

Thesis for the Degree of Doctor of Engineering

Landslide Susceptibility Analysis  
Using Landsat Image & GIS  
Technics in Jeju

JEJU NATIONAL UNIVERSITY  
GRADUATE SCHOOL

Department of Civil & Ocean Engineering

He-Chun Quan

February 2009

# Landsat영상과 GIS를 이용한 제주도 산사태 취약성분석

指導教授 李秉杰

權赫春

이 論文을 工學 博士學位 論文으로 提出함

2009年 2月

權赫春의 工學 博士學位 論文을 認准함

審査委員長 박상렬 ①

委 員 강인준 ①

委 員 이병걸 ①

委 員 이백수 ①

委 員 남정만 ①

濟州大學校 大學院

2009年 2月

# Landslide Susceptibility Analysis Using Landsat Image & GIS Technics in Jeju

He-Chun Quan

(Supervised by professor Byung-Gul Lee)

A thesis submitted in partial fulfillment of the requirements  
for the degree of Doctor of Engineering

2009. 2.

This thesis has been examined and approved.

Thesis director, *Shang-yeol Park*, Prof. of Jeju National University

Thesis director, *In-joon Kang*, Prof. of Busan National University

Thesis director, *Byung-gul Lee*, Prof. of Jeju National University

Thesis director, *Bai-shou Li*, Prof. of Yanbian University

Thesis director, *jung-man Nam*, Prof. of Jeju National University

*February. 2009*

DEPARTMENT OF CIVIL & OCEAN ENGINEERING  
GRADUATE SCHOOL  
JEJU NATIONAL UNIVERSITY

## CONTENTS

LIST OF FIGURES .....	iii
LIST OF TABLES .....	V
ABSTRACT .....	Vii
<b>CHAPTER 1. INTRODUCTION .....</b>	<b>1</b>
1.1 Background and objectives .....	1
1.2 The study trend .....	3
1.2.1 The study trend in oversea .....	4
1.2.2 The study trend in Korea .....	5
1.3 The materials and methods .....	7
<b>CHAPTER 2. THE BASIC THEORY .....</b>	<b>9</b>
2.1 The definition and causes of the landslide occurrences .....	9
2.2 The landslide analysis methods and stages .....	14
<b>CHAPTER 3. THE GIS DATA IN JEJU .....</b>	<b>19</b>
3.1 The study area .....	19
3.2 The GIS data characteristics .....	20
3.2.1 The topographical characteristic in Jeju Island .....	20
3.2.2 The slope characteristic in Jeju Island .....	22
3.2.3 The aspect characteristic in Jeju Island .....	23
3.2.4 The geological characteristic in Jeju Island .....	25
3.2.5 The soil characteristic in Jeju Island .....	29
3.2.6 The forest characteristic in Jeju Island .....	31
3.2.7 The precipitation and rainfall intensity characteristics in Jeju Island .....	35
3.2.8 The land cover characteristic in Jeju Island .....	39
<b>CHAPTER 4. LANDSLIDE SUSCEPTIBILITY ANALYSIS .....</b>	<b>42</b>
4.1 The landslide susceptibility analysis by using the AHP method .....	42
4.1.1 Theoretical consideration of the AHP method .....	42
4.1.2 The application of AHP method .....	46

4.1.3 The landslide susceptibility analysis using the GIS overlay method and weights .....	60
4.2 The landslide susceptibility analysis using the logistic regression analysis method .....	65
4.2.1 The conception of the logistic regression analysis .....	65
4.2.2 The application of the LRA method to the landslide susceptibility analysis .....	67
4.3 The landslide susceptibility analysis using the artificial neural network .....	69
4.3.1 The conception of the artificial neural network .....	69
4.3.2 Mathematics of the artificial neural network .....	71
4.3.3 The application of ANN to the landslide susceptibility analysis .....	75
<b>CHAPTER 5. IMAGE CHANGE DETECTION .....</b>	<b>80</b>
5.1 Landsat TM data .....	80
5.2 Landsat TM image analysis .....	81
5.3 NDVI image change detection .....	89
5.3.1 The conception of NDVI .....	89
5.3.2 The detection of the NDVI changes .....	91
<b>CHAPTER 6. DISCUSSION .....</b>	<b>95</b>
6.1 The analysis of the susceptibility areas .....	95
6.2 The accuracy analysis of the susceptibility areas by field data .....	99
6.3 The landslide probability analysis .....	102
<b>CHAPTER 7. CONCLUSIONS .....</b>	<b>106</b>
<b>REFERENCES .....</b>	<b>108</b>
<b>요약 .....</b>	<b>113</b>

## LIST OF FIGURES

Fig. 1.1	The flow chart of the landslide susceptibility analysis .....	8
Fig. 2.1	The names of each part in a landslide(Varnes, 1978) .....	10
Fig. 2.2	The main landslide types(wonyung, 2000) .....	10
Fig. 2.3	The factors of a landslide(Bromhead, 1992) .....	12
Fig. 3.1	The study area of Jeju Island .....	19
Fig. 3.2	The 1:25,000 contour map of Jeju Island .....	21
Fig. 3.3	The DEM of Jeju Island generated from the 1:25,000 digital map .....	21
Fig. 3.4	The slope map of Jeju Island .....	23
Fig. 3.5	The aspect map of Jeju Island .....	24
Fig. 3.6	The geological classification map with four levels .....	28
Fig. 3.7	The soil classification map of Jeju Island .....	31
Fig. 3.8	The forest distribution map of Jeju Island .....	32
Fig. 3.9	The tree diameter characteristics of the Halla mountain in Jeju Island .....	34
Fig. 3.10	The isohyet map of Jeju Island .....	37
Fig. 3.11	The isohyet grid map of Jeju Island .....	37
Fig. 3.12	The rainfall intensity map .....	38
Fig. 3.13	The land cover classification map of Jeju Island .....	40
Fig. 4.1	The process of AHP .....	43
Fig. 4.2	The structure of AHP .....	46
Fig. 4.3	The work flow of the converting map .....	63
Fig. 4.4	The weighted overlay model .....	63
Fig. 4.5	The landslide susceptibility map generated by using the AHP method and GIS .....	64
Fig. 4.6	The landslide susceptibility map generated by the logistic regression analysis method .....	68
Fig. 4.7	Components of a typical artificial neural network .....	70
Fig. 4.8	Mathematical model of a neuron .....	70
Fig. 4.9	The flowchart of the neural network training for weight determination .....	76
Fig. 4.10	The comparison of the RMSE values between each learning rate .....	78
Fig. 4.11	The relative importance value of each input factor .....	78

Fig. 4.12	The landslide susceptibility map generated by the artificial neural network method .....	79
Fig. 5.1	The shape of Landsat TM satellite .....	80
Fig. 5.2	Landsat TM images of Jeju Island(2001) .....	83
Fig. 5.3	Histograms of Landsat TM images(2001) .....	84
Fig. 5.4	Landsat TM images of Jeju Island(2002) .....	85
Fig. 5.5	Histograms of Landsat TM images(2002) .....	86
Fig. 5.6	Landsat TM images of Jeju Island(2007) .....	87
Fig. 5.7	Histograms of Landsat TM images(2007) .....	88
Fig. 5.8	The NDVI image generated from the Landsat images in 2001 .....	92
Fig. 5.9	The NDVI image generated from the Landsat images in 2002 .....	92
Fig. 5.10	The NDVI image generated from the Landsat images in 2007 .....	93
Fig. 5.11	The change detection of the NDVI images between 2001 and 2002 .....	93
Fig. 5.12	The change detection of the NDVI images between 2002 and 2007 .....	94
Fig. 6.1	The area distribution in each susceptibility level(AHP method) .....	95
Fig. 6.2	The area distribution in each susceptibility level(LRA method) .....	96
Fig. 6.3	The area distribution in each susceptibility level(ANN method) .....	97
Fig. 6.4	The comparison of areas generated by three methods in each level .....	98
Fig. 6.5	The comparison of areas generated by three methods in level 4 and 5 .....	98
Fig. 6.6	The distribution of the field data .....	99
Fig. 6.7	The ANN model for the landslide probability analysis .....	103
Fig. 6.8	The comparison of each RMSE value .....	104
Fig. 6.9	The importance values of each input factor .....	104
Fig. 6.10	The result of the landslide probability analysis .....	105

## LIST OF TABLES

Table 1.1	The number of death by landslides .....	2
Table 2.1	The abbreviated classification of a landslide .....	11
Table 2.2	Landslide susceptibility analysis techniques and map scales .....	16
Table 2.3	Available input data in Korea for the landslide susceptibility analysis using GIS .....	17
Table 3.1	The classification of geological features .....	28
Table 3.2	The classification of soil types[SCS] .....	30
Table 3.3	The forest distribution of elevations and areas(Unit: $km^2$ , %) .....	32
Table 3.4	The forest distribution in the middle area of mountain(Unit: $km^2$ , %) .....	33
Table 3.5	The result of the precipitation analysis per area(Unit: mm) .....	36
Table 3.6	The area amount of the precipitation by an elevation(annual average) .....	36
Table 3.7	The rainfall intensity of each area in Jeju Island .....	38
Table 3.8	The classification levels .....	41
Table 4.1	The importance measurement .....	44
Table 4.2	Proposal conditions .....	47
Table 4.3	The comparison of the importance between each factor .....	47
Table 4.4	The weight values of every proposal at slope .....	49
Table 4.5	The weight values of every proposal at aspect .....	49
Table 4.6	The weight values of every proposal at geology .....	50
Table 4.7	The weight values of every proposal at soil .....	51
Table 4.8	The weight values of every proposal at rainfall intensity .....	51
Table 4.9	The weight values of every proposal at forest .....	52
Table 4.10	The weight values of every proposal at land cover .....	53
Table 4.11	The weight values of every proposal at each factor .....	53
Table 4.12	The relation between landslide and slope .....	55
Table 4.13	The relation between landslide and aspect .....	55
Table 4.14	The relation between landslide and soil .....	56
Table 4.15	The relation between landslide and forest .....	56
Table 4.16	The relation between landslide and land cover .....	56
Table 4.17	The rating values of slope .....	56
Table 4.18	The rating values of aspect .....	56
Table 4.19	The rating values of geology .....	56



Table 4.20	The rating values of soil .....	57
Table 4.21	The rating values of rainfall intensity .....	57
Table 4.22	The rating values of forest(cm) .....	57
Table 4.23	The rating values of land cover .....	58
Table 4.24	The calculation of RIW between each factor .....	58
Table 4.25	The weight values of each factor in proposal 1 .....	59
Table 4.26	Heuristics proposed by researchers to compute the optimum number of hidden layer nodes .....	76
Table 4.27	The setting values for neural network training .....	77
Table 4.28	The learning rates and momentum .....	77
Table 5.1	The Landsat TM spectral band characteristics .....	81
Table 5.2	Statistic data of Landsat TM images(2001) .....	84
Table 5.3	Statistic data of Landsat TM images(2002) .....	86
Table 5.4	Statistic data of Landsat TM images(2007) .....	88
Table 6.1	Field data .....	100
Table 6.2	The information of the field data .....	101
Table 6.3	The field data recognized as the susceptibility areas in each method .....	102
Table 6.4	Layer numbers .....	103
Table 6.5	The learning rates and momentum .....	103

## ABSTRACT

The purpose of the following study is to compare three different methods AHP, LRA and ANN in generation of a landslide susceptibility map in Jeju Island. First, we made the DEM based on the contour line obtained from a 1:25,000 digital map. To evaluate the landslide susceptibility, we also generated a slope map and aspect map from the DEM. Then, we built a geographical information system as well as a soil map, forest map, rainfall intensity map, geological map, land cover map and so on. According to the importance of factors, which had an influence on landslide susceptibilities, we classified the factors and calculated the weight values by using three different methods.

To calculate the weight of each factor by using the AHP method, which has an influence on landslide, we suggested 8 proposals. These 8 proposals were classified according to the important relation between each factor in a landslide occurrence as 8 different cases and the important value of each factor such as slope and aspect that has an influence on a landslide was defined and we calculate the weight values by using the AHP method.

After calculating the weight values, we progressed a geometric correction through a treatment process to a thematic map of the factors, which has an influence on a landslide and the attribute values ( $A, B, C..$ ) of the layer used in overlay, and set up a slope map, aspect map, rainfall intensity map, geology map, soil map, forest map, and land use map. In the process of a calculation, a weighted overlay operation was used for a transformation function ( $f$ ) applied to the overlay and layers were piling up one another after the generated model was considered all weights of factors which had an influence on a landslide susceptibility. The attribute value ( $U$ ) generated by the overlay was made out a landslide susceptibility map of the study areas and the landslide susceptibility areas were expressed by red and yellow color pixels.

In the logistic method, the landslide occurrence belonged to an independent variable and it was assigned for "0" if no landslide was present or "1" if a landslide was present. Dependent variables contained slope, aspect, soil, geology, forest, rainfall intensity and land cover. The relation between dependent and independent variables could be written as the following equation:

$$\begin{aligned} \ln(P_z/(1 - P_z)) = & (-10.158) + 0.783 * X_1(\text{slope}) + 0.364 * X_2(\text{aspect}) \\ & + 0.523 * X_3(\text{geology}) + 0.668 * X_4(\text{soil}) \\ & + 0.726 * X_5(\text{rainfall intensity}) \\ & + 0.400 * X_6(\text{forest}) + 0.575 * X_7(\text{landcover}) \end{aligned}$$

Finally, the landslide susceptibility map was generated by using the above equation and the GIS method.

In the ANN method, the neuron number of the hidden layer was 14 when calculated by the equation suggested by Kanellopoulas and Wilkinson(1997), the number of the input layer was 7, the number of the output layer was 1, the number of the weights between the input and hidden layer was 98, and the number of the weights between the hidden and output layer was 14. Generally 50000 times of circulation were proceeded to achieve a designed error value. Finally, the relative importance of the landslide factors was calculated by the neural network method and the landslide susceptibility map was generated by using the GIS method.

After the susceptibility maps were generated by using the AHP method, the logistic regression method and the artificial neural network method respectively, each area belonging to each level in the susceptibility maps was compared with one another and with NDVI images to find a more dangerous area from susceptibility areas.

To analyze an accuracy of the susceptibility maps generated by three different methods, we used six areas where a landslide had occurred and six

areas considered more dangerous after a field survey.

Through the comparison between three susceptibility maps and field data, we finally knew that the susceptibility areas generated by the ANN method was more accurate among three methods.

To inspect an accuracy of the susceptibility areas, we also performed a landslide probability analysis of some susceptibility areas and safety areas in the susceptibility map generated by the ANN method. Finally, we knew that probability values belonging to the susceptibility areas were very high and probability values belonging to safety areas were very low. Thus, it indicated that the susceptibility map generated by the ANN method was accurate.

# CHAPTER 1. INTRODUCTION

## **1.1 Background and objectives**

With the development of science and technology, a remote sensing technology that classifies the land surface by using a multispectral spectrum, the extraction of topographical features by using high resolution satellite images and the GIS which is efficiently used for geospatial information in daily life have been developed. With these technologies, it could be possible to predict and reduce the damage made by natural disaster through analyzing and monitoring flood damage, forest fires and landslides.

In Korea, about 70% of the land were mountainous areas and the annual average rainfall was about 1,100~1,400mm. Around 60% of the rainfall were distributed in summer and most of the disaster by a landslide occurred in the season. Landslides from a rainfall accompanied by a typhoon also occurred frequently(Hwang, S. H., 2002).

Since 1970, with the progress of the national land development planning, the number of mountain cutting, coulee filling for road and house constructing has increased throughout Korea. The damage of natural slope causes a landslide and it increases the loss of human life and properties. In particular, with the increase of necessity of land for industry development, the disaster caused by a landslide tended to be larger(Chun, K. S., 2005). Table 1.1 shows the survey data about the loss of human life from 1991 to 2000.

Jeju Island was mostly made of the volcanic rocks and typical volcanic ash soil erupted from the Halla mountain, which was a main crater. Because the mountain was very steep, surrounded by many cliffs and significantly

influenced by a typhoon and rainfall, there might be severe damage caused by landslides. Therefore, it was needed to develop a scientific analysis technology to predict landslides to reduce death of human life and properties. However, it needs to spend time and human resources to collect individual spacial information and field data to analyze landslides. Fortunately, we can overcome difficulties in a field investigation by using a remote sensing, which also makes it easy to acquire morphological and physical information about a broad area. In addition, we can continue to collect, manage and analyze enormous spacial information databases about landslides by using the GIS(Lee, M. J., 2003). In this study, we used three different methods AHP, LRA and ANN to generate the susceptibility maps for landslide susceptibility analysis in Jeju Island.

Table 1.1 The number of death by landslides(disaster prevention association, 2001).

Year	The total number of death	The number of death by Landslides	Rate(%)
1991	240	63	26.3
1992	40	1	2.5
1993	69	12	17.4
1994	72	6	8.3
1995	158	28	17.7
1996	77	2	2.6
1997	38	5	13.2
1998	384	103	26.8
1999	89	23	25.8
2000	49	18	36.7
Sum	1,216	261	-
Average	122	26	17.7

## **1.2 The study trend**

Landslides are significant natural hazards in many areas around the world. Globally, they cause hundreds of billions of dollars in damage, and hundreds of thousands of death and injuries each year(Aleotti and Chowdhury, 1999). Over the past 25 years, many governments and international research institutions have invested considerable resources in assessing landslide hazards and in attempting to produce maps of portraying their spatial distribution(Guzzetti et al., 1999). The core techniques for studying landslides in Korea and abroad are a landslide survey, estimation and prediction of a landslide occurrence and real time monitoring.

An importance of the landslide survey is to develop a technique in consideration of geological features in each country because the geological features and the natural environment in each country are somewhat different. The most important usage of the techniques is to estimate and predict a landslide occurrence. In developed countries, they tried to develop a technique that correctly predicted an occurrence of landslides but the problem was how to exactly examine and apply various variables related to landslides. Before applying the GIS technique, the geological feature of Korea was performed illogically and non-quantitatively while it was more scientifically quantitative by the GIS technique. Especially, important foundation of the technique was built through the comprehensive consideration based on the classification of landslide risks and this technique was in the same level with developed countries.

In the case of the real time to monitor landslides, developed countries have operated a system that could predict a landslide occurrence and make an early warning. They have also upgraded the systems through continuous

research. In Korea, many efforts have been done for the development of the systems to predict landslides but the problem is that the budget for the preparation of equipment for the real time survey is too expensive. Unfortunately, most of this equipment has been used in another research for slope stabilities at a cutting slope(Chun, K. S., 2005).

### 1.2.1 The study trend in oversea

In oversea, it has been tried to portray an objective and quantitative landslide risk map based on a conditional probability model, certainty factor model, and fuzzy set model(Chuang and Fabbri, 1993). There was also some research that analyzed the models through a logistic regression analysis using factors, such as aspect, height, land cover, soil drainage and so on(Dai and Lee, 2002).

The GIS has been applied to predict landslide-occurring areas since the end of 1960's. Newman et al(1978) reported that it was possible to realistically portray a prediction map of landslides by a computer and Carrara(1978) predicted an area where a landslide might occur through a multivariable analysis using a 200m×200m grid and around 25 factors. An application of the GIS to map slope-unstable areas has been increased considerably by rapid development of commercial systems such as ArcInfo and MGE since 1980's. In Italy, Carrara and his colleagues(1992) performed a multivariable analysis of slope instabilities by using the GIS. Their primary research focused on analyzing with a grid, however they changed the direction of their research into the field of morphometric. There was not much modification in the method but they chose the area where a landslide occurred previously as a study-model area to establish a statistical model(Carrara et al., 1992).

Baldelli(1996) and his colleagues portrayed a landslide susceptibility map through a GIS overlay analysis using a geological map, topographic map, DEM, and so on(Baldelli, 1996). Turrini and Visintainer(1998) analyzed



Landslides by using an overlay of data such as erosion rates, drainage rates, tectonic, slope inclination, land cover and so on(Turrini and Visintainer, 1998).

Since 1994, GSC in Canada has performed geological hazards and environmental geoscience programs that included a natural hazard synthesis program, a geological study on a main mountain, a study on a landslide at the eastern part of Canada, a study on a landslide occurrence prediction and so on.

In Japan, although the researchers have made an accurate survey of landslides caused by a natural activity, there are few surveys about the landslides that have already happened before and the distribution of the landslides is not clear yet.

E. Yesilnacar and T. Topal(2005) also performed a study about landslides in Turkey. In their study, two different approaches, logistic regression and neural networks, were applied in order to prepare a susceptibility map. Finally, they also found that the susceptibility map prepared by a neural network was more realistic(E. Yesilnacar and T. Topal, 2005).

### **1.2.2 The study trend in Korea**

Kim et al.(1994) investigated a landslide probability through analyzing five factors related to landslides including slope, aspect, geological features, soil, and land cover by using a wide area overlay analysis using the GIS in Cheongju(Kim et al., 1994).

Sin et al.(1996) constructed a database of spacial and attribute data based on a topographic map, geological map, soil map, water vein map, aerial photograph and satellite images and applied them to analyzing a landslide occurrence probability in Boryeong and Seocheon. In the study, they first interpreted an aerial photograph to predict a possibility of a landslide occurrence and discriminated the distribution and frequency of a wide range of landslides and then calculated the length and density per unit area of a

tectonic line(Sin et al., 1996).

Sim et al.(1997) analyzed an effect of the annual amount of rainfall, monthly amount of rainfall, the accumulated amount of rainfall, and the biggest amount of rainfall in a day on a landslide. In this study, they interpreted a landslide behavior related to the rainfall intensity with regional groups and their main purpose of the research was to devise a form of the data survey to establish a landslide cause, behavior analysis, and preventive measures based on a synthetic report style including the data about ground conditions, precipitation conditions, earthquakes and so on(Sim et al., 1997).

Lee et al.(1999) analyzed a landslide susceptibility based on a probability analysis and statistical analysis that analyzed fourteen factors such as a topographic map(slope, aspect, curvature), soil map(topography, soil, base metal, drainage, effective depth of soil), forest map(Wood type, diameter, age, density), geological map(sheet), and land cover in Yongin and Jangheung(Lee et al., 1999).

Kim et al.(2003) systematically arranged natural factors that could influence a type of landslides and occurrences such as rainfall, topography, geological features, soil, and forest through various scientific articles, research reports and internet websites. Then, he proposed situation of disaster and a type of a landslide occurrence within Korea(Kim et al., 2003).

Lee et al.(2003) constructed a database about the study area, analyzed the relationship between a landslide and a spacial database then analyzed the landslide susceptibility after calculating a weighted value in Gangreung(Lee et al., 2003).

Cheon et al.(2005) constructed GIS databases about the study area and performed an evaluation of the landslide susceptibilities after calculating a weighted value and selecting the optimum alternative to landslide occurrence factors using the AHP method. They also performed tracking strange changes of landslides through change detection of the land cover changes and NDVI of the multirate images at the same area(Cheon et al., 2005).

### **1.3 The materials and methods**

The purpose of the study was to compare three different methods AHP, logistic method and ANN in generation of landslide susceptibility map in Jeju Island. First, we made the DEM based on a contour line obtained from a 1:25,000 digital map. To evaluate a landslide susceptibility, we also generated a slope map and aspect map from the DEM. Then, we built a geographical information system as well as a soil map, forest map, rainfall intensity map, geological map, land cover map and so on. According to the importance of factors, which had an influence on the landslide susceptibility, we classified the factors and calculated weight values by using three different methods and then we got three different susceptibility maps using the GIS method through weighted overlay method.

After the susceptibility maps were generated by using the AHP method, the logistic regression method and the artificial neural network method respectively, each area belonging to each level in the susceptibility maps was compared with one another and with NDVI images to find a more dangerous area from susceptibility areas.

To analyze an accuracy of the susceptibility maps generated by three different methods, we used six areas where a landslide had occurred and six areas considered more dangerous after a field survey.

To inspect an accuracy of the susceptibility areas, we also performed a landslide probability analysis of some susceptibility areas and safety areas in the susceptibility map. Fig. 1.1 showed the working flow of this study.

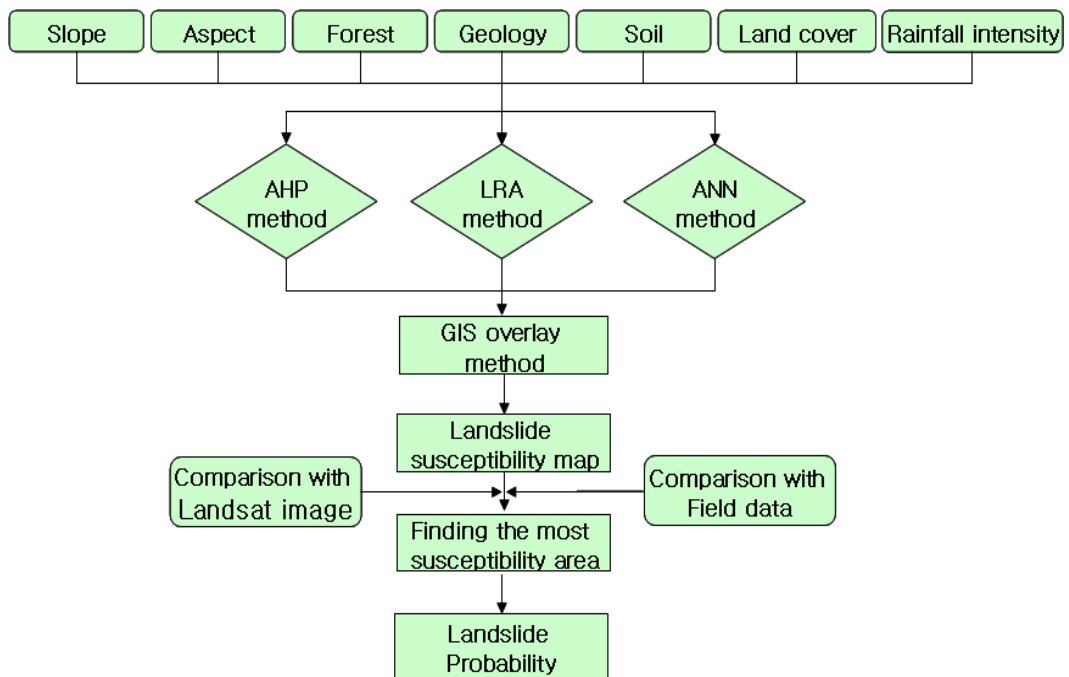


Fig. 1.1 The flow chart of the landslide susceptibility analysis.

## CHAPTER 2. THE BASIC THEORY

### **2.1 The definition and causes of the landslide occurrences**

Landslides mostly occurred at hill areas or mountainous districts and the most crustal movement-caused crushing zone was frequently influenced by rainfall or heavy snow. Landslides mean that a large amount of rock, soil, and a wreckage flow at the bottom while following slope as showed in Fig. 2.1. Landslides have many different types from a small to large scale, and the velocity of landslide movement is also very diverse. In the previous report, landslides were defined as a phenomenon that results from rock or soil and mixtures of them slowly creep or quickly fall due to gravity, slowly slide or flow through a destroyed plane or a complex of two phenomena. Landslides are a failure phenomenon of a natural slope or artificial slope that possesses a feature of the natural slope. Terzaghi defined 'Landslide' as the one that a materials at slope had fast movement. The 'Creep' was defined as the one that moved too slowly to perceive it. In contrast, Varnes integrated these two concepts with 'Slope movement' and he also suggested a 'Mass movement' concept that means the movement of components of the earth surface by gravity.

In Japan, landslides were defined as 'soil and mud flow' and subdivided into 'soil creep', 'slide', 'collapse', 'soil flow', and 'mud flow'. In Korea, they were defined as 'Slope movement' and 'soil and mud flow' except the 'mud flow' during two phenomena. A landslide has six types such as slump, slide, flow, fall, topple, and torrent as shown in Fig. 2.2. A landslide that occurs as two

or more types is called a complex landslide. Skempton and Hutchinson(1969) defined that landslides are a phenomenon that soil or rock flows at the bottom by a shear failure occurring in a slope boundary. Varnes(1978) classified landslide materials into rock and soil, and classified movement forms into fails, topples, slides, rotational, translational, lateral spreads, and flows as shown in Table 2.1.

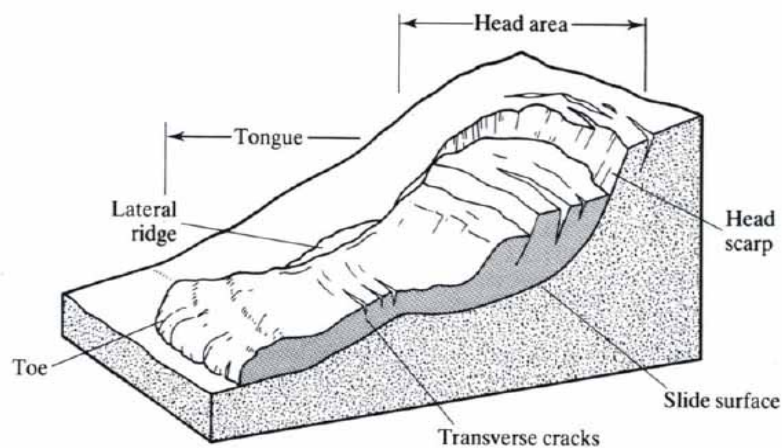


Fig. 2.1 The names of each part in a landslide(Varnes, 1978).

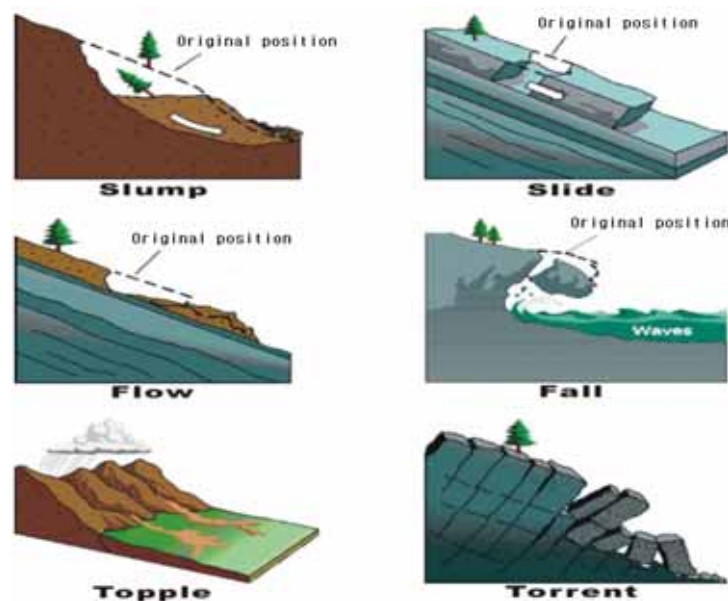


Fig. 2.2 The main landslide types(wonyung, 2000).

Table 2.1 The abbreviated classification of a landslide (Varnes, 1978).

Types of Movement	Types of Materials		
	Bedrock	Engineering Soils	
		Predominantly Coarse	Predominantly Fine
Fails	Rock fall	Debris fall	Earth fall
Topples	Rock topple	Debris topple	Earth topple
Slides	Rock slump	Debris slump	Earth slump
Rotational	Rock block slide	Debris block slide	Earth block slide
Translational	Rock slide	Debris slide	Earth slide
Lateral spreads	Rock spread	Debris spread	Earth spread
Flows	Rock flow (deep crack)	Debris flow (soil creep)	Earth flow (soil creep)
Complex	Combination of two or more principal types of movement		

Landslides are the result of shear damage occurring at the boundary of moving soil or rock. Generally, it is supposed that it occurs when an average shearing stress exists through a sliding face the same as a shear strength of the soil and rock measured in a surveyed field or laboratory. However, by a gradual collapse by an environmental factor of continuous rainfall in an actual field, landslides also occur even though a shearing stress is a little bit more than a maximum strength of the soil and rock measured in the laboratory (Fang, 1991).

A factor which has an influence on a landslide, is comprehensively classified into some natural factors such as geography, rock types, soil types, structure, vegetation, rainfall, groundwater, erosion, and earthquakes and some artificial factors such as land use, cutting, and banking as shown in Fig. 2.3.

Among the natural factors, direct factors include the increase of slope loads from rainfall, the erosion of a lower region of slope from a river, coast erosion by a sea wave, vibrations from earthquakes and occurrences of

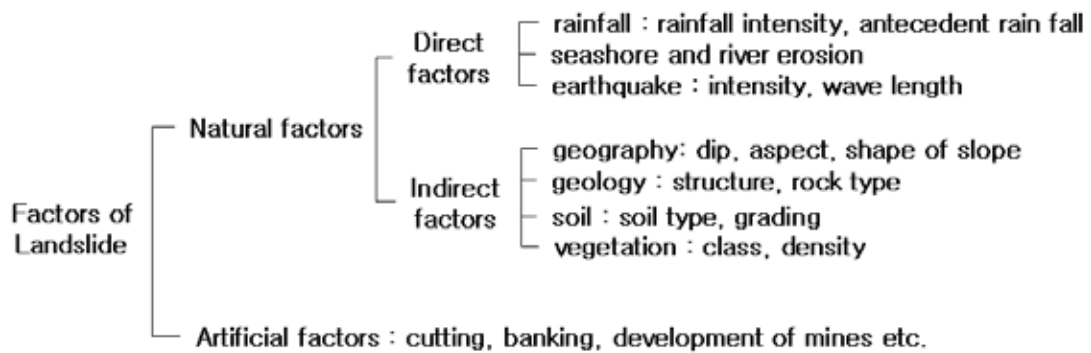


Fig. 2.3 The factors of a landslide (Bromhead, 1992).

cracks(Brand, 1988). In all of them, especially, rainfall is a very important factor that causes a landslide by decreasing the resistance due to the rise of pore water pressure, the overflow of surface water, and the increase of unit weights from soil saturation.

During rainfall in rainy season, a slope failure, in aspect of soil types and landslides often occurs for short time on sandy soil. In a clay soil type, a landslide is caused by the increase of the ground water surface resulted from persistent rainfall. A steep slope is caused by a change of geographic features in a river and coast from the erosive action(Terzaghi, 1950), and erosion at the bottom of slope like erosion in a valley from heavy rain increases instabilities of slope. Most of the slope failures from erosion of a river and coast are a collapse in the soil surface, however, it could be developed into a slope failure. In the case of earthquakes, because of cohesion in soil reduced by movement and friction, a landslide would be able to occur(Walker, 1987). A failure of a steep slope, failure of the soil surface and a fall of rocks included in both of a natural and artificial slope are a typical form of a slope failure generated by earthquakes.

Indirect factors such as another natural factor, can not induce a landslide by itself. However, they can cause instabilities of slope while combined with another factor. Geography, geology, soil and forest are a typical example of



the indirect factors.

Geography has a big association with drainage ability of flowing water and an occurrence of a landslide because it generally has an influence on the concentration, dispersion, and movement of underground water. A slope direction is an important factor to decide whether a landslide occurs and an occurrence type of the relation between geologic structure of a joint, foliation, schistosity and strike, and slope on rock slope.

An inclination of slope plays a role in increasing an impulse of components of slope. Therefore, landslides more easily occur in slope with a big inclination when the other circumstances are under the same condition. Generally, a landslide tends to occur in rock with weak strength or high moisture. The crushing zone and fault on geological structure line also have many influences on landslide. A crushing zone and a fault along a geological structure line also have many influences on landslides. The crushing zone promotes an occurrence of landslides by playing a role of underground water that resulted from the rapid decrease of rock strength and the proceeding of weathering. The occurrence of a joint on slope is affected by an origin of rock and external effects. The slope failure would easily occur due to gravity while a slope direction of a joint is bigger than an angle of an inclination.

Generally, the frequency of landslide occurrences in soil is much higher than that in rock and landslides also easily occurs when the strength of soil is weak or highly moist. The soil is classified into residual soil resulted from weathered country rock and colluvium that is moved and accumulated. The residual soil has a dynamic characteristic that can be changed by weathering the degree of country rock, structure materials, directions and the degeneration degree of country rock.

Colluvium is a soil layer that is made of the residue of weathered rock moved and accumulated at the bottom of slope by gravity and landslides

would occur at the boundary between colluvium and bedrock. The decrease of the shear strength would become a direct cause of landslides while the bedrock is an impermeable layer or a shale. Vegetation can absorb and reduce an influence of rainfall on slope that can prevent erosion of the surface, and the root of vegetation can increase stabilities of slope through increasing the strength of shears(Keller, 1979). Therefore, the distribution and density of vegetation might be an important factor, which could have an influence on slope stabilities.

Artificial factors are mostly made out of a human activity. The change and establishment of a water channel, development of mine, urban and industry, various engineering work and the construction like roads would decrease the resistance of soil or rock by transforming the natural slopes and increase instabilities of slope by changing stress in slope and cause landslides. The increase of a ground water level after finishing the construction of the tunnel and dam also has an influence on a landslide occurrence. In case of cutting slope, with a long period of the exposure to an outside environment, it could also be weathered very quickly by the climatic change and cause landslide even if it was a very strong rock.

## **2.2 The landslide analysis methods and stages**

There are a landslide susceptibility analysis, landslide possibility analysis and landslide risk analysis in analyzing a landslide. These methods can be applied to a large, medium and small level of scale. A landslide susceptibility implies a relative possibility of a landslide occurrence when suffering from an impact such as heavy rainfall or earthquakes. There are many different

methods in analyzing landslide susceptibilities and they are classified according to a scale of input data. Small scale data is analysed by using a scale that is smaller than 1:500,000, medium scale data is analyzed by using input data that scale is between 1:25,000 ~ 1:50,000 and large scale data is analysed by using input data that a scale is greater than 1:5,000. Table 2.2 shows the Landslide susceptibility analysis methods according to a different scale.

Much research on a landslide susceptibility mapping has been done over the last 30 years. Broadly speaking, landslide susceptibility mappings may be qualitative or quantitative and direct or indirect(Guzzetti et al., 1999). Qualitative methods are subjective and they portray hazard levels in a descriptive term. A geomorphological mapping is an example of a qualitative and direct method. Quantitative methods produce numerical estimates(probabilities) of an occurrence of landslide phenomena in any hazard zone. A direct landslide susceptibility mapping involves mapping landslides within a given region by means of field studies, aerial photographic interpretation or other methods(Verstappen, 1983). In the direct mapping, an expert uses knowledge and experience to map an actual or potential landslide hazard. Indirect methods of the landslide susceptibility mapping are essentially stepwise procedures. They first require to recognize and map landslides over a target region or a training area. Identifying and mapping a group of physical factors is directly or indirectly correlated with slope instabilities. Indirect methods then involve an estimate of a relative contribution of instability factors in generating slope failures and the classification of the land surface into domains of different hazard degree(or hazard zoning)(hansen, 1984).

The map overlay method is used for a large scale. This method portrays a landslide susceptibility map by using weight of each factor that is determined by an expert's opinion and justice. A probability method is used for a medium scale. This method portrays a landslide susceptibility map based on the result

from stochastically analyzing the correlation between landslides and each factor related to landslides. Factors involved in a probability analysis are slope and aspect abstracted from the DEM(Digital Elevation Model), the soil, topography, depth, soil drainage and parent material abstracted from curvature and a soil map, wood type, age, diameter and density abstracted from a forest map, a rock floor abstracted from a geology map, a line structure abstracted from Landsat TM and water drainage lineament abstracted from a topographic map(Table 2.3). However, such individual factors mentioned above should have been constructed as GIS database form for the susceptibility analysis even though they transform and calculate in a different form such as a ascii form.

Table 2.2 Landslide susceptibility analysis techniques and map scales  
(Turner and Schuster, 1996).

Technique	Characteristics	Scale
Landslide distribution analysis	Analyze distribution and classification of landslide	r, m, l
Landslide distribution analysis	Analyze temporal changes in landslide pattern	m, l
Landslide density analysis	Calculate landslide density in terrain units or as isopleth map	r
Geomorphologic analysis	Use in-field expert opinion in zonation	r, m, l
Qualitative map combination	Use expert-based weight values of parameter maps	r, m
Bivariate statistical analysis	Calculate importance of contributing factor	m
Multivariate statistical analysis	Calculate prediction formula from data matrix	m
Safety factor analysis	Apply slope stability model	l
Score method	Apply score table	l

(r: regional scale, m: medum scale, l: large scale)

Table 2.3 Available input data in Korea for the landslide susceptibility analysis using GIS(Lee, 2000; Turner and Schuster, 1996).

Types	Layers	Attribute items	Data sources
Landslide	Landslide	Date, type, activity, depth, dimension	Field survey
Geomorphology	geomorphological units	Geomorphological description	Topographic map, Soil map
	Altitude	Altitude	Topographic map
	Slope angle	Slope angle	Topographic map
	Slope direction	Slope direction	Topographic map
	Slope length	Slope length	Topographic map
	Curvature	Concavity/convexity	Topographic map
Engineering Geology	Lithology	Lithology, rock strength, discontinuity spacing	Geological map
	Soil	Material types, depth, USCS, classification	Soil map
		Parent material, soil drainage	
	Structural geology	Fault type, length, dip, dip direction, fold axis, lineament length, direction, density	Geological map, Airphoto, Satellite image, Field Survey
Seismic accelerations	Maximum seismic acceleration	Observation data	
Forest	Forest	Wood type, age, diameter, density	Forest map
Land Use	Land use map	Land use and cover type	Topographic map Satellite image
Hydrology	Meteorological station Drainage, Basin Groundwater table maps	Rainfall, temperature, evapotranspiration Type, order, length, Order, size Depth of groundwater table Water drainage Lineament	Report Topographic map Topographic map Report

Susceptibility in a landslide analysis indicates how much weak a landslide region is in an occurrence of a landslide when the factors that directly cause a landslide like rainfall or earthquakes are generated. A landslide possibility analyzes how often the landslide will happen in a region through the addition of an occurrence possibility of landslide factors like earthquakes to a landslide susceptibility. A landslide risk analyzes the amount of the possibilities of human beings and facilities damage by a landslide through consideration of a

landslide susceptibility or possibility together with damage factors like human life and facilities. It can be written as the following equations:

$$\text{Susceptibility} = f(\text{Landslide, Landslide related factors}) \quad 2.2.1$$

$$\text{Possibility} = f(\text{Susceptibility, Impact factors}) \quad 2.2.2$$

$$\text{Risk} = f(\text{Possibility, Damageable object}) \quad 2.2.3$$

In this study, we made susceptibility maps and analyzed landslide susceptibilities in Jeju Island.

## CHAPTER 3. THE GIS DATA IN JEJU

### 3.1 The study area

The study area, Jeju Island, is a volcanic Island located in the southern coast of Korea as shown in Fig. 3.1 (approximately  $126^{\circ} 05' 10''$  N to  $126^{\circ} 58' 37''$  N,  $33^{\circ} 06' 31''$  E to  $33^{\circ} 35' 55''$  E). Almost Jeju Island was composed of volcanic rocks and original volcanic topographic was well conserved because the formative period was relatively short and the degree of the dissection wasn't far (Lee, B. G., 2003). Jeju Island has about 74km of the east-west distance, 34km of the south-north distance and  $1,848.3\text{km}^2$  of the area. The direction of the major axis is  $N75E^{\circ}$  that parallels with the south coast line of Korea and opposites to the direction of Yodong.

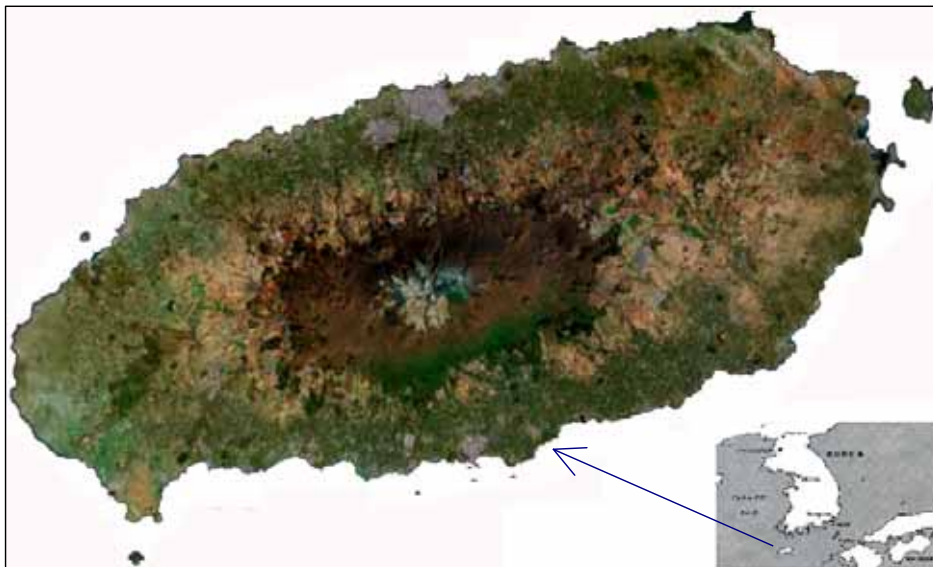


Fig. 3.1 The study area of Jeju Island.

Overall, Jeju Island belonged to Aspite, which was typical feature of shield volcano. Its height is 1950m above the sea level. Its inclination is approximately  $3^{\circ} \sim 5^{\circ}$  from the top of the Halla mountain to the east and west. However, there existed many specific volcanic land forms that were created by the lava, a type of basalt and that repeated eruption from the crater through more than five stages of the period of the volcanic activities.

## **3.2 The GIS data characteristics**

### **3.2.1 The topographical characteristic in Jeju Island**

There are 368 pieces of parasitism volcanoes which are called "oreum", throughout the whole Island. Most of them discontinuously are distributed following a dominant long axis and coast that reached to Seogwipo through Sagyeri from Gosan and also are distributed in the Sinyangri, Seongsan Ilchulbong, Dusanbong, and udo. Almost all of them are constructed from lapillus or volcanic ashes and they are in semiconsolidated or unconsolidated conditions. In the area of the northeast coast and Hyeopjaeri, Sagyeri, and Pyoseonri coast, the sand dune was developed. Fig 3.2 shows a 1:25,000 contour map used in this study that covers all the areas of the Island.

The DEM(Digital Elevation Model) is one of the most important factors in the GIS. The DEM expresses the land surface by a regular grid or arbitrary point connected by a triangle. The purpose of using the DEM is to express the surface of the earth or objects by using a computer and express topography by employing a digital format using a database management system constructed of a discontinuous three dimensional point. An advantage



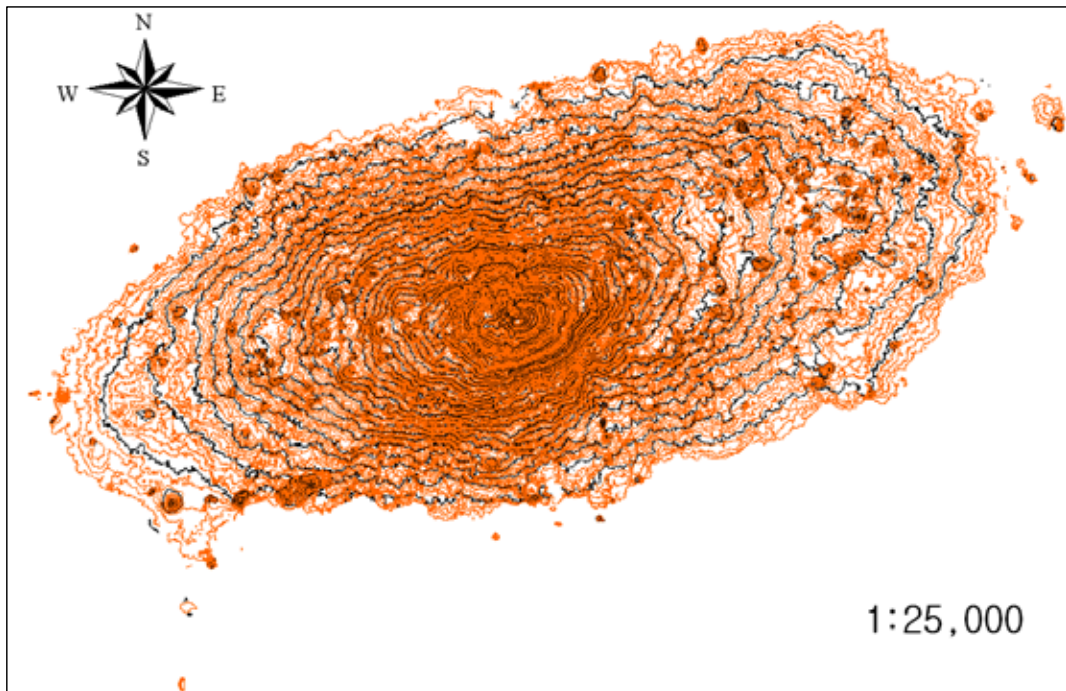


Fig. 3.2 The 1:25,000 contour map of Jeju Island.

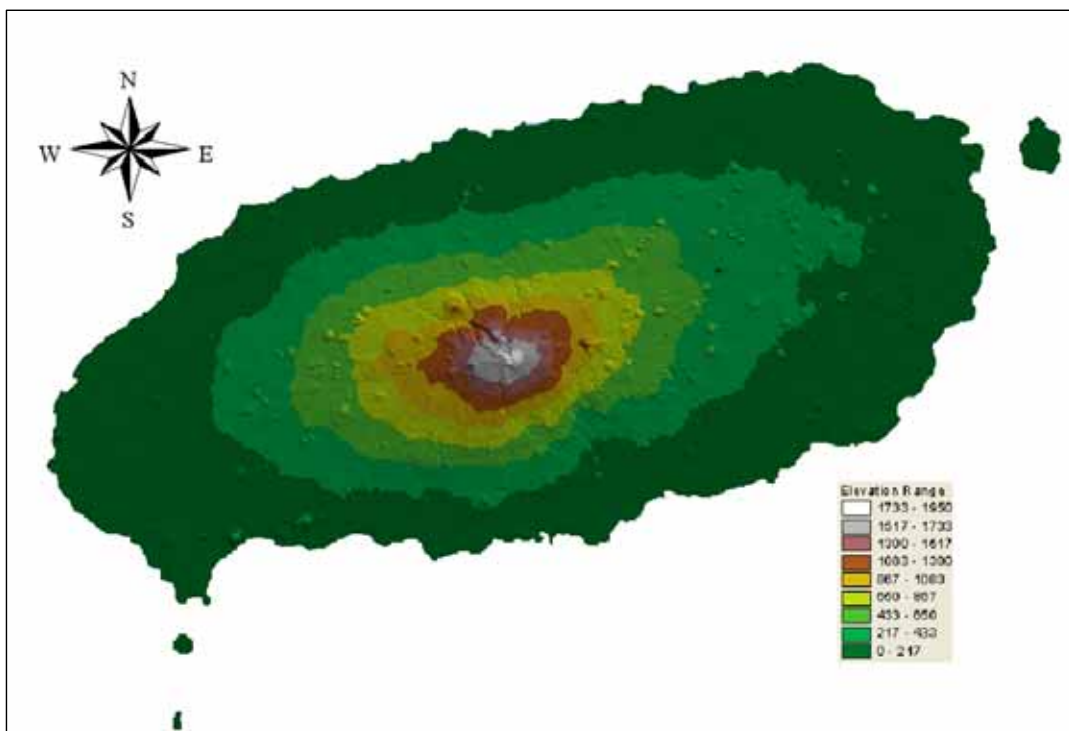


Fig. 3.3 The DEM of Jeju Island generated from the 1:25,000 digital map.

of using the system is to induce many results from the DEM and it is available to combine them with other GIS data. The acquisition of the elevation data is a very important stage in the procedure of generating the DEM because it decides an accuracy of a digital model(Yu. B. M., 2003). In this study, we generated the DEM from the 1:25,000 digital map by using a triangle method as shown in Fig. 3.3.

### **3.2.2 The slope characteristic in Jeju Island**

Slope represents an elevation change between two points by an angle of an inclination. It means that if an angle of an inclination is small, the topography is flat or if an angle of an inclination is big, the topography is steep. A cell value of a grid changes between 0 to 90 degrees and 0 degree represents the horizon and 90 degrees represents the vertical.

The average slope in the whole Jeju Island is analyzed to 8%. The flat area where slope is under 5% is 796.0km<sup>2</sup> and it accounts for 43.6% of the whole area of Jeju Island. The area where slope is under 20% with the frequent utilities of land is 1,627.2km<sup>2</sup> and it accounts for 89.0% of the whole Jeju Island. Thus, most of the areas in Jeju Island are composed of flat geography. According to the districts, the eastern area of Namjeju-gun is analyzed as the flattest area where 91.5% of the areas is under 20% in slope and Seogwipo is analyzed as the steepest area where 21.1% of the area is above 20% in slope.

The average slope in the middle area of the mountain is analyzed as 10%. The area where slope is under 10% accounts for 63.6% of the whole middle area and the area where slope is above 35% accounts for 22.5km<sup>2</sup> from an influence of Oreum. The area under 200~300m in hight where slope is under 10% accounts for 70.6%, the area between 300~400m in hight where slope is under 10% accounts for 64.6% and the area between 400~500m in hight

where slope is under 10% accounts for 60.3%. In conclusion, it indicates that an inclination is rising with the increase of elevation.

According to the districts, the eastern and western area have an easy slope. 82.1% of the eastern area and 73.9% of the western area in Bukjeju-gun are under 10% in slope. 77.9% of the eastern area and 81.6% of the western area in Namjeju-gun are under 10% in slope.

In this study, a slope map of Jeju Island was generated from the DEM as shown in Fig. 3.4.

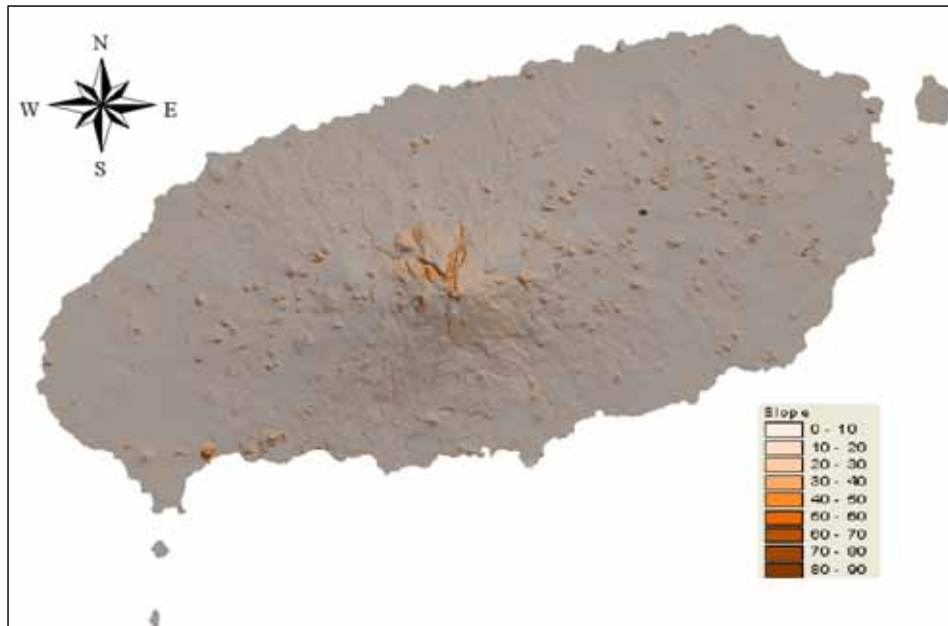


Fig. 3.4 The slope map of Jeju Island.

### 3.2.3 The aspect characteristic in Jeju Island

Aspect map displays the distribution of each direction in the topography by using different colors to each cell of the study area.

The area belonging to northern aspect appears to be highest by 17.6% in the whole island and the area belonging to the eastern and western aspect appears to be lowest by the distribution of 10.4% and 10.2% respectively.

According to elevation, it generally shows a regular characteristic but the area belonging to the northern and northwest aspect shows a high distribution by 18.1% and 13.3% respectively in the coast area under elevation of 200m. According to the districts, Jeju-si mostly came from the northern and northwest aspect and Seogwipo-si mostly came from the southern and southeast and southwest aspect by an influence of geography.

In the middle area of the mountain, the area belonging to the northern aspect appears to be highest by 17.1% and the area belonging to the western aspect appears to be lowest by 9.5%. According to elevation, the area belonging to the northern aspect appears to be highest by 17.1% like a coast area and the area belonging to the northwest aspect shows a distribution of 14.0%. According to the districts, the northern area mostly came from the northern and northwest aspect and the southern area mostly came from the southern and southeast and southwest aspect by an influence of geography.

In this study, a aspect map in Jeju Island was generated from the DEM as shown in Fig. 3.5.

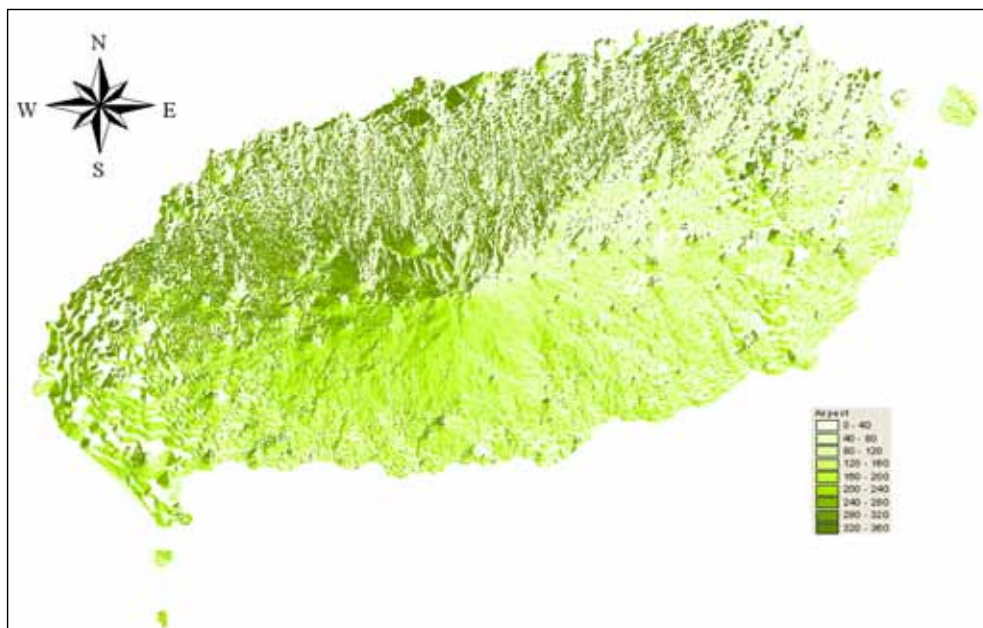


Fig. 3.5 The aspect map of Jeju Island.

### 3.2.4 The geological characteristic in Jeju Island

Jeju Island is constructed of bedrock, basalt and trachyte of the effusive rock, andesite, ejecta, sedimentary rock of the pyroclastic, sand dune and so on. Results from drill cores and pahoehoes whose thickness is less than 0.5m~10m, are distributed under the mean sea level down to 50m depth. Among coulees, there exist shallow paleosol, gravel, pebbly sandstone and sedimentary layers.

In the upper and lower part of the coulees, the clinker, crack and joint are developed and play a good role in the flow of underground water. In the lower part of the basalt, there exists compacted and strong sandstone with the thickness of 20~50m and joint is also very well developed in this area. In the lower part of the basalt, there exist a lot of shellfish fossil and the seogwipo bed constructed of the pebbly sandstone, sandstone, mudstone, psammite mudstone and so on. A hiatus exists at the east side of the line that connected Bukchon and Pyoseone. The depth of the layer's underground distribution is somewhat different from the districts. In the northern and western district, it is distributed with the depth of 30m~70m under the mean sea level. In the southern district from Andeok to Namwon, it is distributed above the mean sea level. In the lower part of the seogwipo bed, there exists U bed constructed of sand and silt with the thickness of 150m and it is distributed broadly under the very deep underground through Jeju Island. In the lower part of the U bed, there exists rudaceous tuff predicted to contrast with cretaceous period tuff in the southeast coast of Korea. In the lower part of the rudaceous tuff, granite, which was generated 58 billion years ago, accomplishes a foundation.

#### 1) Bedrock

Bedrock of Jeju Island was constructed of pyroclastic rock and granite and

pyroclastic was constructed of volcanism sandstone, mudston, rhyolite tuff and lapillus tuff. The quality of rock was estimated to contrast with an oil spring bed in the Cretaceous period. The age of granite was relevant to the last of Paleocene Epoch and it was estimated to intrude pyroclastic rock. Bedrock started from 312m-deep under the maximum sea surface and its average depth was 250m. The distribution of the depth of bedrock was 210m~305m under the sea surface and the average depth was 259m in the southern district and it was known as that the distribution depth was similar to the eastern district. In the northern district, the distribution depth of bedrock was 156m~206m under the sea surface and it was lower than the eastern and southern district.

## 2) U bed

U bed was named because it was not distributed to the land surface and could not be applied to a geographical designation. U bed was distributed to 82m~145m-deep (average 115.3m) area under the sea surface and its average thickness was 134.7m(minimum 111m, maximum 180m). In the southern district, U bed was distributed to the depth of 15m~205m(average 72.6m) under the sea surface and its average thickness was 171.4m(minimum 90m, maximum 228m) thicker than that in the eastern district. In the northern district, the distribution depth was 136m~165m under the sea surface and the thickness was 70m~250m. The U bed was detected from the depth of 86m in the western district.

## 3) Sedimentary rock of the pyroclastic(Seogwipo bed)

Seogwipo bed was distributed over a southern coast cliff of the Cheonjiyeon waterfall in Seogwipo-si with the height about 30m and about 11km-scale on the ground but it was broadly distributed under the ground that was less than 400m of the altitude in the western district of Bukchon

and Pyoseon. Its thickness was about an average of 100m.

A geological medium which composes geological features of the surface of the earth in almost all the areas is trachyte or basalt lava flow, clinker constructed of the flow of the lava, scoria, pyroclastic bed and aqueous pyroclastic bed, and unconsolidated superimposed clastic rock formed in a volcanic activity rest period. Almost all these features have an excellent permeability. Especially, it permeates more than 40% of the recession into underground according to a permeability of geological features of Sumgol and Gotjawal.

#### 4) Volcanic rock

Jeju Island was constructed of relatively various volcanic rocks from trachyte to basalt. The latter was broadly distributed to the district from Seogwipo to Sagye except Hagwi-ri Aewol-eup of Bukjeju-kun and around the head of the Hallasan.

Trachyte and sanidine limited in the districts from Seogwipo to Sagye-ri and Hagwi-ri Aewol-eup and around the head of the Hallasan were much thicker, closer, and stronger than basalt and the developed vertical joint played a good role in contents and flows of underground water. A tuff sedimentary layer constructed of volcanic block, gravel, sand and ashes was intermittently distributed into the side area of the coast of Seongsanpo and Seogwipo, between Hwasun and Songak and between Suwolbong and Yongsu. Its permeability was very low because it was a consolidated or semi-consolidated sedimentary rock layer. Therefore, it played a role of cap rock to restrain a run-off of underground water.

#### 5) Cinder cone and Sand dune

Cinder cone and tuff cone distributed throughout Jeju Island were composed of 360 parasitic cone pieces called "oreum". The "oreum" with a predominant

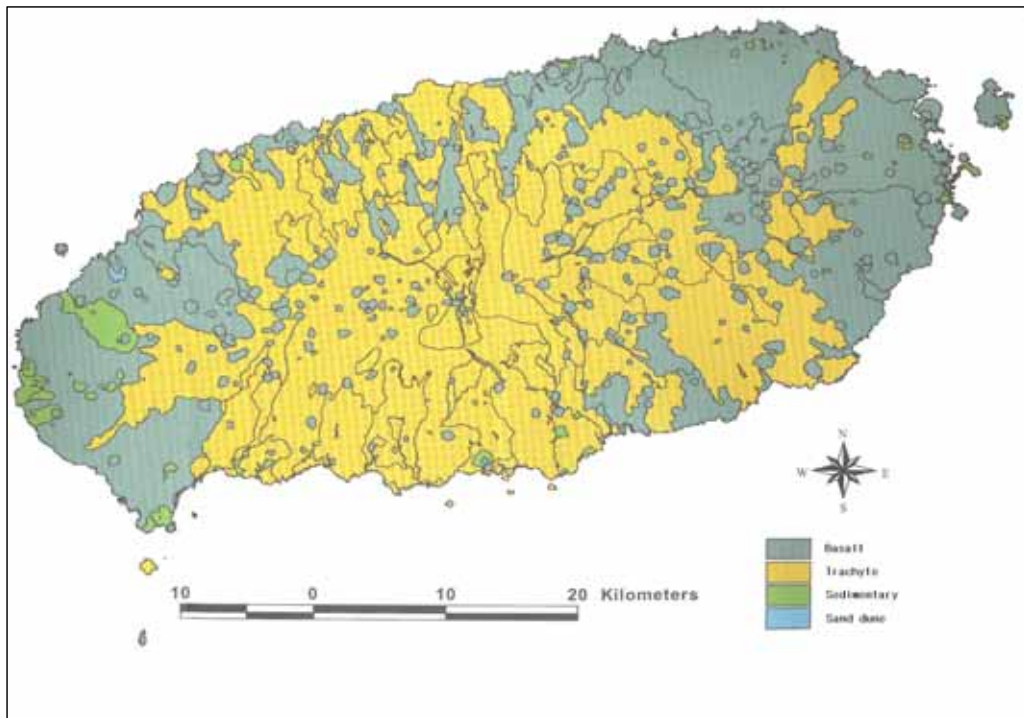


Fig. 3.6 The geological classification map with four levels.

Table 3.1 The classification of geological features.

Classification	Typical names of rock	Reference
Basalt	feldspar, augite, olivine, aphonitic basalt	including variety of close and vesicular basalt
Trachyte	sanidine, andesite	it was very close so it's permeability is lower than basalt
Sedimentary layer	tuff, conglomerate, seogwipo bed, seongsan bed, paleosol	lower permeability
Sand dune layer	Sand dune, sand of beach	

major axis was distributed discontinuously following the coast that reached to Seogwipo via Sagyeri from Gosan and was also distributed to the Sinyangri, Seongsan Ilchulbong, Dusanbong and udo. Almost all these areas were



constructed of lapillus or volcanic ashes and they were in semi-consolidated or unconsolidated conditions. A sand dune layer formed after sand of the coast was carried by wind on the inland side was distributed to the district of Gujwa, Seongsan, Pyoseon, Hyeopjae, Hwasun. Sand dune in the districts of Gimnyeong, Sangdo and Pyoseon was distributed to a deep place, but outside of the area was limited to an area near the coast relatively.

Fig. 3.6 shows a geological map used in this study and it is generally classified into 4 levels as shown in Table 3.1.

### 3.2.5 The soil characteristic in Jeju Island

Most soil in Jeju Island was composed of typical volcanic ash soil. A main basic material was basalt and some of the parts were derived from trachyte and andesite.

The soil in Jeju Island can be classified into dark-brown soil, strong dark-brown soil, chernozem and brown forest soil according to an earth color. Among them, the dark-brown soil is an un-volcanic ash soil and the rest three types (strong dark-brown soil, chernozem and brown forest soil) are a volcanic ash soil. Most dark-brown soil is distributed to the coast less than 200m under the sea level with 311.6km<sup>2</sup> square. The average available depth of soil in Jeju Island is 60cm and the area of 610.2km<sup>2</sup> where the available depth of soil is 50~75cm is more broadly distributed and it accounts for 33% of the total area of Jeju Island.

The bulk density of soil of Jeju Island is lower than other districts. Especially, the density of chernozem and brown forest soil is very low so it has a high porosity, low resistance to wind erosion, a high permeability and fast downward permeation. The chemical characteristic of the soil is that hydrogen ion concentrations are relatively higher than 5.0 based on the chemical characteristic of the volcanic ash soil of the basalt, andesite as the

basic material and the high precipitation of the Jeju area. A base saturation is very low, a natural fertility is low and an available phosphorus is very low. Therefore, pollutants are easy to eluviate because of good drainage of the soil. However, because of higher ability of absorption and fixation to the nitrogen than a phosphoric acid, it is easy to be polluted by nitrogen.

Table 3.2 The classification of soil types[SCS].

Soil types	Characteristics of Soil	Distribution areas	Permeability of geological structure
A	Permeability coefficient is very big, floating stuff with a gravel, drainage is very good, lowest runoff potential	Ara, Daehol, Gamsan, Gapa, Geumak, Gujwa, Haengwon, Hallim, heukak, Jeokak, Miak, Minak, Onpyeong, Sanbang, Sineom, Wollyeong, Haean	Sungol, Yongam cave
B	Permeability coefficient is generally big, sandy soil with a gravel, drainage is generally good	Byeongak, Gimnyeong, Gunsan, Hamo, hangyeong, Jocheon, Jungeom, Namwon, Noksan, Nongo, Noro, Pyoseon, Sara, Seokto, songdang, Wimi, Yongdang, rock area, lava flow	Gotjawal, scoria layer
C	Permeability coefficient is generally small, generally fine sand of soil type, drainage is generally bad	Aewol, Donggwi, Donghong, Gueom, Gyorae, Ido, Inseong, Jeju, Jisan, Jungmun, Mudeung, Nakcheon, Ora, Pyeongdae, Songak, Topyeong, Tosan, Yonggang, River flooding area, Sea overflowing area	
D	Permeability is very small, clay of soil type, nearly impermeability, highest runoff potential	Daejeong, Gangjeong, Haean, Hawon, Iho, Mureung, Udo, Wolpyeong, Yeongrak, Yongheung, Yongsu	

- Data source: 1. Classification of soil for runoff rate presumption (Journal of the Korean Society of Agriculture Engineers , VOL 37 No.6, P.12~33)
2. Jeju Island middle mountain area synthesis investigation report(1997, Jeju Island)
3. Jeju international free city special law operation regulation announcement 1

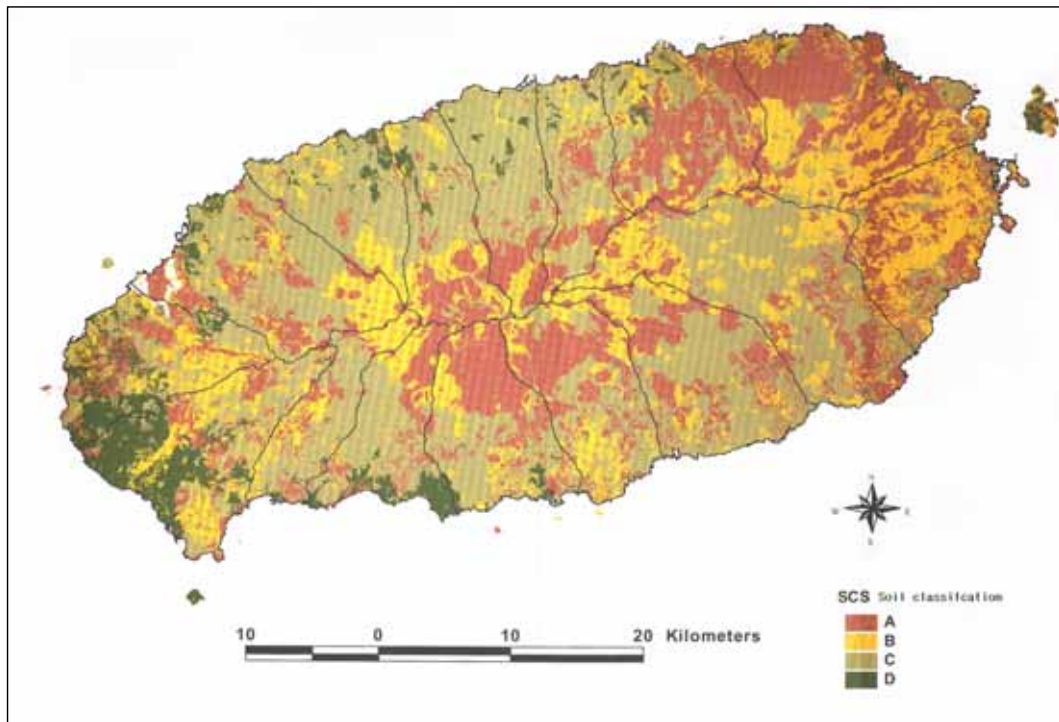


Fig. 3.7 The soil classification map of Jeju Island.

Fig. 3.7 shows a soil map of Jeju Island used in this study and Table 3.2 shows a characteristic and structure of the classified soil.

### 3.2.6 The forest characteristic in Jeju Island

#### 1) The forest distribution

There are 1,800 kinds of native plants in Jeju Island and the area of forest that forms a colony is about  $460.1\text{km}^2$ . About 47.6% ( $218.8\text{km}^2$ ) of them are distributed to the mountains area above an elevation of 600m and 17.3% ( $79.6\text{km}^2$ ) are distributed to the coast area under an elevation of 200m. When it comes to forest types, the broad-leaved forest accounts for  $274.2\text{km}^2$  (59.6%), the needle-leaved forest accounts for  $164.1\text{km}^2$  (36.7%) and the broad and needle mixed forest just accounts for  $21.8\text{km}^2$  (4.7%). By the districts, the

broad-leaved forest is distributed intensively to Seogwipo-si and the eastern district but the needle-leaved forest like a japanese black pine is distributed mostly to the western district of Bukjeju-gun as shown in Table 3.3 and Fig. 3.8.

Table 3.3 The forest distribution of elevations and areas(Unit:  $km^2$ , %).

Section		Sum	Broad-leaved forest	Needle-leaved forest	Broad and needle mixed forest	
Sum		460.1(100.0)	274.2(59.6)	164.1(36.7)	21.8(4.7)	
Elevation	under 200m	79.6(17.3)	31.2(39.1)	45.2(56.7)	3.2(4.2)	
	200~600m	161.7(35.1)	77.9(48.2)	74.9(46.3)	8.9(5.5)	
	above 600m	218.8(47.6)	165.1(75.5)	44.0(20.1)	9.7(4.4)	
Area	Jejusi	80.7(17.5)	52.5(65.0)	26.2(32.5)	2.0(2.5)	
	Seogwiposi	105.0(22.8)	60.1(57.2)	36.8(35.1)	8.1(7.7)	
	Bukjejugun		157.1(34.2)	91.8(58.4)	60.8(38.7)	4.5(2.9)
		eastern	69.8(15.2)	42.8(61.3)	25.5(36.5)	1.5(2.2)
		western	87.3(19.0)	49.0(56.1)	35.3(40.5)	3.0(3.4)
	Namjejugun		117.3(25.5)	69.8(59.5)	40.3(34.4)	7.1(6.1)
		eastern	86.0(18.6)	51.8(60.2)	28.8(33.5)	5.3(6.3)
		western	31.3(6.8)	18.0(57.5)	11.5(36.7)	1.8(5.8)

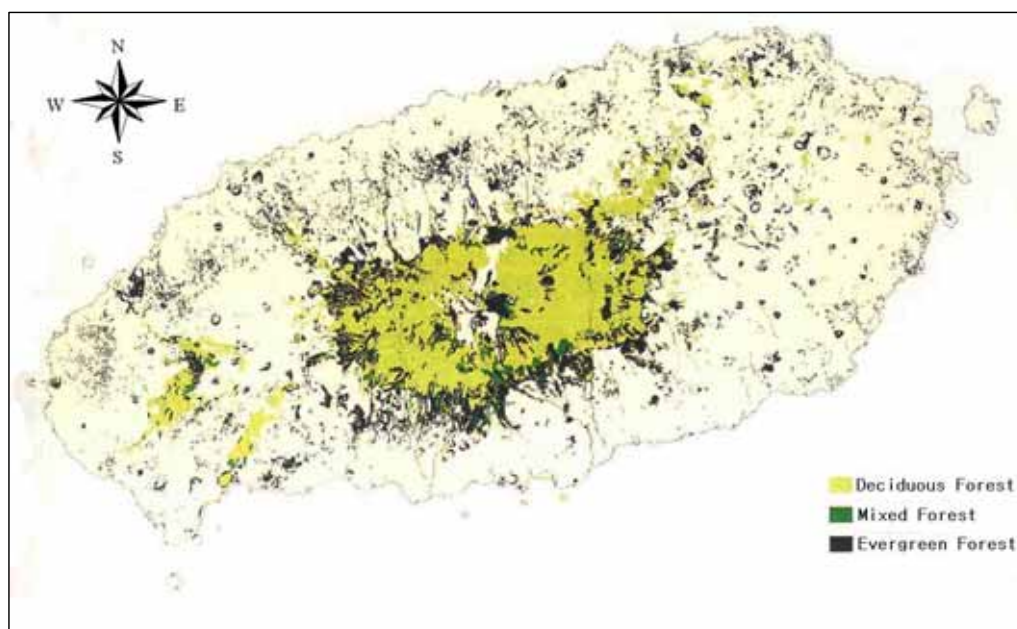


Fig. 3.8 The forest distribution map of Jeju Island.

About 24.9%(161.5 $km^2$ ) of the middle district are forest and prevalence is higher than that in all the areas of Jeju Island (24.9%). By species of trees in the middle district of the mountain, the broad-leaved forest accounts for 77.7  $km^2$  (48.2%), the needle-leaved forest accounts for 74.9 $km^2$  (46.3%) and the broad and needle mixed forest just accounts for 8.9 $km^2$  (5.5%) as shown in Table 3.4. The highest district of the forest density in the middle district of the mountain is between the hight of 400~500m and 55.3% of this area were constructed of a forest.

Table 3.4 The forest distribution in the middle area of the mountain  
(Unit:  $km^2$ , %).

Section	Sum	Broad-leaved forest	Needle-leaved forest	Broad and needle mixed forest
Middle area	161.7(100.0)	77.9(48.2)	74.9(46.3)	8.9(5.5)
200~300m	35.0(100.0)	13.2(37.7)	19.2(54.9)	2.6(7.4)
300~400m	36.7(100.0)	16.6(45.2)	18.6(50.7)	1.5(4.1)
400~500m	45.9(100.0)	24.5(53.4)	19.2(41.8)	2.2(4.8)
500~600m	44.1(100.0)	23.6(53.5)	17.9(40.6)	2.6(5.9)

## 2) The vegetation age distribution

The average age of the trees is 23 years old in the island and 10~20 years-old trees account for 35.1% of the total forest area and the trees more than 50 years old just accounts for 1.4%. A colony more than 40 years old is distributed intensively to the mountain area above an elevation of 600m and colony less than 20 years old is distributed intensively to a coast area. By the districts, more than 30% of the trees in Jeju-si and Seogwipo-si are 20~30 years old and more than 40% of the trees in Bukjeju-gun and Namjeju-gun are 10~20 years old.

The average age of the trees in the middle district of the mountain is 18

years old and the trees more than 50 years old do not exist. A colony between 40~50years old accounts for 2.3% and a colony between 30~40 years old just accounts for 8.0%. A colony between 10~20years old accounts for 53.1% of the total forest in middle district of the mountain and is distributed intensively between an elevation of 200~400m. The other side, a colony between 20~30years old is distributed intensively between an elevation of 400~600m.

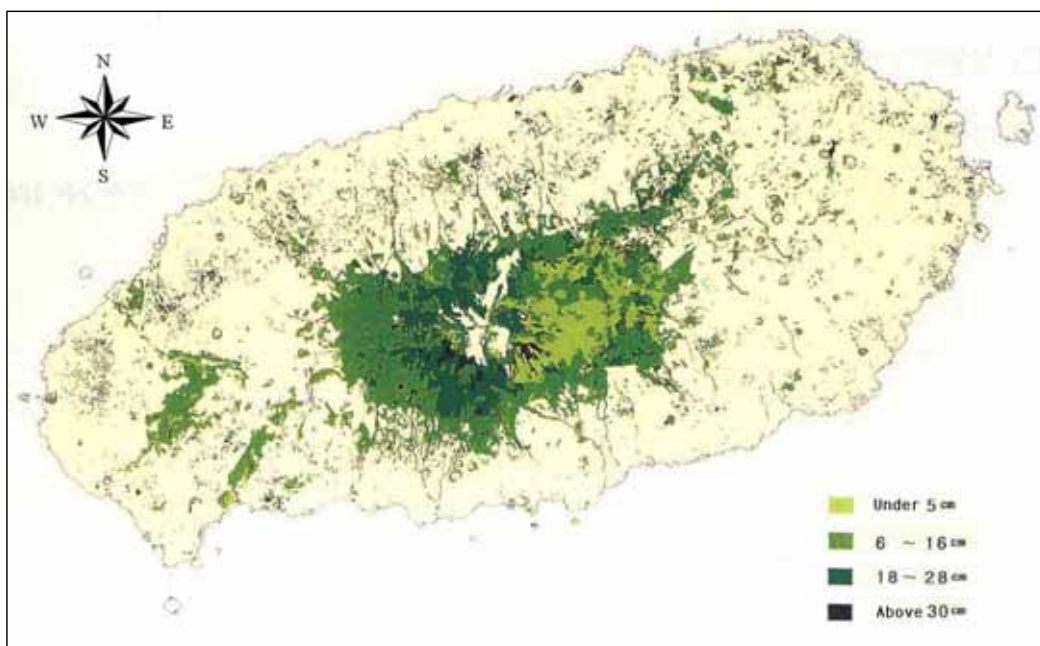


Fig. 3.9 The tree diameter characteristics of the Halla mountain in Jeju Island.

### 3) The vegetation diameter distribution

A diameter means a tree diameter in the hight of human's breast(about 1.2m) and the average diameter of the tree in Jeju Island is about 13cm. The trees that a diameter is less than 5cm account for 18.2% of the total forest, a diameter between 6~16cm accounts for 60.1% of the forest and the trees that a diameter is larger than 30cm just account for 1.2%. The small trees that a diameter is between 6~16cm are distributed to the middle area of the

mountain of an elevation of 200~600m and the trees that a diameter is between 17~29cm are distributed intensively to mountain areas above an elevation of 600m as shown in Fig. 3.9.

The average diameter of the trees is about 10cm in the middle area of the mountain. Large trees that diameter is larger than 30cm are rare and small trees that diameter is less than 5cm account for 15.3% of the total middle area of the mountain. The forest that a diameter is between 6~16cm accounts for 74.2% and the forest that a diameter is between 17~29cm accounts for 10.5% of the total middle area of the mountain. By an elevation, trees that a diameter is less than 5cm are distributed over 500~600m areas and trees that a diameter is between 6~16cm are distributed equally over the middle area of the mountain and trees that a diameter is between 17~29cm are mostly distributed over 400~600m areas.

### **3.2.7 The precipitation and rainfall intensity characteristics in Jeju Island**

According to the precipitation data from the last 10 years, the annual average amount of precipitation was 1,975mm in Jeju Island and the precipitation in the pluvial year and the least rainfall year was 2,945mm and 1,419mm, respectively. By the districts, the precipitation in the southern and western district was 2,339mm and 1,299mm, respectively and it showed a big difference. It was analyzed that the precipitation in the southeast district was larger than that in the northwest district by a geological influence of the Hallasan as shown in Table 3.5. On the other side, the area precipitation was evaluated according to an altitude under following three levels(below 200m, 200m~600m, and above 600m) based on the last 10-years'(1993~2002) precipitation data. The result showed that the annual average precipitation of the districts(54.3% of the total Jeju Island area) under an elevation of 200m

and 200~600mm was 1,651mm and 2,184mm, respectively. The annual average precipitation of the high districts(13.5% of the total Jeju Island area) in Hallasan that was above an elevation of 600m is 2,784mm(Table 3.6).

The distribution of the precipitation was shown in Fig 3.11. It was made by a grid format and was classified into some different levels by using an isohyet line extracted from an isohyet map as shown in Fig 3.10.

Table 3.5 The result of the precipitation analysis per area(Unit: mm).

Areas	Annual average precipitation		The pluvial year (1996)	The least rainfall year (1999)
	Data about recently ten years (1993~2002)	The whole period data (1923~2002)		
The whole Jeju	1,975	1,972	1,419	2,945
Northern area	2,027	2,046	1,215	3,047
Southern area	2,339	2,347	1,738	3,355
Eastern area	2,077	2,037	1,571	3,276
Western area	1,299	1,293	1,022	1,844

Table 3.6 The area amount of the precipitation by an elevation (annual average).

Section	Area( $km^2$ )	Area rate(%)	Area amount of precipitation(mm)	
			(1993)	recently
The whole Jeju	1,828.3	100.0	1,872	1,975
Under 200m	993.4	54.3	1,625	1,651
200~600m	589.0	32.2	1,989	2,184
Above 600m	245.9	13.5	2,578	2,784



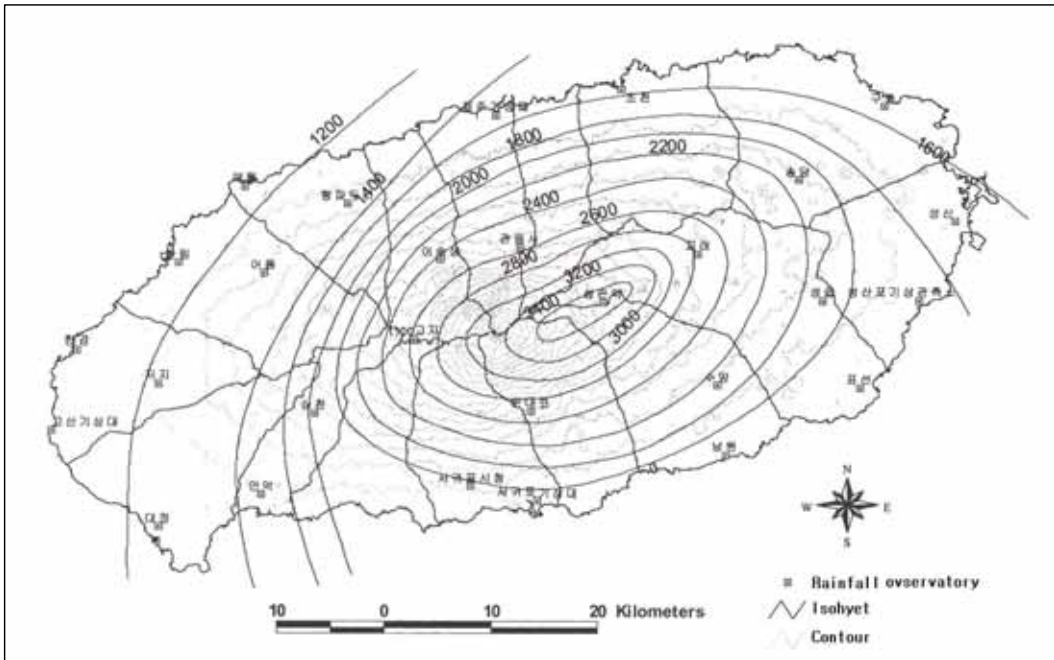


Fig. 3.10 The isohyet map of Jeju Island.

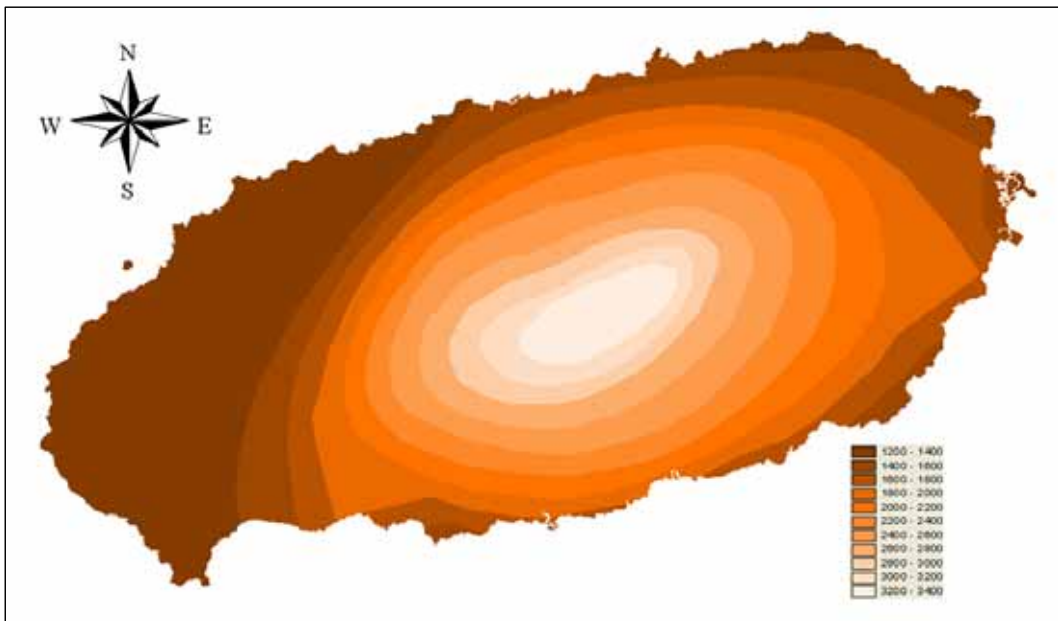


Fig. 3.11 The isohyet grid map of Jeju Island.

Rainfall intensity is a very important natural direct factor for an occurrence of a landslide. To calculate the rainfall intensity of each area in Jeju,

Probabilistic Rainfall - Intensity Formula for every 50 years was used as shown in Table 3.7. Using a rainfall intensity value we made a rainfall intensity map to all the areas in Jeju Island as shown in Fig. 3.12. After the comparison between precipitation and rainfall intensity, we found that the rainfall intensity had a more significant influence on an landslide occurrence so we used this rainfall intensity map to analyze a landslide susceptibility.

Table 3.7 The rainfall intensity of each area in Jeju Island.

Area	Probabilistic Rainfall - Intensity Formula
Jeju	$I = \frac{531.41}{t^{0.44315}} = 21.174$
Gosan	$I = \frac{1142.3}{(t+27.0)^{0.63093}} = 11.481$
Seongsan	$I = \frac{760.91}{(\sqrt{t}-1.9133)} = 21.116$
Seogwipo	$I = \frac{544.62}{(t)^{0.46403}} = 18.643$

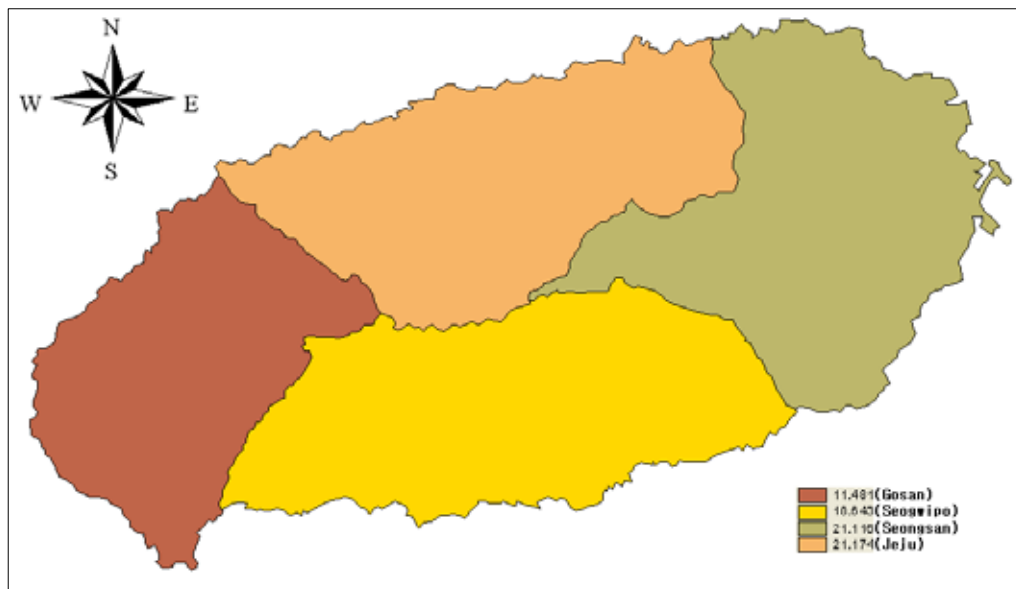


Fig. 3.12 The rainfall intensity map.

### 3.2.8 The land cover characteristic in Jeju Island

#### 1) The land cover classification

A land cover classification is one of the most representative and typical methods of a remote sensing and it can classify physical circumstances of the earth surface like a forest, grassland, and concrete pavement. The land cover classification generally applies a supervised classification by using the previous information. This procedure is divided into two steps such as an investigation step that appoints features of each classification item and an analysis step.

In the investigation step, a definite area by the classification item is created through a map or field survey in image. The data of the statistical characteristic by the classification item will be made out based on the data distribution of the area. A selected area will directly influence a subsequent result of the classification step so the selection will be performed carefully and it usually undergoes the rule of trial and error.

In the analysis step, all the pixels will be classified sequentially by a regular standard by using the data of the statistical characteristic mentioned above. On this occasion, minimum distance algorithm, parallelepiped algorithm, maximum likelihood algorithm and others will be applied according to a setting method of a classification criterion.

In this study, the whole area of Jeju Island was classified into 6 classes as shown in Fig. 3.13. So this classified image was applied to an analysis of a landslide in this study after the classification item of each class was decided and an estimation of an accuracy was performed through a field survey.

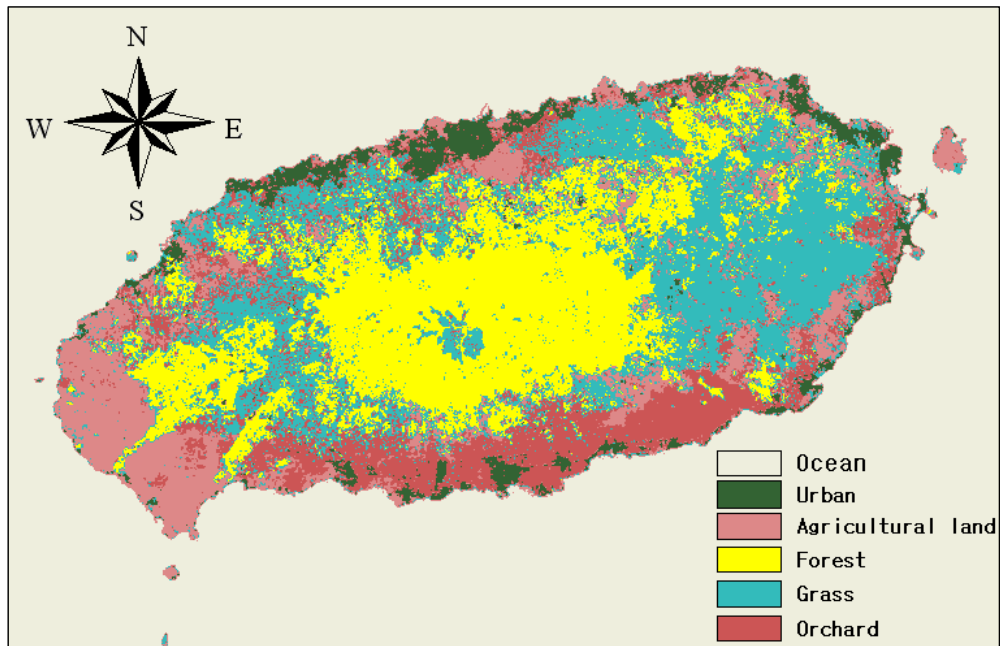


Fig. 3.13 The land cover classification map of Jeju Island.

## 2) The land cover classification standard

The U.S. Geological Survey classified land cover(use) into IV levels and they constructed the system by analyzing satellite images and area photographs. In Korea, the Environment Division(1999) presented a land cover classification device by using satellite images in a long view after collecting the opinions taken from the Ministry of Construction and Transportation, National Geographic Information Institute, the Office of Forestry and others.

The land cover classification system of the Environment Division included 7 levels that were urban, agricultural land, forest land, rangeland, wetland, barren land and water. The detailed contents were described as the following.

The urban area included residential, commercial and services, transportation, communications, utilities, artificially developed sites and facilities for a community. The agricultural land included cropland like a rice fields, farms, orchards and others. The forest included deciduous forest, evergreen forest and mixed forest was formed naturally or artificially. The rangeland included

a green tract of land, graveyards, hills where the density of the trees was not so large, facilities like golf and parks in the center of the cities. The wetland included a swamp or fore shore, salt fields and others. The barren land included a mining area like mine and quarry, sandy beach of the coast, sandy plain of riverside and undeveloped areas. The water area included rivers, lakes, oceans and others. The classification levels used in this study are divided as shown in Table 3.8.

Table 3.8 The classification levels.

Large classes	Detailed classes
Water	river / ocean
Residential	urban(commercial/industrial) / transportation
Forest land	deciduous / evergreen / mixed forest land
Rangeland	pasture / confined feeding operations
Orchards land	orchards(orange)
Agricultural land	rice field / farm

A pattern of the land cover throughout Jeju Island was showed in Fig. 3.13. The forest land is distributed broadly centering on Hallasan, the urban is distributed around Jeju-si and Seogwipo-si and through the coast line, the orchards are distributed mostly to the southern area like Seogwipo-si and Namjeju-gun, the agricultural land is distributed mostly to the western area and the range land is distributed mostly to the eastern area.

# CHAPTER 4. LANDSLIDE SUSCEPTIBILITY ANALYSIS

## **4.1 The landslide susceptibility analysis by using the AHP method**

### 4.1.1 Theoretical consideration of the AHP method

AHP was firstly introduced by the T. L. Saaty and it was the abbreviation of the words, "Analytic Hierarchy Process", and could be explained as a hierarchical analysis process. When solving a problem in decision with the AHP method, there are four steps(Johnson, 1980; Zahedi, 1986).

Step 1: Establish a decision making level.

Step 2: Collect initial data by the pair comparison of a decision making factor.

Step 3: Estimate a relative weight of the decision making factor using a eigen value method.

Step 4: Combine all the relative weights of the decision making factor.

If we analyze it in detail, the steps would be classified into 6 steps as shown in Fig. 4.1.

Step 1: The first step would be the most important step in AHP. In step 1, a decision maker should classify a problem in decision making into a level related to a decision making factor(Saaty, 1980). In the top of the hierarchy, the broad purpose, the general purpose of the decision maker, would be treated. The attributes that were useful for the quality of the decision making

were involved in lowering a lower rank hierarchy. The details of the attributes were added increasingly with lowering the hierarchy. The alternative to the decision making remained in the last hierarchy(Zahedi, 1986).

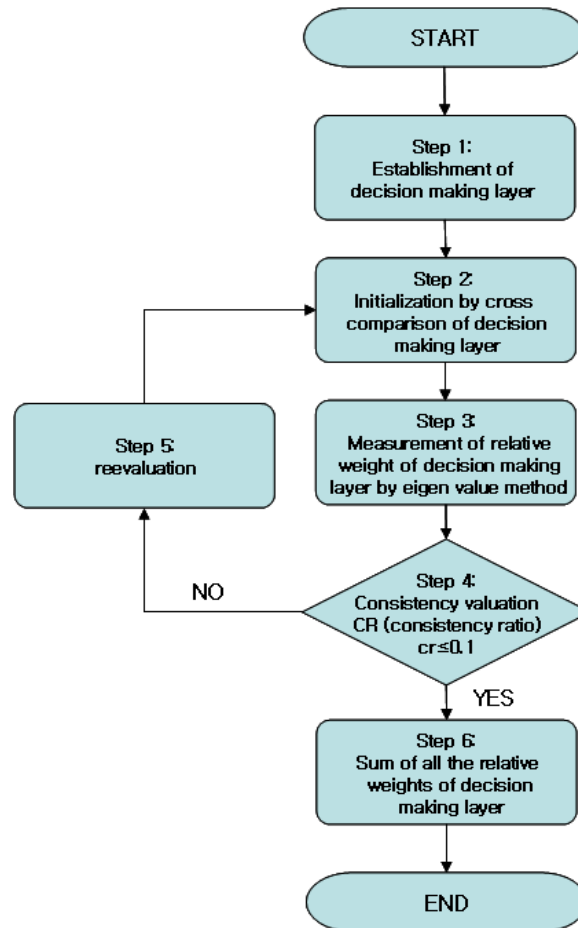


Fig. 4.1 The process of AHP.

Step 2: In the second step, initial matrix values of the factor comparison were obtained by the comparison with each factor. First, Saaty(1977) insisted that the amount of the factors of each level be restricted within at most 9 pieces because the pair comparison was needed in each level. In addition, Saaty explained a standard about an importance like Table 4.1.

Table 4.1 The importance measurement.

Degrees of importance	Definitions
1	equal importance
3	weak importance of one over another
5	essential or strong importance
7	demonstrated importance
9	absolute importance
2, 4, 6, 8 was individually estimated as middle degree of importance	

Second, the composition of the initial values of the matrix was as the following.

if  $A = (a_{ij})$ ,  $(i = 1, 2, \dots, n)$  then  $a_{ij}$  was confined to the following next regulation.

I) If  $a_{ij} = \alpha$  then  $a_{ji} = 1/\alpha$ ,  $\alpha \neq 0$

II) If the relative weights of the factor of i and j are the same then it becomes as  $a_{ij} = 1$ ,  $a_{ji} = 1$ . naturally,  $a_{ij} = 1$ .

Step 3: In this step, a relative weight of the decision making factor is estimated by an eigen value method. The relationship between relative weight of  $W_i$ ,  $W_j$  and  $a_{ij}$  is

$W_i/W_j = a_{ij}$  ( $i, j = 1, 2, 3 \dots \dots, n$ ). Accordingly, the matrix A can be written as follows:

$$A = \begin{pmatrix} W_1/W_1 & W_1/W_2 & \dots\dots & W_1/W_n \\ W_2/W_1 & & \dots\dots & W_2/W_n \\ \cdot & \cdot & \dots\dots & \cdot \\ \cdot & \cdot & \dots\dots & \cdot \\ W_n/W_1 & W_n/W_2 & \dots\dots & W_n/W_n \end{pmatrix}$$

but,

$$a_{11} = W_1/W_1, a_{12} = W_1/W_2, \dots a_{1j} = W_1/W_j \dots a_{1n} = W_1/W_n,$$



$$\text{so } \frac{W_1}{W_1} W_1 = W_1, \frac{W_1}{W_2} W_2 = W_1, \dots \frac{W_1}{W_n} W_n = W_1$$

$$\therefore W_i = a_{ij} W_j \quad (i, j = 1, 2, \dots n)$$

$$W_i = \frac{1}{n} \sum_{j=1}^n a_{ij} W_j \quad (i, j = 1, 2, \dots n).$$

$$\text{if } W = (W_i)^t \quad \text{then} \quad n W = A W.$$

let  $\bar{W}$  as estimate of  $W$ ,

$$\bar{A} \bar{W} = \lambda_{max} \bar{W}$$

but,  $\bar{A}$  is a real value of the matrix by the pair comparison.

$\lambda_{max}$  is the biggest eigenvalue of  $\bar{A}$ .  $\bar{W}$  is an eigenvalue of the right side.

Step 4: In this step, an estimation of consistency consideration was performed by the CR(consistency ratio). First, the CI(consistency index) was calculated by using the following equation.

$$CI = (\lambda_{max} - n) / (n - 1)$$

In the equation,  $CR$  was expressed as the following equation to understand the consistency of  $\bar{A}$  matrix.

$$CR = CI/RI$$

where  $RI$  was the random index. Zahedi said that if a standard of judgment is  $CR \leq 0.1$ , it has a consistency of consideration relatively(Zahedi, 1986).

Step 5: Reevaluate the initial values. If the value of CR is  $CR \geq 0.1$ , it has to pass through a reevaluation process.

Step 6: In step 4, if a value of  $CR$  is lower than 0.1, it is relatively considered to have a consistency of consideration. In this case, it is needed to sum all the relative weights of each hierarchy for the decision making and the process of this is accomplished in step 6.

#### 4.1.2 The application of AHP method

In this study, to calculate weight of each factor having an influence on a landslide, using AHP method, we suggested 8 proposals as shown in Fig. 4.2. These 8 proposals were classified according to an important relation between each factor in a landslide occurrence as 8 different cases as shown in Table 4.2. An important value of each factor such as a slope and aspect that had an influence on a landslide was defined according to Table 4.1 and then we calculated the weight value by the AHP method as shown in Table 4.3. An importance of each factor at each proposal was also defined according to Table 4.1 and the results that the weight was calculated by the AHP method were shown in the tables from Table 4.4 to Table 4.10 and all the weight values in each proposal were finally shown in Table 4.11 synthetically.

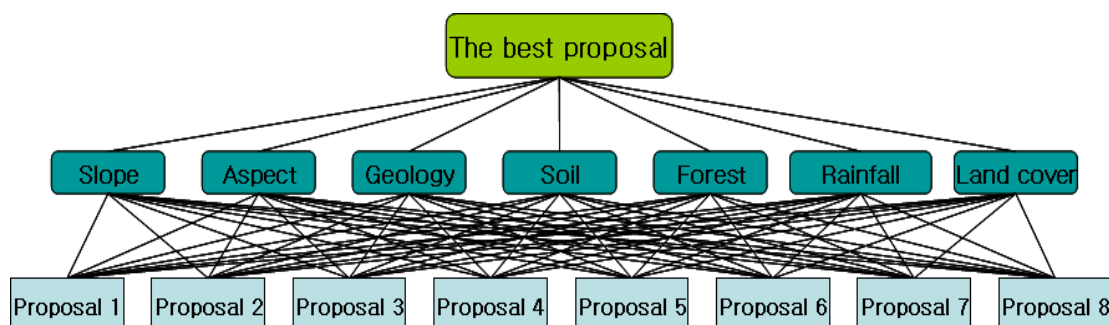


Fig. 4.2 The structure of AHP.

Table 4.2 Proposal conditions.

Proposal	Conditions
Proposal 1	Slope>Rainfall intensity>Soil>Forest>Geology>Landcover>Aspect
Proposal 2	Slope>Geology>Rainfall intensity>Soil>Landcover>Forest>Aspect
Proposal 3	Slope>Forest>Geology>Landcover>Rainfall intensity>Soil>Aspect
Proposal 4	Slope>Soil>Landcover>Forest>Rainfall intensity>Geology>Aspect
Proposal 5	Slope>Rainfall intensity>Landcover>Geology>Soil>Forest>Aspect
Proposal 6	Slope>Geology>Soil>Landcover>Forest>Rainfall intensity>Aspect
Proposal 7	Slope>Soil>Forest>Rainfall intensity>Landcover>Geology>Aspect
Proposal 8	Slope>Forest>Rainfall intensity>Geology>Soil>Landcover>Aspect

Table 4.3 The comparison of the importance between each factor.

Factors	Slope	Aspect	Geology	Soil	Rainfall intensity	Forest	Land cover
Slope	1	2	2	2	2	2	2
Aspect	1/2	1	1/2	1/2	1/2	1/2	1/2
Geology	1/2	2	1	1/2	1/2	1/2	1/2
Soil	1/2	2	2	1	1/2	2	2
Rainfall intensity	1/2	2	2	2	1	2	2
Forest	1/2	2	2	1/2	1/2	1	2
Land cover	1/2	2	2	1/2	1/2	1/2	1
<b>RIW</b>	<b>0.24</b>	<b>0.07</b>	<b>0.09</b>	<b>0.16</b>	<b>0.20</b>	<b>0.13</b>	<b>0.11</b>

To perform a consistency estimation of consideration according to the initial matrix values of factors by comparison with stage 4, some processes were proceeded as follows.

First, according to the above table, let's express the matrix A as follows:

$$A = \begin{pmatrix} 1 & 2 & 2 & 2 & 2 & 2 & 2 \\ 0.5 & 1 & 0.5 & 0.5 & 0.5 & 0.5 & 0.5 \\ 0.5 & 2 & 1 & 0.5 & 0.5 & 0.5 & 0.5 \\ 0.5 & 2 & 2 & 1 & 0.5 & 2 & 2 \\ 0.5 & 2 & 2 & 2 & 1 & 2 & 2 \\ 0.5 & 2 & 2 & 0.5 & 0.5 & 1 & 2 \\ 0.5 & 2 & 2 & 0.5 & 0.5 & 0.5 & 1 \end{pmatrix}$$

According to  $Ax = \lambda x$ ,  $(A - \lambda I)x = 0$ ,  $\det(A - \lambda I) = 0$ ,

The value of  $\lambda$  was calculated as follows:

$$\lambda = \begin{pmatrix} 7.3489 \\ 0.1274 + 1.4801i \\ 0.1274 - 1.4801i \\ -0.1296 + 0.5886i \\ -0.1296 - 0.5886i \\ -0.1722 + 0.1694i \\ -0.1722 - 0.1694i \end{pmatrix}$$

So  $\lambda_{max} = 7.3489$

$$CI = (\lambda_{max} - n)/(n - 1) = 0.05815$$

To calculate  $CR$ , the value of  $RI$  was generated randomly as follows:

$RI$	0.6813	0.3795	0.8318	0.6028	0.7095	0.4289	0.3046
------	--------	--------	--------	--------	--------	--------	--------

From the above table, we took the middle value as  $RI = 0.6028$

$$CR = CI/RI = 0.05815/0.6028 = 0.0965$$

Finally, it satisfied the condition of  $CR = 0.0965 \leq 0.1$  so that the initial values were not need to reset.

Table 4.4 The weight values of every proposal at slope.

Slope	P1	P2	P3	P4	P5	P6	P7	P8
P1	1	1	1	1	1	1	1	1
P2	1	1	1	1	1	1	1	1
P3	1	1	1	1	1	1	1	1
P4	1	1	1	1	1	1	1	1
P5	1	1	1	1	1	1	1	1
P6	1	1	1	1	1	1	1	1
P7	1	1	1	1	1	1	1	1
P8	1	1	1	1	1	1	1	1
<b>RIW</b>	<b>0.13</b>	<b>0.13</b>	<b>0.13</b>	<b>0.13</b>	<b>0.13</b>	<b>0.13</b>	<b>0.13</b>	<b>0.13</b>

To obtain the above matrix value, a consistency estimation of consideration was proceeded as follows:

$$\lambda_{max} = 0$$

$$CI = (\lambda_{max} - n) / (n - 1) = -1.143$$

$$CR = CI / RI = -1.143 / 0.5028 = -2.273$$

So it satisfied the condition of  $CR = -2.273 \leq 0.1$ .

Table 4.5 The weight values of every proposal at aspect.

Aspect	P1	P2	P3	P4	P5	P6	P7	P8
P1	1	1	1	1	1	1	1	1
P2	1	1	1	1	1	1	1	1
P3	1	1	1	1	1	1	1	1
P4	1	1	1	1	1	1	1	1
P5	1	1	1	1	1	1	1	1
P6	1	1	1	1	1	1	1	1
P7	1	1	1	1	1	1	1	1
P8	1	1	1	1	1	1	1	1
<b>RIW</b>	<b>0.13</b>	<b>0.13</b>	<b>0.13</b>	<b>0.13</b>	<b>0.13</b>	<b>0.13</b>	<b>0.13</b>	<b>0.13</b>

To obtain the above matrix value, a consistency estimation of consideration was proceeded as follows:

$$\lambda_{max} = 0$$

$$CI = (\lambda_{max} - n) / (n - 1) = -1.143$$

$$CR = CI / RI = -1.143 / 0.5028 = -2.273$$

So it satisfied the condition of  $CR = -2.273 \leq 0.1$ .

Table 4.6 The weight values of every proposal at geology.

Geology	P1	P2	P3	P4	P5	P6	P7	P8
P1	1	1/4	1/3	2	1/2	1/4	2	1/2
P2	4	1	2	5	3	1	5	3
P3	3	1/2	1	4	2	1/2	4	2
P4	1/2	1/5	1/4	1	1/3	1/5	1	1/3
P5	2	1/3	1/2	3	1	1/3	3	1
P6	4	1	2	5	3	1	5	3
P7	1/2	1/5	1/4	1	1/3	1/5	1	1/3
P8	2	1/3	1/2	3	1	1/3	3	1
<b>RIW</b>	<b>0.06</b>	<b>0.25</b>	<b>0.16</b>	<b>0.04</b>	<b>0.10</b>	<b>0.25</b>	<b>0.04</b>	<b>0.10</b>

To obtain the above matrix value, a consistency estimation of consideration was proceeded as follows:

$$\lambda_{max} = 8.1151$$

$$CI = (\lambda_{max} - n) / (n - 1) = 0.0164$$

$$CR = CI / RI = 0.0164 / 0.5028 = 0.0327$$

So it satisfied the condition of  $CR = 0.0327 \leq 0.1$ .

Table 4.7 The weight values of every proposal at soil.

Soil	P1	P2	P3	P4	P5	P6	P7	P8
P1	1	2	4	1/2	3	1	1/2	3
P2	1/2	1	3	1/3	2	1/2	1/3	2
P3	1/4	1/3	1	1/5	1/2	1/4	1/5	1/2
P4	2	3	5	1	4	2	1	4
P5	1/3	1/2	2	1/4	1	1/3	1/4	1
P6	1	2	4	1/2	3	1	1/2	3
P7	2	3	5	1	4	2	1	4
P8	1/3	1/2	2	1/4	1	1/3	1/4	1
<b>RIW</b>	<b>0.15</b>	<b>0.09</b>	<b>0.03</b>	<b>0.24</b>	<b>0.05</b>	<b>0.15</b>	<b>0.24</b>	<b>0.05</b>

To obtain the above matrix value, a consistency estimation of consideration was proceeded as follows:

$$\lambda_{max} = 8.0981$$

$$CI = (\lambda_{max} - n) / (n - 1) = 0.014$$

$$CR = CI / RI = 0.014 / 0.5028 = 0.0279$$

So it satisfied the condition of  $CR = 0.0279 \leq 0.1$ .

Table 4.8 The weight values of every proposal at rainfall intensity.

Rainfall intensity	P1	P2	P3	P4	P5	P6	P7	P8
P1	1	2	4	4	1	5	3	2
P2	1/2	1	3	3	1/2	4	2	1
P3	1/4	1/3	1	1	1/4	2	1/2	1/3
P4	1/4	1/3	1	1	1/4	3	1/2	1/3
P5	1	2	4	4	1	5	3	2
P6	1/5	1/4	1/2	1/3	1/5	1	1/3	1/4
P7	1/3	1/2	2	2	1/3	3	1	1/2
P8	1/2	1	3	3	1/2	4	2	1
<b>RIW</b>	<b>0.24</b>	<b>0.15</b>	<b>0.05</b>	<b>0.06</b>	<b>0.24</b>	<b>0.03</b>	<b>0.09</b>	<b>0.15</b>

To obtain the above matrix value, a consistency estimation of consideration was proceeded as follows:

$$\lambda_{max} = 8.0619$$

$$CI = (\lambda_{max} - n) / (n - 1) = 0.0202$$

$$CR = CI / RI = 0.0202 / 0.5028 = 0.0401$$

So it satisfied the condition of  $CR = 0.0401 \leq 0.1$ .

Table 4.9 The weight values of every proposal at forest.

Forest	P1	P2	P3	P4	P5	P6	P7	P8
P1	1	3	1/3	1	3	2	1/2	1/3
P2	1/3	1	1/5	1/3	1	1/2	1/4	1/5
P3	3	5	1	3	5	4	2	1
P4	1	3	1/3	1	3	2	1/2	1/3
P5	1/3	1	1/5	1/3	1	1/2	1/4	1/5
P6	1/2	2	1/4	1/2	2	1	1/3	1/4
P7	2	4	1/2	2	4	3	1	1/2
P8	3	5	1	3	5	4	2	1
<b>RIW</b>	<b>0.10</b>	<b>0.04</b>	<b>0.25</b>	<b>0.10</b>	<b>0.04</b>	<b>0.06</b>	<b>0.16</b>	<b>0.25</b>

To obtain the above matrix value, a consistency estimation of consideration was proceeded as follows:

$$\lambda_{max} = 8.1151$$

$$CI = (\lambda_{max} - n) / (n - 1) = 0.0164$$

$$CR = CI / RI = 0.0164 / 0.5028 = 0.0327$$

So it satisfied the condition of  $CR = 0.0327 \leq 0.1$ .



Table 4.10 The weight values of every proposal at land cover.

Land cover	P1	P2	P3	P4	P5	P6	P7	P8
P1	1	1/2	1/3	1/4	1/4	1/3	1/2	1
P2	2	1	1/2	1/3	1/3	1/2	1	2
P3	3	2	1	1/2	1/2	1	2	3
P4	1/4	1/3	1/2	1	1	2	3	4
P5	1/4	1/3	1/2	1	1	2	3	4
P6	3	2	1	1/2	1/2	1	2	3
P7	2	1	1/2	1/3	1/3	1/2	1	2
P8	1	1/2	1/3	1/4	1/4	1/3	1/2	1
<b>RIW</b>	<b>0.05</b>	<b>0.08</b>	<b>0.14</b>	<b>0.23</b>	<b>0.23</b>	<b>0.14</b>	<b>0.08</b>	<b>0.05</b>

To obtain the above matrix value, a consistency estimation of consideration was proceeded as follows:

$$\lambda_{max} = 7.3563$$

$$CI = (\lambda_{max} - n) / (n - 1) = -0.092$$

$$CR = CI / RI = -0.092 / 0.5028 = -0.1829$$

So it satisfied the condition of  $CR = -0.1829 \leq 0.1$ .

The values of RIW from Table 4.4 to Table 4.10 were shown in Table 4.11 synthetically.

Table 4.11 The weight values of every proposal at each factor.

<RIW>	P1	P2	P3	P4	P5	P6	P7	P8
Slope	0.13	0.13	0.13	0.13	0.13	0.13	0.13	0.13
Aspect	0.13	0.13	0.13	0.13	0.13	0.13	0.13	0.13
Geology	0.06	0.25	0.16	0.04	0.10	0.25	0.04	0.10
Soil	0.15	0.09	0.03	0.24	0.05	0.15	0.24	0.05
Rainfall intensity	0.24	0.15	0.05	0.06	0.24	0.03	0.09	0.15
Forest	0.10	0.04	0.25	0.10	0.04	0.06	0.16	0.25
Landcover	0.05	0.08	0.14	0.23	0.23	0.14	0.08	0.05

To select the best proposal, the values of RIW calculated in Table 4.3 and the weights by each proposal suggested in Table 4.11 were converted to the matrix format as follows and the best proposal was selected by a maximum value after these two matrixes were multiplied. All the procedures are as follows:

From Table 4.3, the values are converted to matrix as follows:

$$A = ( 0.24 \ 0.07 \ 0.09 \ 0.16 \ 0.20 \ 0.13 \ 0.11 )$$

and from Table 4.11, the weight values at a different proposal are converted to the matrix as follows:

$$B = \begin{pmatrix} 0.13 & 0.13 & 0.13 & 0.13 & 0.13 & 0.13 & 0.13 & 0.13 \\ 0.13 & 0.13 & 0.13 & 0.13 & 0.13 & 0.13 & 0.13 & 0.13 \\ 0.06 & 0.25 & 0.16 & 0.04 & 0.10 & 0.25 & 0.04 & 0.10 \\ 0.15 & 0.09 & 0.03 & 0.24 & 0.05 & 0.15 & 0.24 & 0.05 \\ 0.24 & 0.15 & 0.05 & 0.06 & 0.24 & 0.03 & 0.09 & 0.15 \\ 0.10 & 0.04 & 0.25 & 0.10 & 0.04 & 0.06 & 0.16 & 0.25 \\ 0.05 & 0.08 & 0.14 & 0.23 & 0.23 & 0.14 & 0.08 & 0.05 \end{pmatrix}$$

Therefore, a proposal that contains a maximum value is the best to analyze a landslide susceptibility when calculating a form of  $A * B$ . The result is as follows:

$$A * B = ( 0.1362 \ 0.1212 \ 0.1174 \ 0.1326 \ 0.1358 \ 0.1160 \ 0.1299 \ 0.1253 )$$

and the proposal is ordered according to the above value and it is written as follows:

**P1(0.1362)>P5(0.1358)>P4(0.1326)>P7(0.1299)>P8(0.1253)>P2(0.1212)>P3(0.1174)>P6(0.1160)**

In this study, we selected proposal 1 to analyze a landslide susceptibility. To do this, the rating was calculated after calculating the weights of each factor. The weight was relatively important in factors such as slope, curvature, and soil texture. The rating was relatively important in classes of each factor. For example, if slope was more important than soil texture in a landslide occurrence, a relatively important value was the weight; if a 30° slope was more hazardous than a 5° slope, a relatively important value was

the rating. Because there were no fixed or standard values of weight and rating for a landslide related to the factors, a determination of a weight and rating value was very important in a landslide-susceptibility analysis and the weight and rating should be determined based on an objective analysis, not on subjective experts opinions(Lee S. L. et al., 2004).

To objectively determine a rating value, we used the following statistic data extracted from the Gyeonggi-do Yongin area as shown in Table 4.12 to 4.16.

In a slope map, a rating value was calculated based on Table 4.12 and the AHP method after it was classified into four levels such as  $0^{\circ} \sim 10^{\circ}$ ,  $10^{\circ} \sim 25^{\circ}$ ,  $25^{\circ} \sim 40^{\circ}$ ,  $40^{\circ} \sim 90^{\circ}$  and the result was shown in Table 4.17. The rating of the other factors, which had an influence on a landslide susceptibility, was also calculated by the same way used in the slope map and the result was shown in Table 4.18 to Table 4.23. Here, the classification of the geology was just based on its intensity and drainage characteristics and the classification of the rainfall intensity was based on the data of Table 3.7.

Table 4.12 The relation between landslide and slope.

Range	Landslide occurred(%)
$0^{\circ} \sim 10^{\circ}$	6
$10^{\circ} \sim 25^{\circ}$	50
$25^{\circ} \sim 40^{\circ}$	40
$40^{\circ} \sim 90^{\circ}$	4
Total	100

Table 4.13 The relation between landslide and aspect.

Range	Landslide occurred(%)
S, SE, SW	32
N, NE, E	38
W, NW, F	30
Total	100

Table 4.14 The relation between landslide and soil.

Range	Landslide occurred(%)
Poorly drained	0
Somewhat poorly drained	2
Well drained	46
Excessively well drained	52
<b>Total</b>	<b>100</b>

Table 4.15 The relation between landslide and forest.

Range	Landslide occurred(%)
Non-forest	5
Very small diameter	27
Small diameter	68
Medium diameter	0
<b>Total</b>	<b>100</b>

Table 4.16 The relation between landslide and land cover.

Range	Landslide occurred(%)
Grass	2
Forest	93
Urban	1
Barrren	1
Rice field	3
<b>Total</b>	<b>100</b>

Table 4.17 The rating values of slope.

Slope	0° ~10°	10° ~25°	25° ~40°	40° ~90°
0° ~10°	1	1/3	1/4	1/2
10° ~25°	3	1	1/2	2
25° ~40°	4	2	1	3
40° ~90°	2	1/2	1/3	1
<b>RIW</b>	<b>0.09</b>	<b>0.28</b>	<b>0.47</b>	<b>0.16</b>

Table 4.18 The rating values of aspect.

Aspect	S, SE, SW	N, NE, E	W, NW
S, SE, SW	1	2	3
N, NE, E	1/2	1	2
W, NW	1/3	1/2	1
<b>RIW</b>	<b>0.54</b>	<b>0.30</b>	<b>0.16</b>

Table 4.19 The rating values of geology.

Geology	Sand dune layer	Sedimentary layer	Trachyte	Basalt
Sand dune layer	1	2	3	4
Sedimentary layer	1/2	1	2	3
Trachyte	1/3	1/2	1	2
Basalt	1/4	1/3	1/2	1
<b>RIW</b>	<b>0.47</b>	<b>0.28</b>	<b>0.16</b>	<b>0.09</b>

Table 4.20 The rating values of soil.

Soil	A	B	C	D
A	1	2	3	4
B	1/2	1	2	3
C	1/3	1/2	1	2
D	1/4	1/3	1/2	1
<b>RIW</b>	<b>0.47</b>	<b>0.28</b>	<b>0.16</b>	<b>0.09</b>

Table 4.21 The rating values of rainfall intensity.

Rainfall intensity	Gosan	Seongsan	Seogwipo	Jeju
Gosan	1	1/3	1/2	1/3
Seongsan	3	1	2	1
Seogwipo	2	1/2	1	1/2
Jeju	3	1	2	1
<b>RIW</b>	<b>0.11</b>	<b>0.35</b>	<b>0.19</b>	<b>0.35</b>

Table 4.22 The rating values of forest(cm).

Forest (diameter)	d< 5	d=6~16	d=18~28	d>30
d< 5	1	2	3	4
d=6~16	1/2	1	2	3
d=18~28	1/3	1/2	1	2
d>30	1/4	1/3	1/2	1
<b>RIW</b>	<b>0.47</b>	<b>0.28</b>	<b>0.16</b>	<b>0.09</b>

Table 4.23 The rating values of land cover.

Land cover	Residential	Range land	Forest land	Agricultural land	Orchards land
Residential	1	1/4	1/5	1/3	1/2
Rangeland	4	1	1/2	2	3
Forest land	5	2	1	3	4
Agricultural land	3	1/2	1/3	1	2
Orchards land	2	1/3	1/4	1/2	1
<b>RIW</b>	<b>0.06</b>	<b>0.26</b>	<b>0.42</b>	<b>0.16</b>	<b>0.10</b>

According to proposal 1, we calculated the weight values by using the AHP method as shown in Table 4.24 and all the weight and rating values were shown in Table 4.25.

Table 4.24 The calculation of *RIW* between each factor.

Factors	Slope	Aspect	Geology	Soil	Rainfall intensity	Forest	Land cover
Slope	1	7	5	3	2	4	6
Aspect	1/7	1	1/3	1/5	1/6	1/4	1/2
Geology	1/5	3	1	1/3	1/4	1/2	2
Soil	1/3	5	3	1	1/2	2	4
Rainfall intensity	1/2	6	4	2	1	3	5
Forest	1/4	4	2	1/2	1/3	1	3
Land cover	1/6	2	1/2	1/4	1/5	1/3	1
<b>RIW</b>	<b>0.35</b>	<b>0.03</b>	<b>0.07</b>	<b>0.16</b>	<b>0.24</b>	<b>0.10</b>	<b>0.05</b>

Table 4.25 The weight values of each factor in proposal 1.

	Factor (weight value)	Classification	Rating value
Proposal 1	Slope (35%)	0° ~10°	9%
		10° ~25°	28%
		25° ~40°	47%
		40° ~90°	16%
	Aspect (3%)	S, SE, SW	54%
		N, NE, E	30%
		W, NW	16%
	Geology (7%)	Basalt	9%
		Trachyte	16%
		Sedimentary layer	28%
		Sand dune layer	47%
	Soil (16%)	A	47%
		B	28%
		C	16%
		D	9%
	Rainfall intensity (24%)	Gosan	11%
		Seongsan	35%
		Seogwipo	19%
		Jeju	35%
	Forest (10%)	d<5	47%
		d=6~16	28%
		d=18~28	16%
		d>30	9%
Land cover (5%)	Residential	6%	
	Forest land	42%	
	Rangeland	26%	
	Agricultural land	16%	
	Orchards land	10%	

#### **4.1.3 The landslide susceptibility analysis using the GIS overlay method and weights**

Geo-spatial information that constitutes GIS (geographical information system) was discriminated from position and attribute information. Position information provides positive or relative positions of an object for a spatial analysis. Descriptive information is composed of graphic information, image information and attribute information. Graphic information is the data that described as a figure or map. Image information is the data that described as a general photograph, aerial photograph, satellite image, video and various images. Attribute information is the data that expresses characteristics of the nature, culture, society, administration, economy and environment, and it must be connected with a figure or image information as well as make it possible of the geo-spatial analysis (Yu, B. M., 1998).

The utilization of geographical information system covers various fields like land, resources, urban, environments, transportation, agriculture, oceans and the military. In an application for the geographical information system, Land Information System, Geographic Information System, Urban Information System, Automated Mapping and Facility Management and others compose a main part.

The geographical information system inputs and saves various information related to land, resource and environments according to its location and characteristic and it is synthetically treated with stages so that it is developing matching a purpose of utilization, analysis, and output.

Position and descriptive information is saved in data-base in a digital format suited to a computer according to prescribed scales, projections, and coordinates. The data-base is conceptually composed of a layer or plane so that different main information is recorded in each layer. In this way, many layers recorded digitally according to a main subject composed data bank of



the given problems and if individual data bank accomplishes the unification of the coordinates according to a given base map, it is called an overlay or composite analysis.

The data analysis is a main function of GIS and an analysis method has a spatial analysis and statistical analysis. The spatial analysis uses a spacial composition of information expressed in one or more data layer. The statistical analysis like many tools mentioned in GIS is a statistical process needed for a qualitative guarantee during a preparation process, a summary of the data collections like a data report or a new data addition during an analysis in a general information flow of GIS. Generally, GIS composes a new map by overlapping a map through arithmetical operations and it is also possible to trace a network connection, measure direction or distance and analyze them statistically.

A change in the attribute value that appears to be a result by an overlap occurs from an influence of one point or polygon, or an attribute value of the circumference area in the same position at many layers used in an overlay. In other words, new attribute value generated by an overlay is converted and generated by a function so that attribute values corresponded to many layers used in the overlay are able to defined as a function, which can be written as follows:

$$U=f(A, B, C, \dots) \quad 4.1.1$$

$U$ : Attribute value generated by an overlay

$f$ : Conversion function applied to an overlay

$A, B, C..$  : Attribute value of layers used in  
an overlay

At this time, an applicable function is possible to apply from a simple operation like addition or subtraction to a more complicated operation or numerical formula through a pattern.

The process of an overlay was accomplished by an object of the respective

grids of the unit structure in the grid structure but it was generally applied to an object of a point, line and plane with a foundation of a point of basic structure in the vector structure.

In a function and process of an overlay, a mathematical overlay based on a logic is possible except an overlay for the information composition of a simple layer through a possible transformation function. The mathematical overlay provides a modeling function for the extraction of information useful for actualities or a decision making. The mathematical overlay is to get a new numerical value by an allowance of a regular calculation targeted at the value of the same area of the other layers for the numerical value existing in a layer(Kim, G. H., 2000).

In this study, we first progressed a geometric correction through a treatment process as shown in Fig. 4.3 to a thematic map of the factors which had an influence on a landslide and the attribute values( $A, B, C...$ ) of the layer used in overlay, and set up a slope map, aspect map, rainfall intensity map, geology map, soil map, forest map, and land use map. In the process of a calculation, a weighted overlay operation was used for a transformation function( $f$ ) applied to an overlay and layers were piled up one another after a generated model considered all the weights of the factors which had an influence on a landslide susceptibility like Fig. 4.4. An attribute value( $U$ ) generated by an overlay was made out of a landslide susceptibility map of the study area and a susceptibility area of a landslide was expressed by a red and yellow color in Fig. 4.5 and it was known as that the susceptibility areas of Jeju Island were mostly distributed to the commit areas of the Halla mountain.

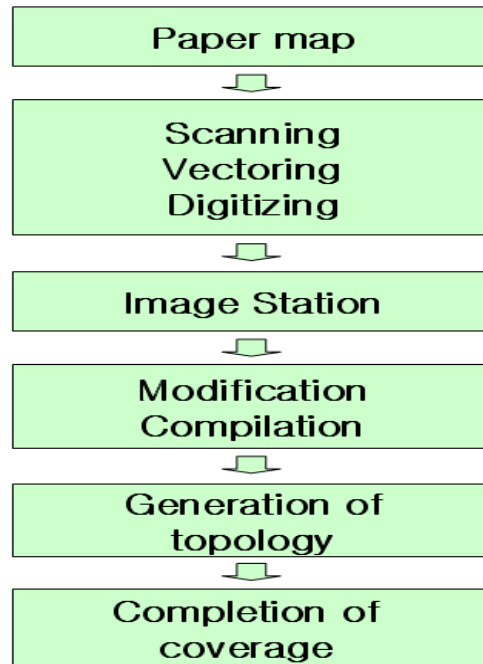


Fig. 4.3 The work flow of the converting map.

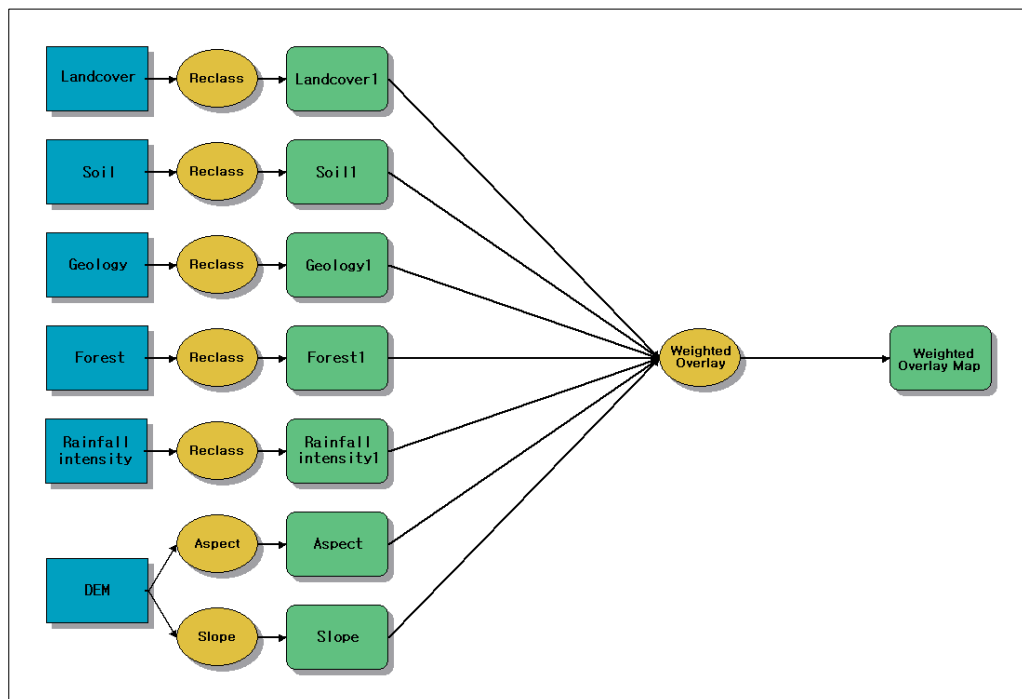


Fig. 4.4 The weighted overlay model.

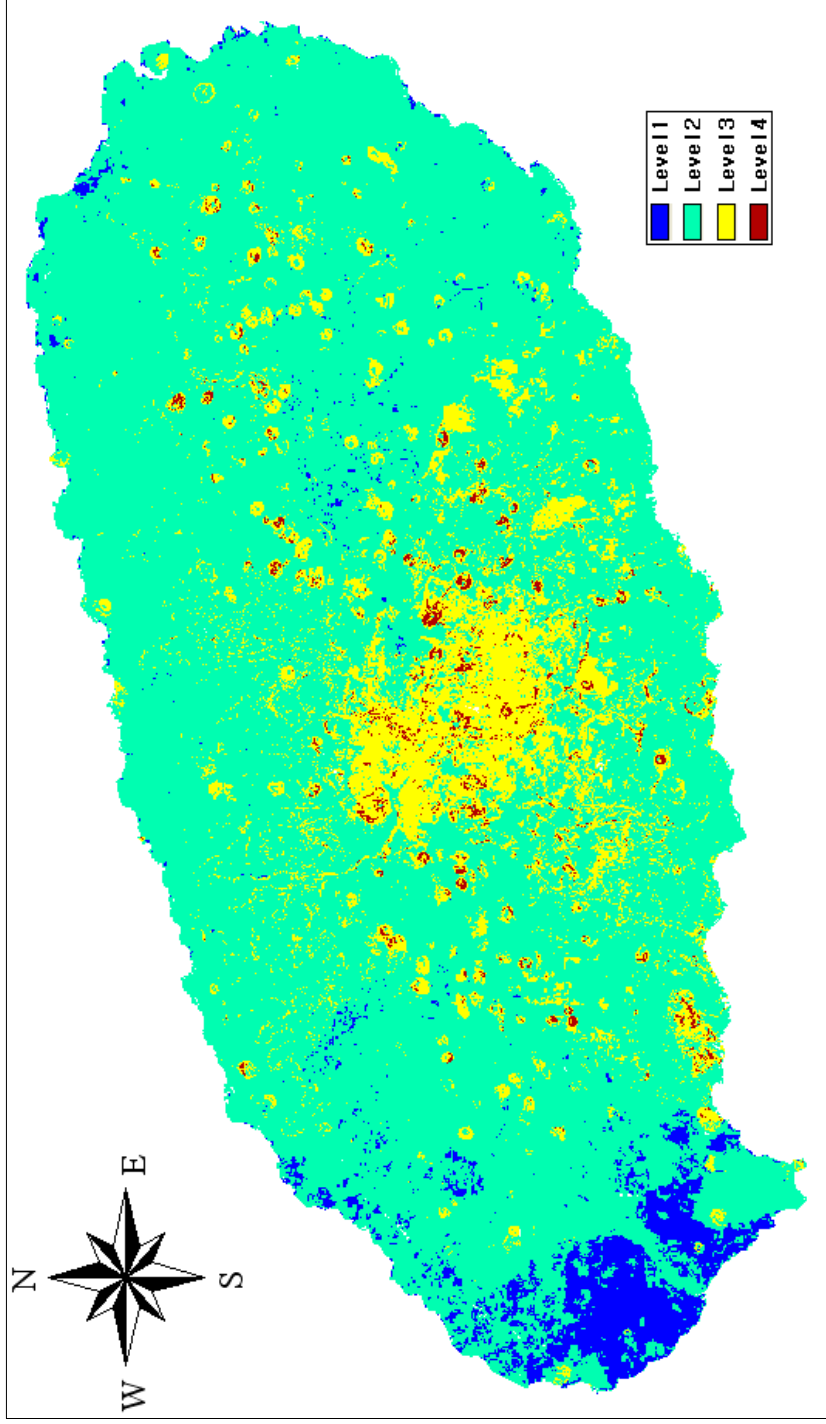


Fig. 4.5 The landslide susceptibility map generated by using the AHP method and GIS.

## **4.2 The landslide susceptibility analysis using the logistic regression analysis method**

### **4.2.1 The conception of the logistic regression analysis**

Logistic regression analysis is one of the statistic methods that estimates causalities between a dependent variable and independent variable just having two values. In other words, it is possible to directly estimate a possibility of occurring events. Regression analysis is one of the analysis methods that estimates or explains one independent variable from many dependent variables after measuring many dependent variables and one independent variable, and estimates the relations between these variables.

In the regression analysis, a linear regression model can be used if it has a linear relation between an independent and dependent variable and a multiple regression model can be used if it has a nonlinear relation between an independent and dependent variable. Regression analysis is applied when a dependent variable is a quantitative variable but it can also be applied for using a dummy variable when a dependent variable is a qualitative variable. Furthermore, regression analysis is applied when an independent variable is a continuous variable but it can also be applied when an independent variable is a classification variable. In this case, it is operated by using a logistic model.

Logistic regression analysis and discriminant analysis are very similar to a form of an independent variable. It is the case that one individual belongs to one group between two or more groups and it is also one of the methods to analyze data when an independent variable is measured by a nominal scale. Generally, a discriminant analysis is used when a dependent variable beyond an interval scale and variables have a multivariate normal distribution.

Logistic analysis is used when a qualitative scale like a nominal scale and ordinal scale is mixed with an interval scale and the assumption that variables have a multivariate normal distribution is not so clear.

Logistic regression analysis is similar to regression analysis by seeing from an analysis form because it can be expressed to a general linear regression formula if an independent variable is changed into a log function. The model assumed in logistic is shown in following equation:

$$P_z = 1/(1 + e^{-z}) = e^z/(1 + e^z)$$

$$Z = \alpha + \beta_1 X_1 + \beta_2 X_2 + \dots + \beta_p X_p$$

and it is changed into

$$\ln(P_z/(1 - P_z)) = \alpha + \beta_1 X_1 + \beta_2 X_2 + \dots + \beta_p X_p$$

so a probability that an event occurs can be written as follows:

$$P_z(\text{didn't happen}) = 1 - P_z(\text{happen})$$

The logistic regression model is not linear and it is constructed from a nonlinear curve. In other words, the relation between a dependent variable and probability of an occurrence was nonlinear. The probability assumption always existed between 0 and 1 regardless of the value of Z. In the linear regression model, a population parameter of the model was estimated by least-squares method but it was estimated by a maximum-likelihood method in the logistic regression model.

#### 4.2.2 The application of the LRA method to the landslide susceptibility analysis

LRA(logistic regression analysis) was applied to use independent variables to create a mathematical formula to predict a probability that an event occurs on any given parcel of land. The key of the logistic regression is that dependent variables are dichotomous and independent variables in the model are predictors of the dependent variables and can be measured by a nominal, ordinal, interval or ratio scale. The relationship between dependent variables and independent variables is nonlinear(E. Yesilnacar et al., 2005).

In this study, a landslide occurrence belonged to an independent variable and it would be assigned to "0" if no landslide was present or "1" if a landslide was present. Dependent variables contained slope, aspect, soil, geology, forest, rainfall intensity and land cover. The sample data was obtained from the study area and the relation between dependent and independent variables could be written as the following equation:

$$\begin{aligned} \ln(P_z/(1 - P_z)) = & (- 10.158) + 0.783 * X_1(\text{slope}) + 0.364 * X_2(\text{aspect}) \\ & + 0.523 * X_3(\text{geology}) + 0.668 * X_4(\text{soil}) \\ & + 0.726 * X_5(\text{rainfall intensity}) \\ & + 0.400 * X_6(\text{forest}) + 0.575 * X_7(\text{landcover}) \end{aligned}$$

Finally, a landslide susceptibility map was generated by using the equation as shown in Fig. 4.6.

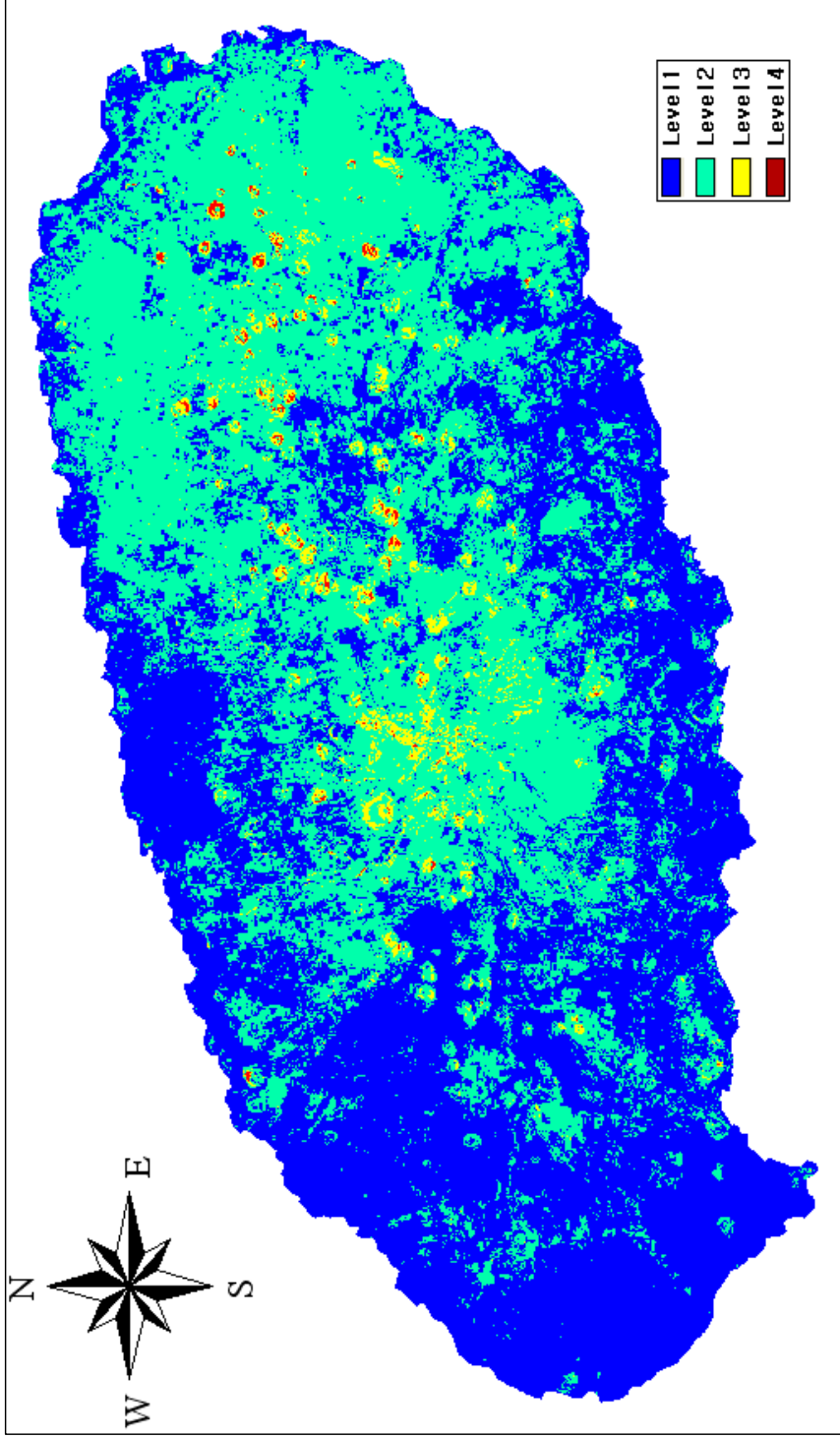


Fig. 4.6 The landslide susceptibility map generated by the logistic regression analysis method.



## **4.3 The landslide susceptibility analysis using the artificial neural network**

### **4.3.1 The conception of the artificial neural network**

A neuron is a cell in the brain whose principal function is the collection, processing, and dissemination of electrical signals (Russell and Norvig, 2003). Neural networks simulate the thinking process of human beings, whose brains use interconnected neurons to process incoming information (Jensen et al., 1999; Hengl, 2002). A neural network reaches a solution not via a step-by-step algorithm or a complex logical program, but in a nonalgorithmic, unstructured fashion based on the adjustment of the weights connecting the neurons in the network (Rao and Rao, 1993). Neural networks have been used to classify various types of remote sensor data and have in certain instances produced results superior to those of traditional statistical methods (E.g., Benediktsson et al., 1990; Jensen et al., 1999; Ji, 2000). This success can be attributed to two of the important advantages of neural networks: 1) freedom from normal distribution requirements and 2) the ability to adaptively simulate complex and nonlinear patterns given proper topological structures (Atkinson and Tatnall, 1997; Jensen et al., 1999)

The topological structure of a typical back-propagation neural network is shown in Fig. 4.7 (Civco, 1993; Benediktsson and Sveinsson, 1997). The artificial neural network normally contains neurons arranged in three types of layers: an input layer, a hidden layer(s) and an output layer.

The neurons in the input layer might be the multispectral reflectance values for individual pixels plus their texture, surface roughness, terrain elevation, slope, aspect, etc. The use of neurons in the hidden layer(s) enables the

simulation of nonlinear patterns in the input data. A neuron in the output layer might represent a single thematic map land-cover class, e.g., agriculture.

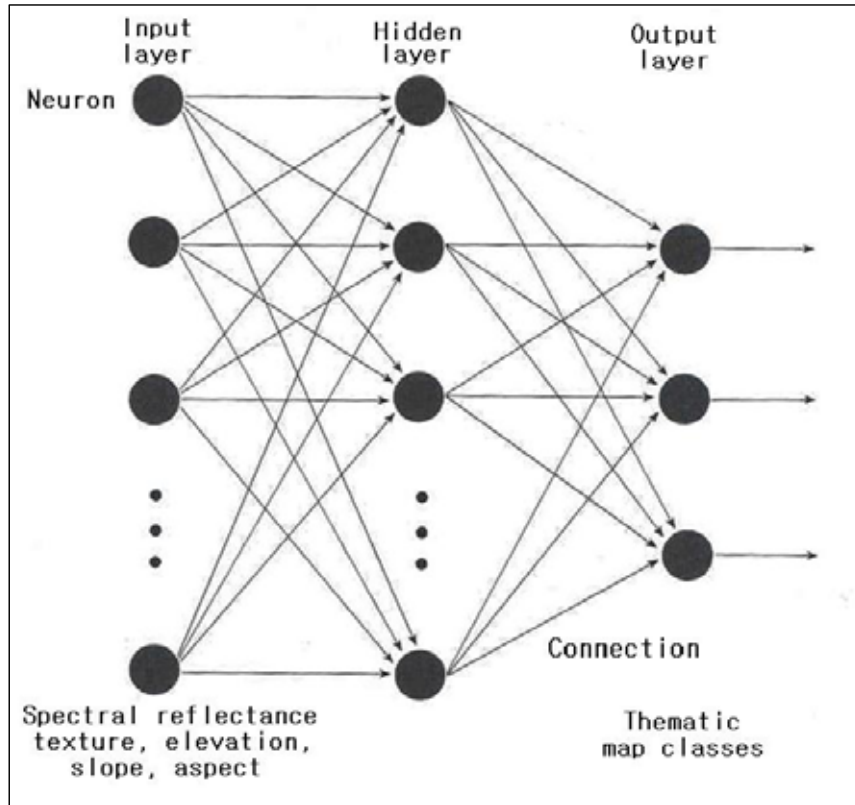


Fig. 4.7 Components of a typical artificial neural network.

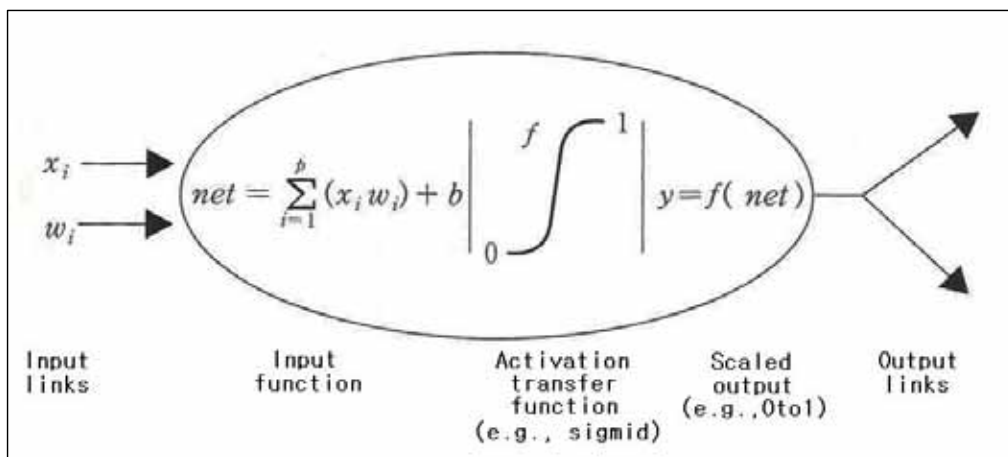


Fig. 4.8 Mathematical model of a neuron.

### 4.3.2 Mathematics of the artificial neural network

An artificial neural network(ANN) is defined by neurons, topological structure, and learning rules. The neuron is the fundamental processing unit of an ANN for computation(Jensen et al., 1999). Analogous to the human brain's biological neuron, an artificial neuron is composed of inputs(dendrites), weights(synapses), processing units(cell bodies), and outputs(axons)(Hagan, et al., 1996). Each input  $x_i$  is multiplied by the scalar weight  $w_i$  to form  $x_i w_i$ , a term that is sent to the "summing unit" of the processing unit(Fig. 4.8). An offset,  $b$ , may be added to the total. The summation output:

$$net = \sum_{i=1}^P (x_i w_i) + b \quad 4.3.1$$

referred to as net input, goes into an activation transfer function  $f$  that produces scaled neuron output  $y$ (between 0 and 1, or -1 to 1)through a transform algorithm. Thus,  $y$  can be calculated as(jensen et al., 1999):

$$y = f(net) = f\left[\sum_{i=1}^P (x_i w_i) + b\right] \quad 4.3.2$$

The topological structure of an ANN defines the overall architecture of the network, including the framework and interconnection of neurons that are organized into layers. As previously discussed, a typical ANN consists of three or more layers(Fig 4.7): one input layer, one output layer, and one or more hidden layers(Jensen et al., 2001). Neurons within and between layers can be connected to form a user defined, task-oriented network. Decision processes can be duplicated or approximated through an ANN's ability to learn and recall. Learning is made possible by feeding the input layer with training data. By comparing the current activation of neurons in the output layer to a desired output response, the difference can be obtained and used to adjust weights connecting neurons in the network. It is the weights that

primarily determine the behavior of the network, so the goal of learning is to achieve a set of weights that will produce an output most resembling the target(Jensen et al., 1999). This adaptive learning process repeats until changes in network weights drop below a preset threshold, which indicates a user-defined accuracy. Once learned, the network can recall stored knowledge to perform either classification or prediction on new input data(Lloyd, 1996).

The desirable properties of non-normality and nonlinearity of an ANN can be attributed not only to the network's massively parallel distributed structure, but also to the transfer function for each neuron(Haykin, 1994). A neuron is basically a nonlinear device that may take continuous and differential functions as the transfer function. Therefore, ANNs are capable of modeling any complex system, be it physical or human(Bischof et al., 1992; Civco, 1993; Gong et al., 1996; Qiu and Jensen, 2004).

There are two commonly used artificial neural network learning paradigms:

1) The Pattern Associator ANN Algorithm

A pattern associator(PA) model is a primitive neural network that consists of only one input layer and one output layer and operates under the assumption of linearity(Haykin, 1994). It is based on the least-mean-square (LMS)algorithm. The LMS algorithm is driven by the difference between the target activation and the obtained activation. The idea is to adjust the weights of the connection to reduce the meansquare error. First, the network is initialized by setting all the weights to zero(Haykin, 1994):

$$w_k(1) = 0 \tag{4.3.3}$$

$$\text{for } k = 1, 2, 3, \dots, p$$

where  $p$  is the number of inputs and  $w_i(1)$ is the weight associated with input  $k$  in the first iteration. For every iteration  $t$ ,  $t = 1, 2, \dots$ , the obtained activation  $y$  can be calculated:

$$y(t) = \sum_{j=1}^P [x_j(t) \bar{w}_j(t)] \quad 4.3.4$$

where  $x_j(t)$  is the value of input  $j$  at iteration  $t$ .

Thus, the difference between the desired activation  $d(t)$  and obtained activation  $y(t)$  at iteration  $t$  can be computed:

$$e(t) = d(t) - y(t) \quad 4.3.5$$

Then, in the next iteration ( $t + 1$ ), the weight of input  $k$  is adjusted as

$$\bar{w}_k(t + 1) = w_k(t) + \eta \cdot e(t) \cdot x_k(t) \quad 4.3.6$$

where  $\eta$  is a positive constant known as the learning rate.

If  $y(t)$  is greater than  $d(t)$ ,  $e(t)$  computed from Equation 4.3.5 will be a negative value. When applied to Equation 4.3.6,  $w_k(t + 1)$  will be adjusted (penalized) to a smaller number. If  $d(t)$  is greater than  $y(t)$ ,  $w_k(t + 1)$  will be adjusted (rewarded) to a larger number. The difference between the desired and obtained activation is thus minimized at the learning rate  $\eta$ . The ideal choice for  $\eta$  is the largest value that does not lead to oscillation (Benediktsson, 1990; Jensen et al., 1999).

The traditional PA usually uses a linear transfer function in its output neuron, so that the activation of the output neuron is simply equal to the net input (Jensen et al., 1999). In this sense, the LMS learning process emulates a linear regression analysis, except that it is free from any assumption of data distribution. Like regression analysis, the traditional PA fails to achieve a good result when the data being modeled are not linear. Variants to the linear PA adopt nonlinear transform function such as a continuous sigmoidal function that resembles regression with a logarithmic transformation. These variants have the ability of modeling simple nonlinearity without distribution constraints.

2) The error back-propagation ANN algorithm

Back-propagation(BP)neural networks were first proposed by Werbos(1974) to improve the efficiency of multilayer network training(Jensen et al., 1999). This network has a hierarchical architecture with fully interconnected layers. Typically, one or more hidden layers are used to enable the network to learn complex tasks. the training is based on an error-correction learning rule. Each neuron in the network may include a nonlinear transfer function at the output end, producing smooth signals to other neurons. One of the common forms of nonlinearity is a sigmoidal transfer function defined by the logistic function(Haykin, 1994; Hagan et al., 1996):

$$f(net) = \frac{1}{1 + e^{(-net)}} \quad 4.3.7$$

Initialized with all the synaptic weights and thresholds set to small random numbers, the network is fed with training patterns. Each learning iteration of the network consists of two passes: a forward pass and a backward pass. In the forward pass, the net input of the  $j$ th neuron of layer  $l$  is calculated:

$$net_j^l(t) = \sum_{i=0}^P (y_i^{(l-1)}(t)w_{ji}^l(t)) \quad 4.3.8$$

and the output activation is computed using the transfer function (Equation 4.3.7):

$$y_j^l(t) = f[net_j^l(t)] \quad 4.3.9$$

The difference between the desired response and output activation of neuron  $j$  at the output layer is obtained by:

$$e_j(t) = d_j(t) - o_j(t) \quad 4.3.10$$

In the backward pass, a local error gradient,  $\delta$ , is computed layer by layer:

$$\delta_j^L(t) = e_j^l(t)o_j(t)[1 - o_jx(t)] \quad 4.3.11$$

for neuron  $j$  in output layer  $L$ , and

$$\delta_j^l(t) = j_j^l(t)[1 - y_j(t)] \sum_k \delta_j^{(l+1)}(t) w_{kj}^{(l+1)}(t) \quad 4.3.12$$

for neuron  $j$  in hidden layer  $l$ .

With this information, the synaptic weights in layer  $l$  can be adjusted according to a generalized LSM rule (Haykin, 1994; Hagan et al., 1996):

$$w_{ji}^l(t+1) = w_{ji}^l(t) + \alpha [w_{ji}^l(t) - w_{ji}^l(t-1)] + \eta \delta_j^l(t) y_i^{(l-1)}(t) \quad 4.3.13$$

where  $\eta$  is the learning rate and  $\alpha$  is the momentum constant for speeding up learning without running into the risk of oscillation. In a special case when  $\alpha$  equals zero, the generalized LSM rule becomes the standard LSM rule. In the backward pass, weights are adjusted in a manner that changes are proportional to the error gradient. Because this pass is started from the output layer and error correction is propagated backward to the previous layer, this process is called *error back-propagation*. The knowledge inherent in the training data is obtained through the iteration of forward and backward passes until all the parameters in the network are stabilized (Jensen et al., 2001). This is signified by the decrease of average squared error to a minimum or acceptable level.

### 4.3.3 The application of ANN to the landslide susceptibility analysis

A flowchart of neural networks training for weight determination showed in Fig. 4.9 was used in this study. Kavzoglu (2001) suggested that an appropriate sample size needed for neural network analysis be between  $30 \cdot N_i \cdot (N_i + 1)$  and  $60 \cdot N_i \cdot (N_i + 1)$ , so the sample size used in this study was decided according to the suggestion. The neural network analysis was performed after samples were abstracted from the study area.

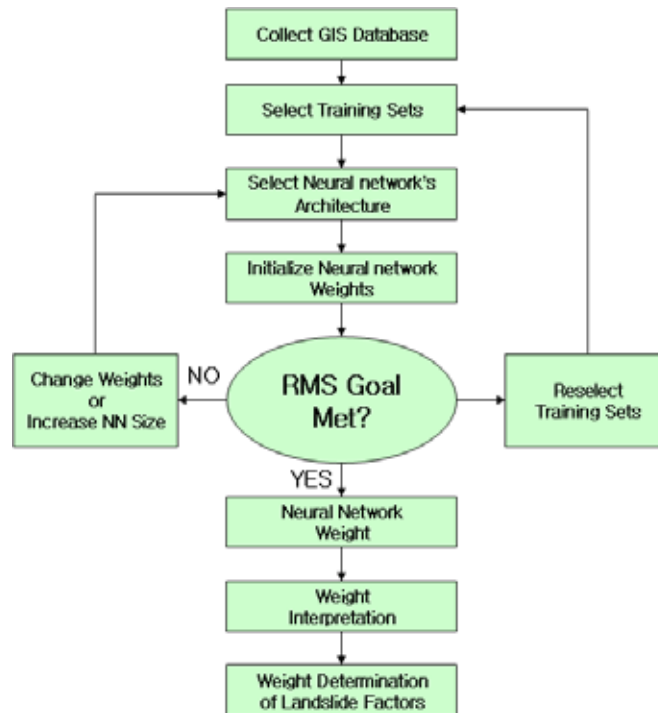


Fig. 4.9 The flowchart of the neural network training for weight determination.

Table 4.26 Heuristics proposed by researchers to compute the optimum number of hidden layer nodes(modified from Kavzoglu, 2001).

Proposed by	Heuristic	Calculated hidden nodes ( $N_i = 7, N_o = 1, N_p = 2000$ )
Hecht-Nielsen(1987)	$2 \cdot N_i + 1$	15
Hush(1989)	$3 \cdot N_i$	21
Ripley(1993)	$(N_i + N_o)/2$	4
Paola(1994)	$\frac{2 + N_o \cdot N_i + N_o \cdot (N_i^2 + N_i)/2 - 3}{N_i + N_o}$	4
Wang(1994)	$2 \cdot N_i/3$	5
Aldrich et al.(1994)	$N_p/k(N_i + N_o)(k = 10)$	25
Aldrich et al.(1994)	$N_p/k(N_i + N_o)(k = 7)$	36
kaastra and Boyd(1996)	$\sqrt{N_i \cdot N_o}$	3
Kanellopoulas and Wilkinson(1997)	$2 \cdot N_i$	14

$N_i$ : number of input nodes.

$N_o$ : number of output nodes

$N_p$ : number of training samples.

$k$ : noise factor(varies between 4 and 10), index number representing percentage of false measurements in the data or degree of error.



Table 4.27 The setting values for neural network training.

Setting factors	Values
Input layer	7
Hidden layer	14
Output layer	1
The number of weights between input and hidden layer	98
The number of weights between hidden and output layer	14
Learning cycles	50000

Table 4.28 The learning rates and momentum.

No Factor	1	2	3	4	5	6	7	8
Learning rate	0.01	0.01	0.01	0.01	0.1	0.1	0.1	0.1
Momentum	0.1	0.3	0.5	0.7	0.1	0.3	0.5	0.7
No Factor	9	10	11	12	13	14	15	16
Learning rate	0.3	0.3	0.3	0.3	0.5	0.5	0.5	0.5
Momentum	0.1	0.3	0.5	0.7	0.1	0.3	0.5	0.7

The neuron number of the hidden layer was 14 when calculated by the equation suggested by Kanellopoulas and Wilkinson(1997) as shown in Table 4.26, the number of the input layer was 7, the number of the output layer was 1, the number of weights between the input and hidden layer was 98 and the number of weights between the hidden and output layer was 14 as shown in Table 4.27. Generally, 50000 times of circulation were proceeded to achieve a designed error value. To calculate a relative importance of each input factor, we used 16 pairs of the learning rates and momentum values as shown in Table 4.28. According to the result of the comparison of the RMSE value, we found that the RMSE value was minimized when learning rates and momentum values were 0.1 and 0.7 as shown in Fig. 4.10 so we used this value to calculate the relative importance. Finally, the relative importance

of each input factor calculated by a neural network method was shown in Fig. 4.11 and a landslide susceptibility map was shown in Fig. 4.12.

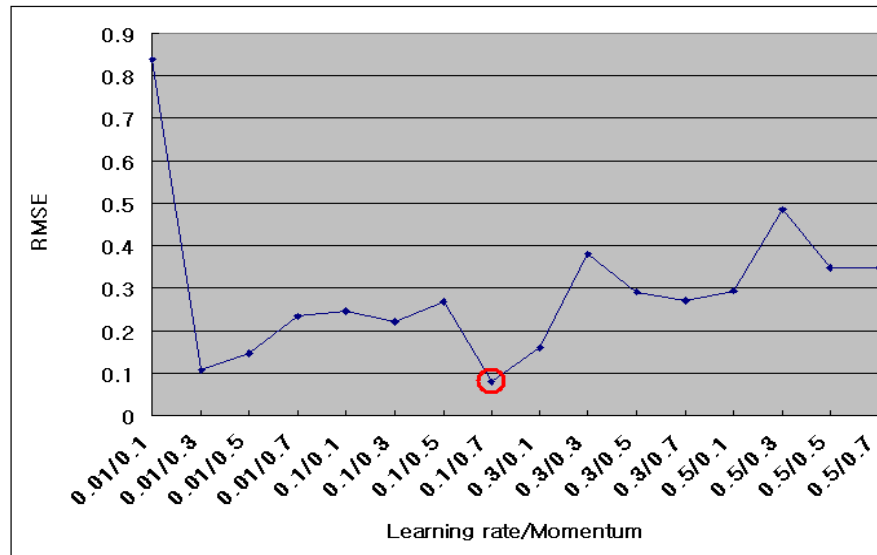


Fig. 4.10 The comparison of the RMSE values between each learning rate and momentum.

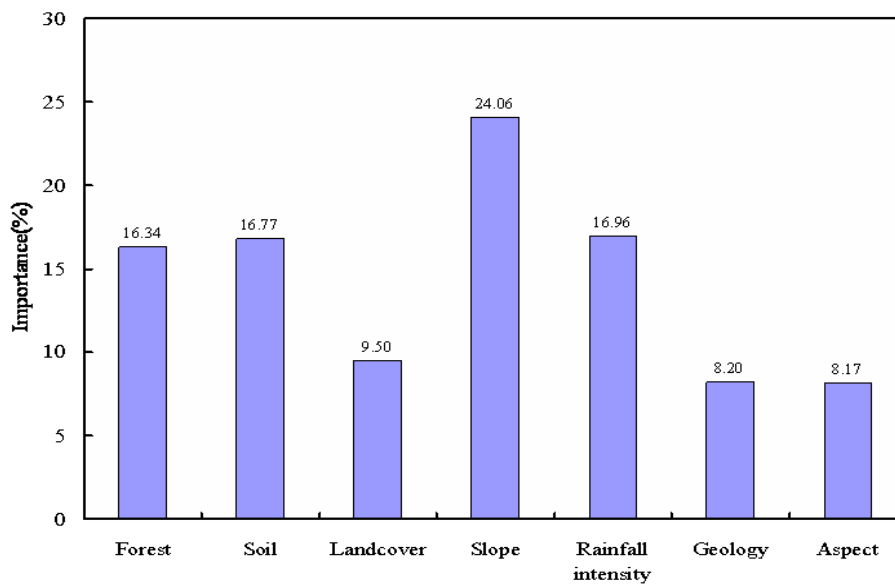


Fig. 4.11 The relative importance value of each input factor.

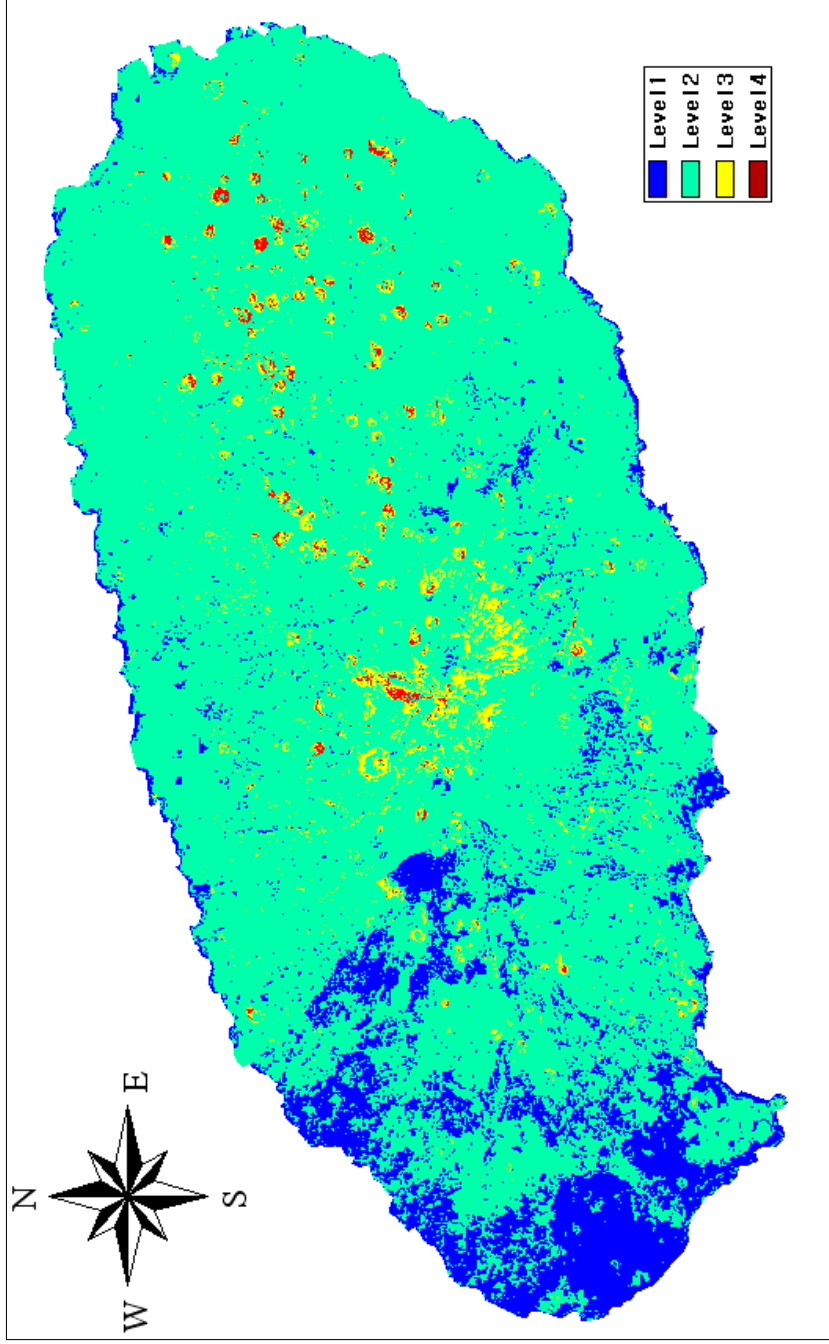


Fig. 4.12 The landslide susceptibility map generated by the artificial neural network method.

## CHAPTER 5. IMAGE CHANGE DETECTION

### 5.1 Landsat TM data

A shape of Landsat satellite machine is shown in Fig. 5.1. Landsat Thematic Mapper sensor systems were launched on July 16, 1982(Landsat 4), and on March 1, 1984(Landsat 5).

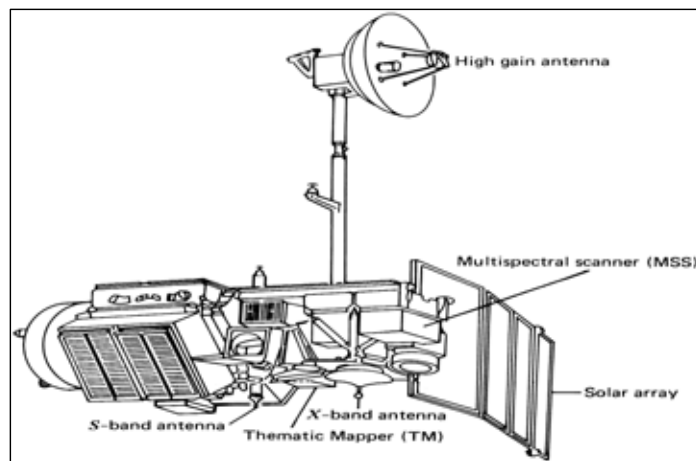


Fig. 5.1 The shape of Landsat TM satellite (Lillesand & Kiefer, 2000).

The TM is an optical-mechanical whiskbroom sensor that records energy in a visible, reflective-infrared, middle-infrared and thermal infrared regions of electromagnetic spectrum. It collects multispectral imagery that has higher spatial, spectral, temporal, and radiometric resolution than the Landsat MSS. Landsat TM data has a ground-projected IFOV of  $30 \times 30$ m from band 1 to band 7 except band 6. The thermal infrared band 6 has a spatial resolution of  $120 \times 120$ m. The TM spectral bands represent important departures from the

bands found on the traditional MSS and also carried onboard Landsat 4 and 5. The original MSS bandwidths were selected based on their utility for vegetation inventories and geologic studies. Conversely, the TM bands were chosen after years of the analysis for their value in water penetration, discrimination of vegetation types and vigor, plant and soil moisture measurements, differentiation of clouds, snow and ice, and identification of hydrothermal alterations in certain rock types (Table 5.1).

Table 5.1 The Landsat TM spectral band characteristics.

Bands	Wave Length ( $\mu\text{m}$ )	Pixel (m)	Principal Application
1(Blue)	0.45-0.52	30	Useful for soil/vegetation discrimination
2(Green)	0.52-0.60	30	For vegetation discrimination vigor assesment and culture feature identification
3(Red)	0.63-0.69	30	Sense in a cholorophyll absorption and culture feature identification
4(Near Infrared)	0.76-0.90	30	For vegetation types, vigor, and biomass content, delineating water bodies and soil moisture content
5(Mid Infrared)	1.55-1.75	30	Indicative of vegetation moisture and soil moisture
6(Thermal Infrared)	10.4-12.5	120	Useful in vegetation stress analysis, soil moisture discrimination and thermal mapping
7(Mid Infrared)	2.08-2.35	30	For discrimination of mineral and rock type. Also sensitive to vegetation moisture content

## 5.2 Landsat TM image analysis

In this study, Landsat TM data (2898×1897 Landsat pixels) on May 20, 2007, March 11, 2002 and March 24, 2001 was selected for this study. Fig. 5.2, 5.4 and 5.6 shows the Landsat TM images from band 1 to 7 taken in a different time. To get available data through an analysis of Landsat images, we first used a histogram to analyze the images.

Histograms are a useful graphic representation of information contents of a remotely sensed image. Histograms for each band of imagery are often displayed and analyzed in many remote sensing investigations because they provide an analyst with an appreciation of the quality of original data (e.g., whether it is low in contrast, high in contrast or multimodal in nature). In fact, many analysts routinely provide before (original) and after histograms of the imagery to document an effect of applying an image enhancement technique (Jahne, 1997; Gonzalez and Woods, 2002). It is instructive to review how a histogram of a single band of imagery,  $k$ , composed of  $i$  rows and  $j$  columns with a brightness value  $BV_{ijk}$  at each pixel location is constructed.

Individual bands of remote sensor data are typically quantized (digitally recorded) with brightness values ranging from  $2^8$  to  $2^{12}$  (if  $quant_k = 2^8$  then brightness values range from 0 to 255;  $2^9 =$  values from 0~511;  $2^{10} =$  values from 0~1023;  $2^{11} =$  values from 0~2047; and  $2^{12} =$  values from 0~4095). The majority of the remote sensor data quantized to 8 bits, with values ranging from 0 to 255 (e.g., Landsat 5 Thematic Mapper and SPOT HRV data). The greater the quantization is, the higher the probability is. That is, subtle spectral reflectance (or emission) characteristics may be extracted from the imagery.

Tabulating a frequency of an occurrence of each brightness value within the images provides statistical information that can be displayed graphically in a histogram (Hair et al., 1998). A range of quantized values of a band of imagery and  $quant_k$  is provided on the abscissa (x axis) while a frequency of an occurrence of each of these values is displayed on the ordinate (y axis).

Fig. 5.3, 5.5 and 5.7 shows a histogram of each band of Landsat TM images and Table 5.2, 5.3 and 5.4 shows a statistical value of each image used in this study.

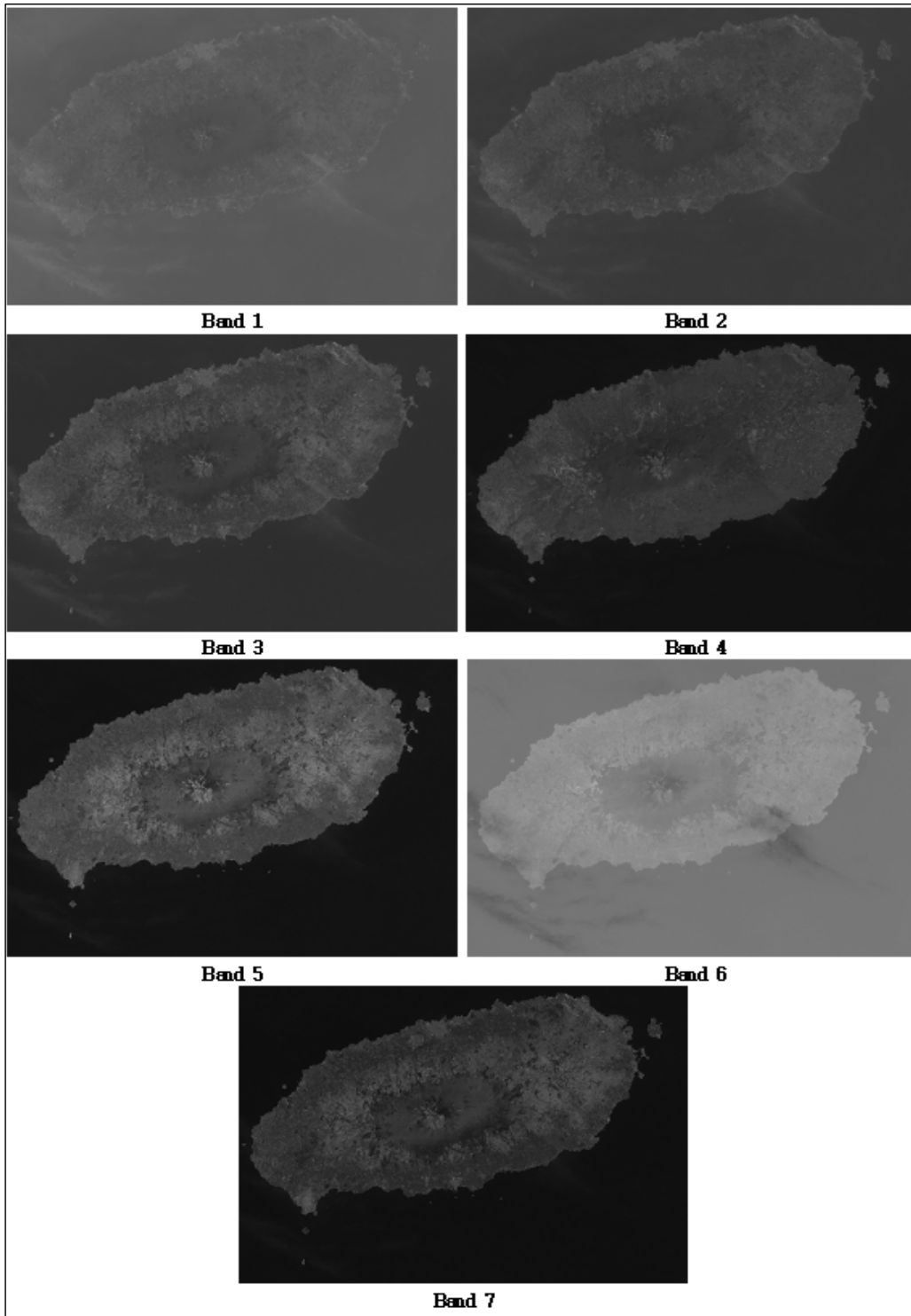


Fig. 5.2 Landsat TM images of Jeju Island(2001).

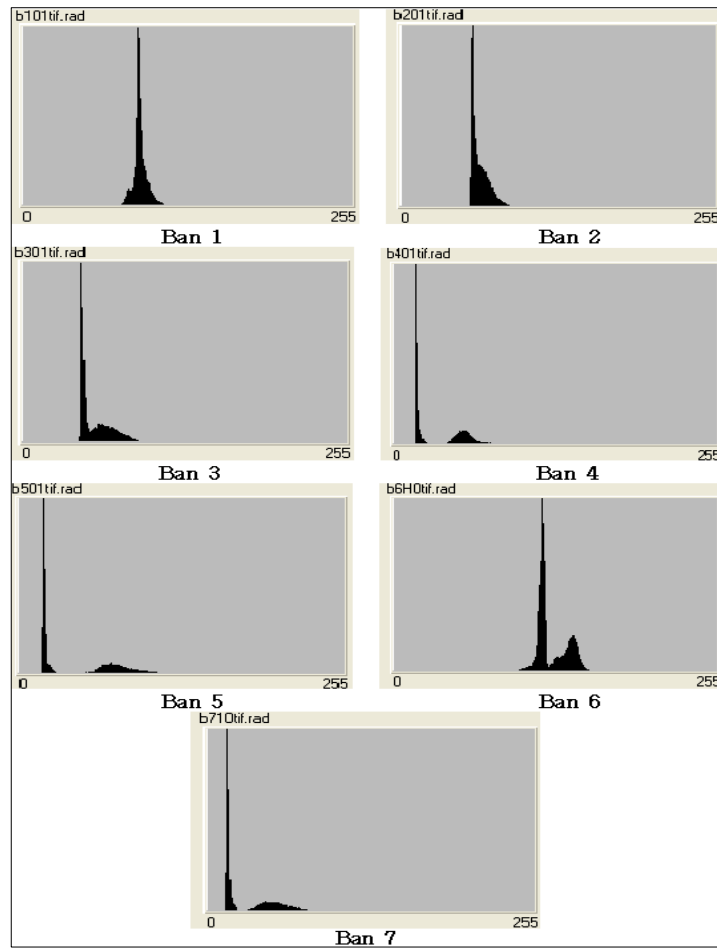


Fig. 5.3 Histograms of Landsat TM images(2001).

Table 5.2 Statistic data of Landsat TM images(2001).

Types	Band 1	Band 2	Band 3	Band 4	Band 5	Band 6	Band 7
Sample percent	0.521	0.521	0.521	0.521	0.521	0.521	0.521
Number	7682491	7682491	7682491	7682491	7682491	7682491	7682491
Mean	66.95	46.70	41.79	25.19	31.73	92.37	23.28
Median	89	59	48	19	19	118	16
Mode	0	0	0	0	0	0	0
Variance	1617.24	812.85	728.12	499.81	999.38	3144.60	475.60
Std. Deviation	40.21	28.51	26.98	22.36	31.61	56.08	21.81
Minimum	0	0	0	0	0	0	0
Maximum	128	104	118	114	133	168	103
Range	128	104	118	114	133	168	103



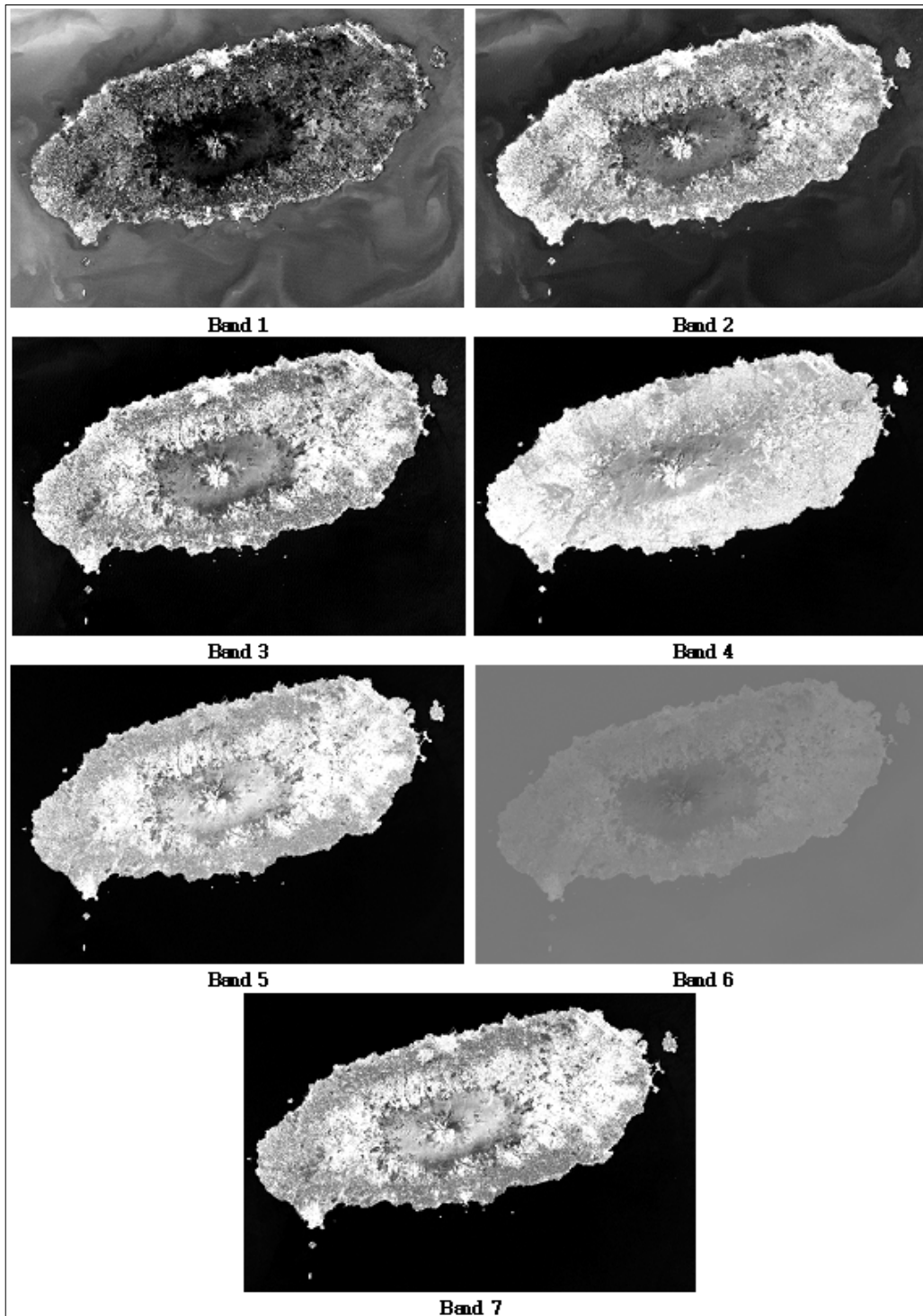


Fig. 5.4 Landsat TM images of Jeju Island(2002).

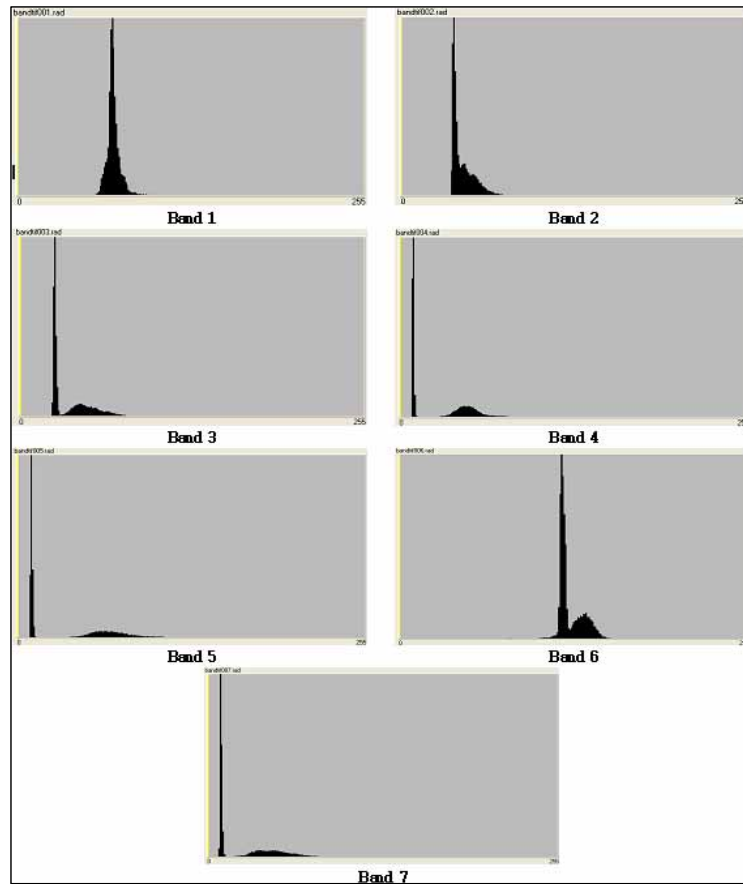


Fig. 5.5 Histograms of Landsat TM images(2002).

Table 5.3 Statistic data of Landsat TM images(2002).

Types	Band 1	Band 2	Band 3	Band 4	Band 5	Band 6	Band 7
Sample percent	0.521	0.521	0.521	0.521	0.521	0.521	0.521
Number	7682491	7682491	7682491	7682491	7682491	7682491	7682491
Mean	52.1	33.01	26.63	19.27	24.68	92.05	18.18
Median	69	39	26	10	10	119	9
Mode	0	0	0	0	0	0	0
Variance	984.84	435.94	402.88	466.01	893.18	3079.18	423.94
Std. Deviation	31.38	20.88	20.07	21.59	29.89	55.49	20.59
Minimum	0	0	0	0	0	0	0
Maximum	144	137	165	113	143	165	126
Range	144	137	165	113	143	165	126

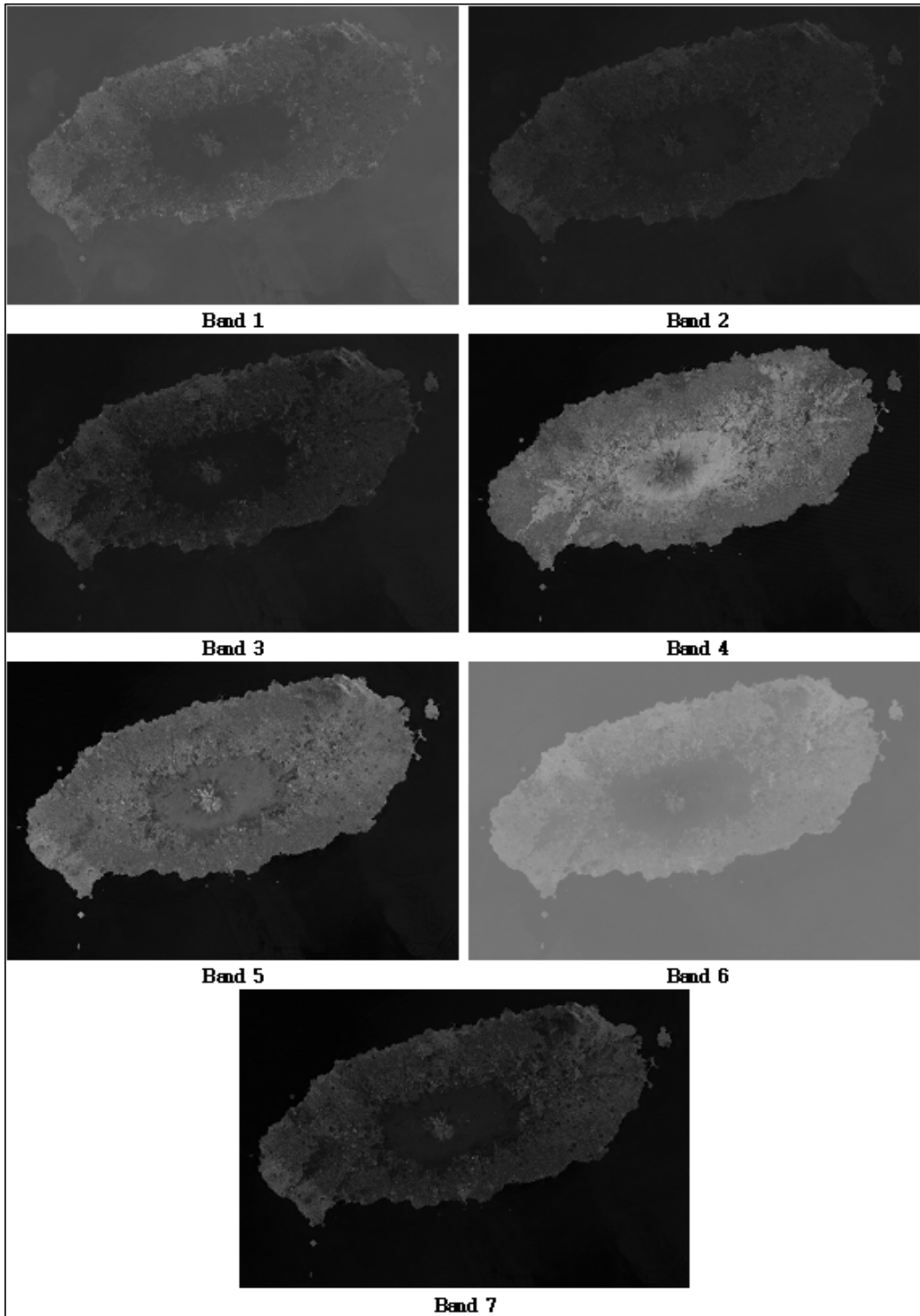


Fig. 5.6 Landsat TM images of Jeju Island(2007).

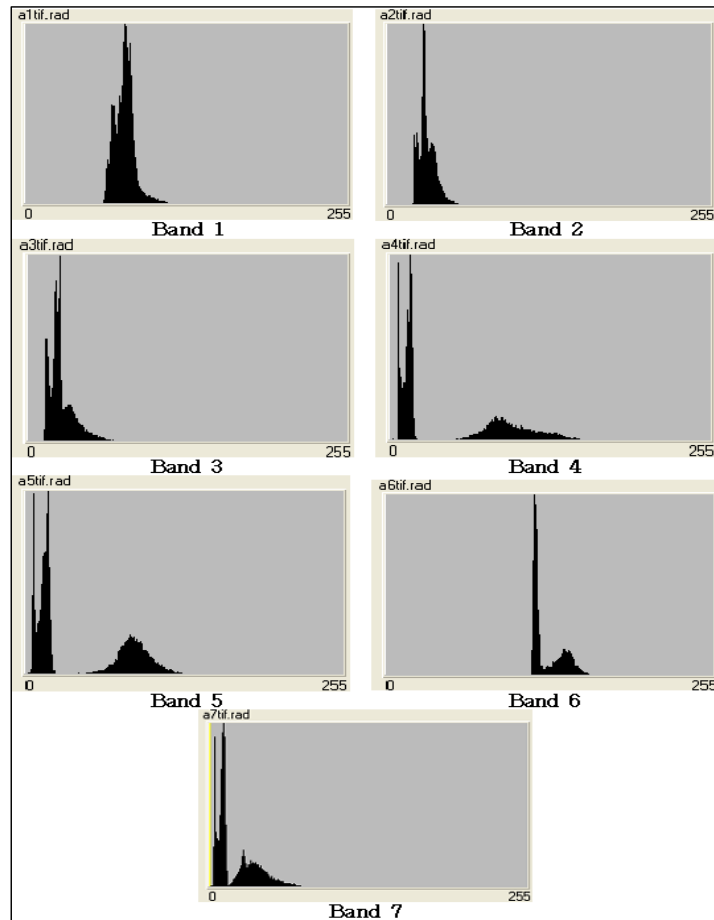


Fig. 5.7 Histograms of Landsat TM images(2007).

Table 5.4 Statistic data of Landsat TM images(2007).

Type	Band 1	Band 2	Band 3	Band 4	Band 5	Band 6	Band 7
Sample percent	0.521	0.521	0.521	0.521	0.521	0.521	0.521
Number	7682491	7682491	7682491	7682491	7682491	7682491	7682491
Mean	57.835	22.803	20.187	35.214	32.248	91.947	15.003
Median	75	28	23	15	15	117	10
Mode	0	0	0	0	0	0	0
Variance	1262.79	222.60	223.32	1830.43	1425.47	3179.60	280.15
Std. Deviation	35.54	14.92	14.94	42.78	37.76	56.39	16.74
Minimum	0	0	0	0	0	0	0
Maximum	161	83	109	167	212	165	156
Range	161	83	109	167	212	165	156

## **5.3 NDVI image change detection**

### **5.3.1 The conception of NDVI**

The multispectral image data detected by satellites and aircrafts showed that ground objectives possessed specific characteristics in a different spectrum and it would be useful to obtain the information that we needed. Expecially, among the image data of land surface, which was a main interesting area by satellites like Landsat, more than 95% of the information were largely about soil and vegetation. Therefore, it was possible to assume the vegetation distribution or density of the land surface by using the imaging data. For example, healthy vegetation reflected very well in a near infrared part of the spectrum. Green leaves had 20 percents or less of reflectance from 0.5 to 0.7 micron ranges(green to red) and about 60 percents from 0.7 to 1.3 micron ranges(near infra-red). On the other hand, the reflectance of the withered vegetation without chlorophyll was higher in a visible ray part of the spectrum but lower in a near infrared part of the spectrum than the healthy vegetation. It was also possible to make a formula for the calculation of the vegetation density based on reflectance properties with each wavelength range and combination of the special quality of the spectrum, which was called a vegetation index. The vegetation index had been developed as a measure that could quantitatively express a leaf area, distribution area of vegetation, height of trees and wood types. It is a popular method because it can be embodied by many different ways like rates, differences and linear combination between each observed images in different wavelength range. A calculation principle of the vegetation index is to extract an image of a vegetation condition by applying some formulas to the images

taken in the two ranges and using reflectance differences between a visible ray (especially red part) and near-infrared part of the spectrum in the healthy vegetation.

NDVI (Normalized Difference Vegetation Index) was one of the popular vegetation indexes. It emphasized on the reflectance characteristics of the vegetation by calculating spectrum differences from the two visible rays and near-infrared images and it was generalized by the division of the sum of the two images. Generally, the reflectance of the vegetation in each spectrum was influenced by an incident angle of sunlight, a viewing angle of a satellite and a condition of the atmosphere, and it could be reduced by a generalization.

If imaging data was a Landsat TM or ETM, the NDVI could be calculated by the following equation.

$$NDVI = \frac{TM_4 - TM_3}{TM_4 + TM_3} \quad 5.3.1$$

Where NDVI was an index that indicated vitality of the vegetation,  $TM_4$  was an image of band 4 in the Landsat TM and  $TM_3$  was an image of band 3 in the Landsat TM.

Because the value of the reflectance by the visible ray was higher than that of the near-infrared part, the value of the NDVI became a minus and the value of the NDVI approaches zero when the area had a similar reflectance characteristic like the area of rock and barren soil. In the healthy vegetation, the value of the NDVI became positive because the reflectance by the visible ray was lower than the near-infrared part. In most areas covered by vegetation, NDVI had the value between 0.1~0.6 when it did not consider the condition of that the vegetation contained a moisture.

The following equation generalizes the range of the NDVI values calculated by the above equation.

$$NDVI = \left( \frac{TM_4 - TM_3}{TM_4 + TM_3} + 1 \right) \times 128 \quad 5.3.2$$

In other words, the value of the NDVI calculated by the first equation had the value between -1 and +1 but the value of the NDVI calculated by the second equation distributed to the range between 0 and 255. Thus, the second equation had an advantage of making it easy to discriminate the value of the NDVI visually.

### 5.3.2 The detection of the NDVI changes

In this study, we calculated a value of the NDVI from the images obtained in 2001, 2002 and 2007 by using equation 5.3.2 to compare the differences between the NDVI images. Fig. 5.8, 5.9 and 5.10 shows the NDVI images generated by the Landsat images taken in 2001, 2002 and 2007 respectively. Fig. 5.11 shows the differences between NDVI images in 2001 and 2002. Fig. 5.12 shows the differences between NDVI images in 2002 and 2007. The areas marked by the red circles indicate that the NDVI values were significantly decreased in Fig. 5.11 and 5.12. From Fig. 5.11 and Fig. 5.12, we found some areas where the NDVI values were significantly decreased and the areas were indicated by the blue circles. From the conception of the NDVI, we discovered that the susceptibility area where the NDVI values were significantly decreased was more dangerous than other susceptibility areas. To find this dangerous area, we compared the NDVI change images with the susceptibility area generated by the ANN method. The susceptibility area is indicated by the red circles in Fig. 5.11 and 5.12. After the comparison of them, we knew that the areas that overlaid by the red and blue circles were more dangerous areas than other susceptibility areas as shown in Fig. 5.11 and 5.12.

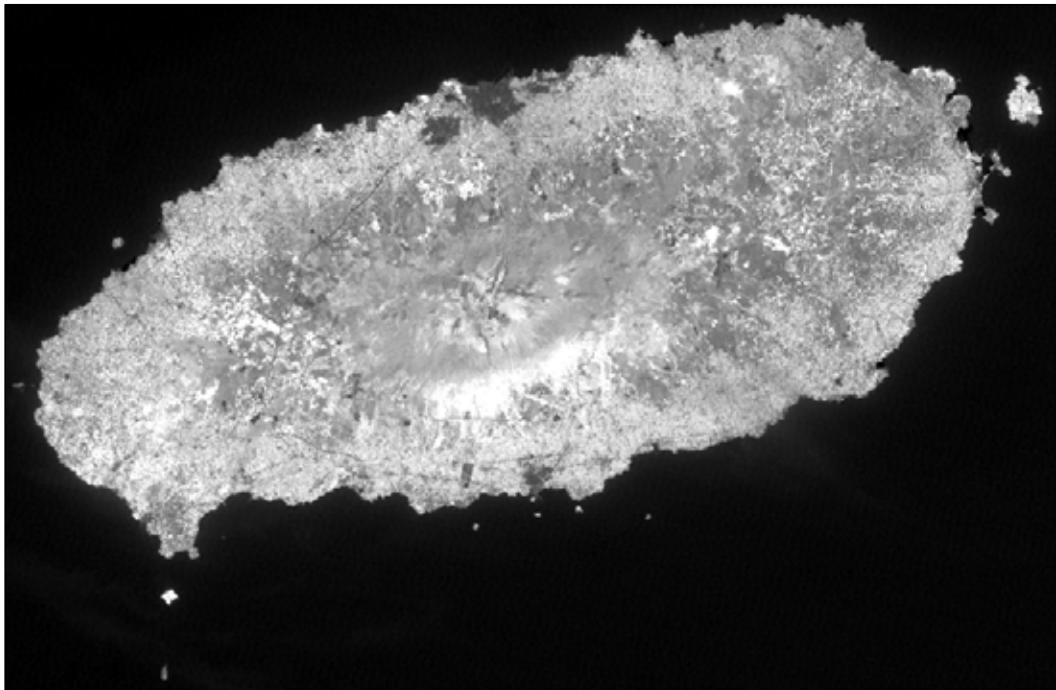


Fig. 5.8 The NDVI image generated from the Landsat images in 2001.

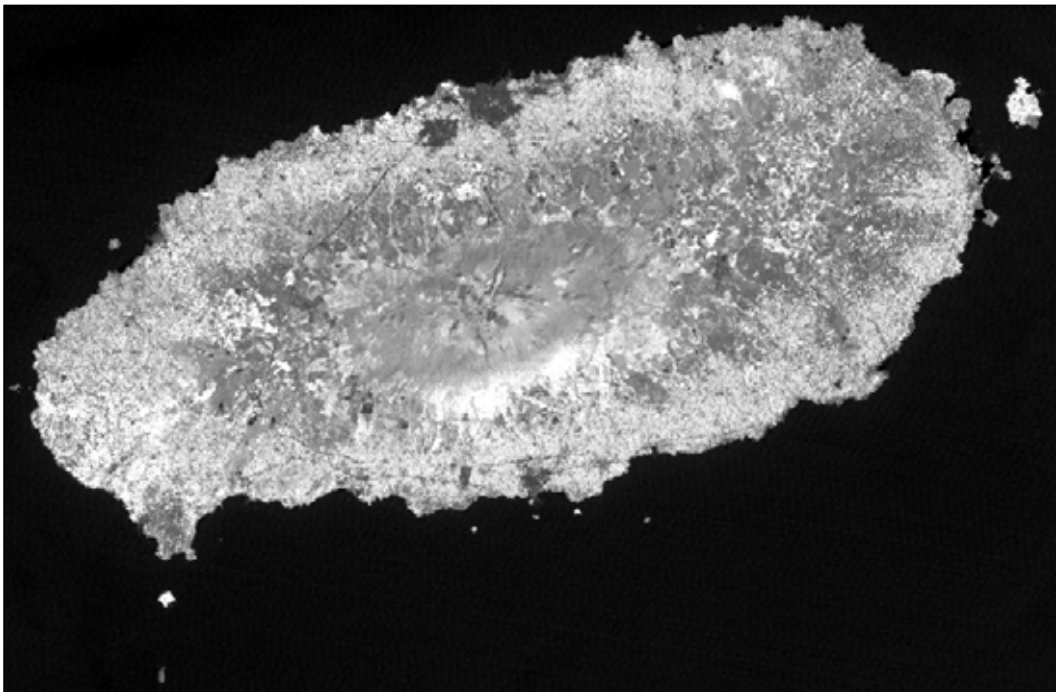


Fig. 5.9 The NDVI image generated from the Landsat images in 2002.



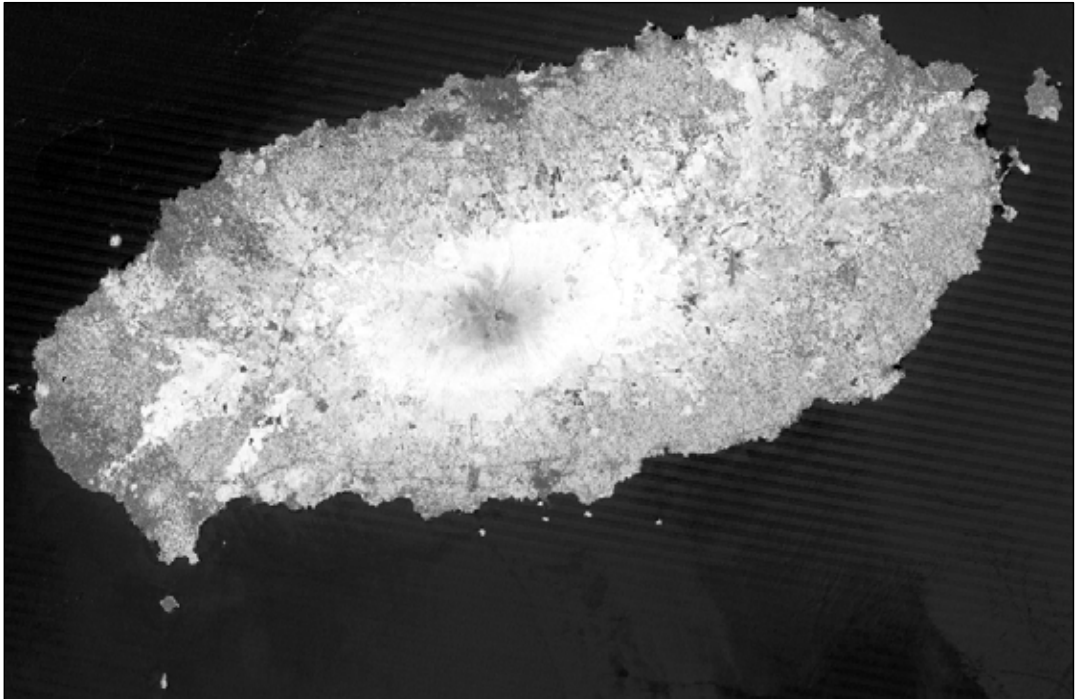


Fig. 5.10 The NDVI image generated from the Landsat images in 2007.

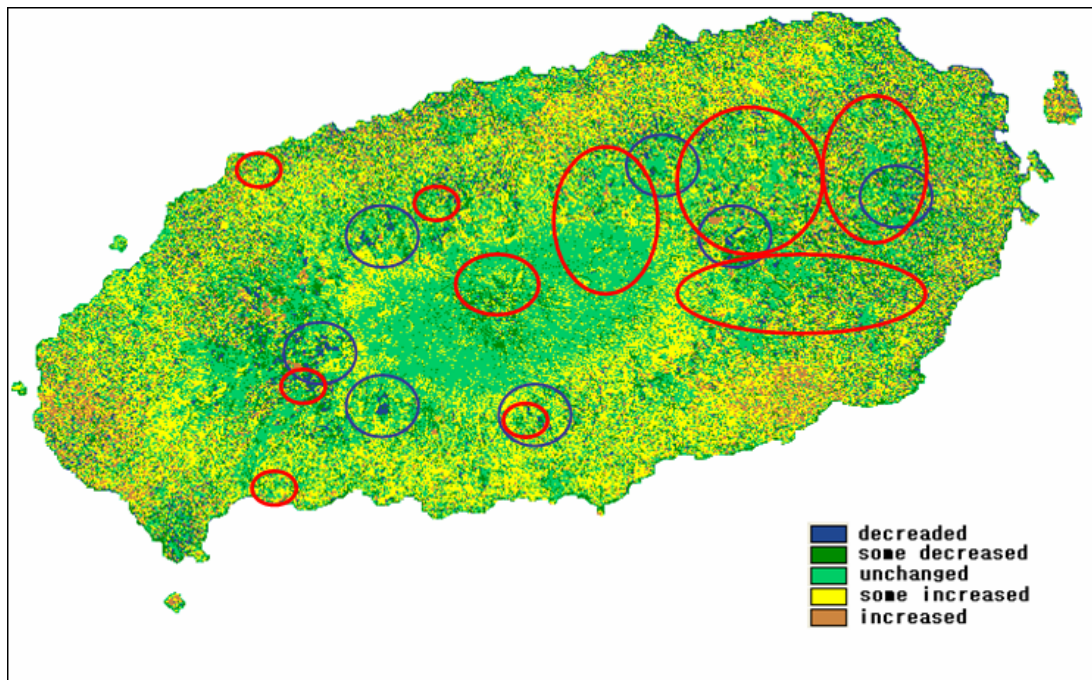


Fig. 5.11 The change detection of the NDVI images between 2001 and 2002.

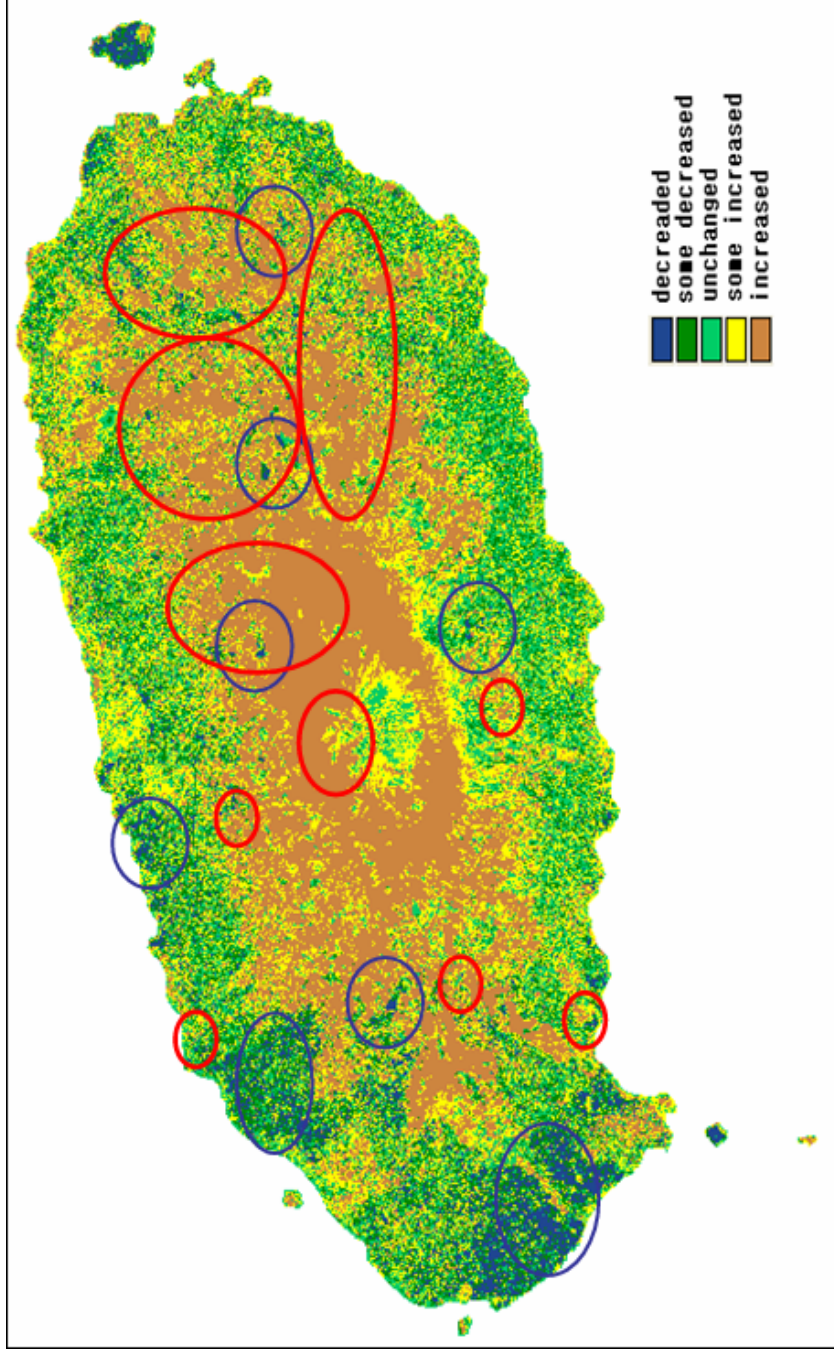


Fig. 5.12 The change detection of the NDVI images between 2002 and 2007.

## CHAPTER 6. DISCUSSION

### 6.1 The analysis of the susceptibility areas

To analyze landslide susceptibilities throughout Jeju Island, the three methods such as the AHP, logistic regression analysis, and artificial neural network methods were used to portray susceptibility maps. After comparing the results, we obtained the subsequent results.

In the AHP method, a weight value of slope, aspect, soil, geology, rainfall intensity, land cover and forest that had an influence on a landslide was calculated by using the AHP method. The safe and hazardous areas were calculated by means of the susceptibility map generated by a weighted overlay arithmetic operation using weight. Fig. 6.1 shows the area distribution

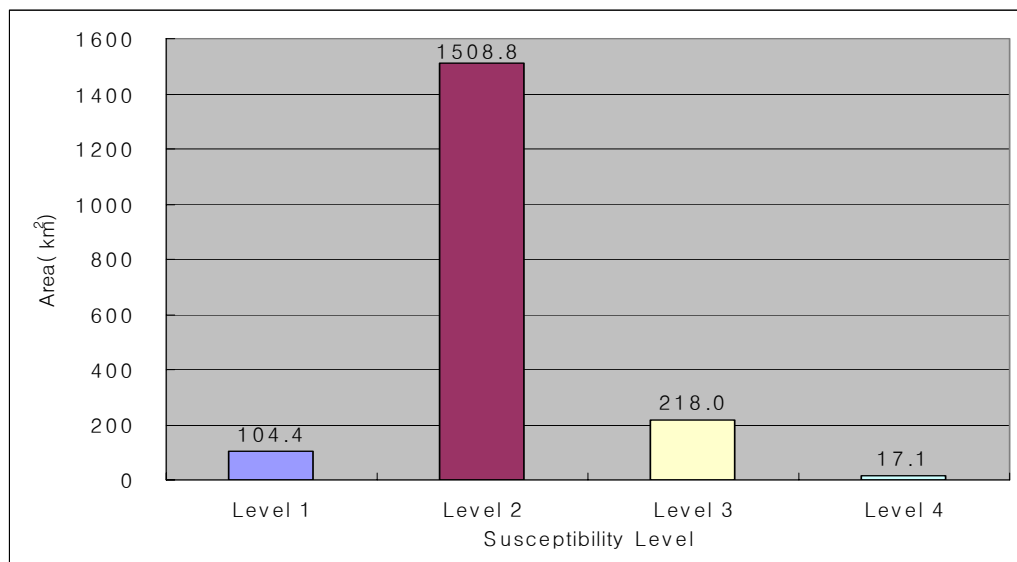


Fig. 6.1 The area distribution in each susceptibility level(AHP method).

in each susceptibility level. In this figure, level 1 meant a very safe area and level 4 meant a very hazardous area. Level 2 and 3 belong to between these two levels. Thus, level 1 and 2 was the area where a possibility of a landslide occurrence was very low.

In the logistic regression method, the equation as shown in below was generated by using the sample data gotten from the study area and the susceptibility map was portrayed by using the equation and the GIS method.

$$\begin{aligned} \ln(P_z/(1 - P_z)) = & (-10.158) + 0.783 * X_1(\text{slope}) + 0.364 * X_2(\text{aspect}) \\ & + 0.523 * X_3(\text{geology}) + 0.668 * X_4(\text{soil}) \\ & + 0.726 * X_5(\text{rainfall intensity}) \\ & + 0.400 * X_6(\text{forest}) + 0.575 * X_7(\text{landcover}) \end{aligned}$$

The value of  $P_z$ (occurrence probability) was between 0 to 1 and this interval was classified into 4 levels the same as the AHP method. thus, the value of  $P_z$  in a very hazardous area of level 4 was between 0.8~1. The areas belonging to each level were compared by a graph as shown in Fig. 6.2.

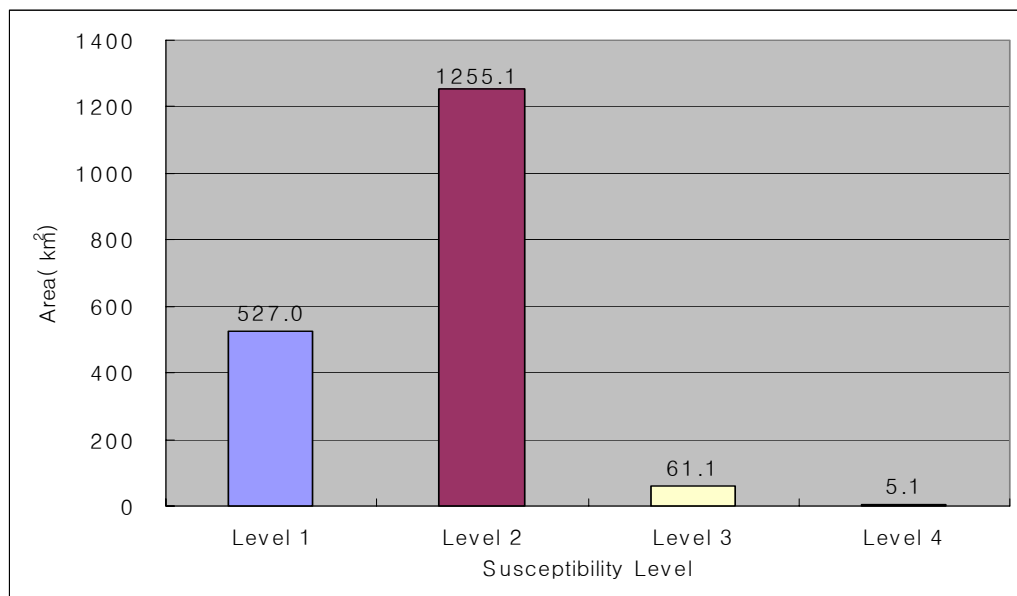


Fig. 6.2 The area distribution in each susceptibility level(LRA method).

In the artificial neural network method, the neuron number of the hidden layer was 14, the number of the input layer was 7, the number of the output layer was 1, the number of the weights between the input and hidden layer was 98, and the number of the weights between the hidden and output layer was 14. Generally, 50000 times of circulation were proceeded to achieve a designed error value.

The susceptibility map generated by ANN was classified into 4 levels the same as the AHP method and the areas belonging to each level was compared by a graph as shown in Fig. 6.3.

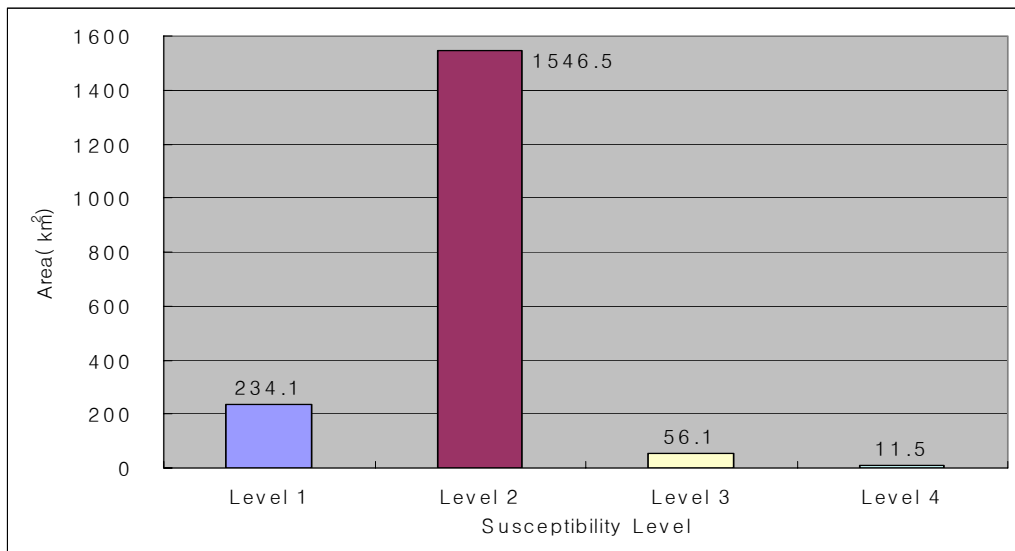


Fig. 6.3 The area distribution in each susceptibility level(ANN method).

Fig. 6.4 shows the comparison of the areas belonging to each level and Fig. 6.5 shows the comparison of the areas just belonging to level 3 and 4 in each susceptibility map generated by three different methods. According to the figure, the area belonging to level 3 and 4 generated by the AHP method was biggest as 218.0km<sup>2</sup> and 17.1km<sup>2</sup>, the second as 56.1km<sup>2</sup> and 11.5km<sup>2</sup> was the area generated by the ANN method, and the smallest as 61.1km<sup>2</sup> and 5.1km<sup>2</sup> was the area generated by the LRA method .

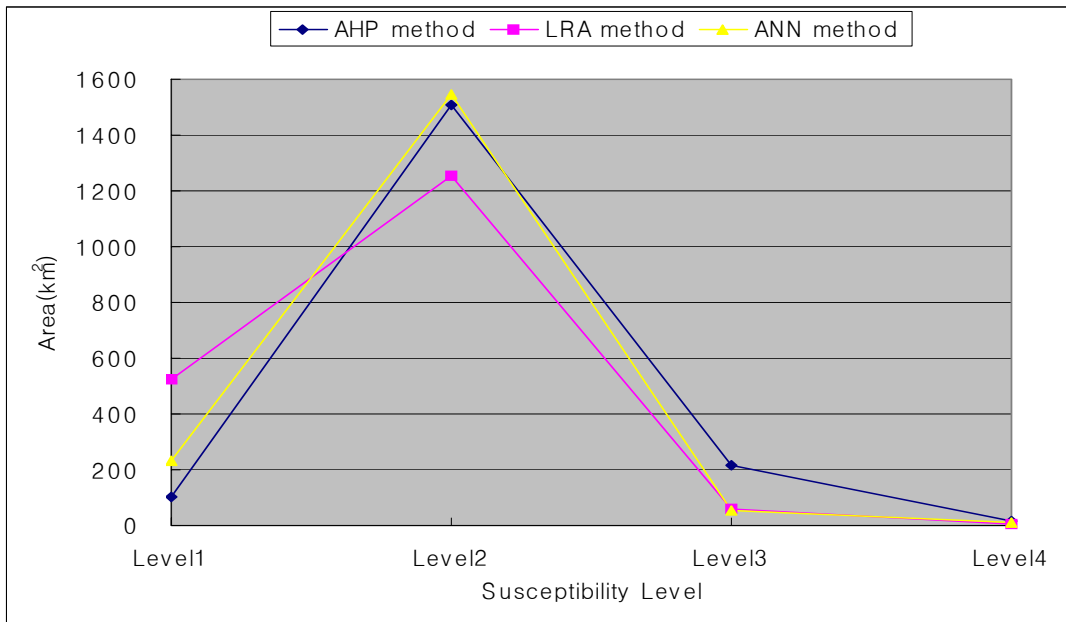


Fig. 6.4 The comparison of areas generated by three methods in each level.

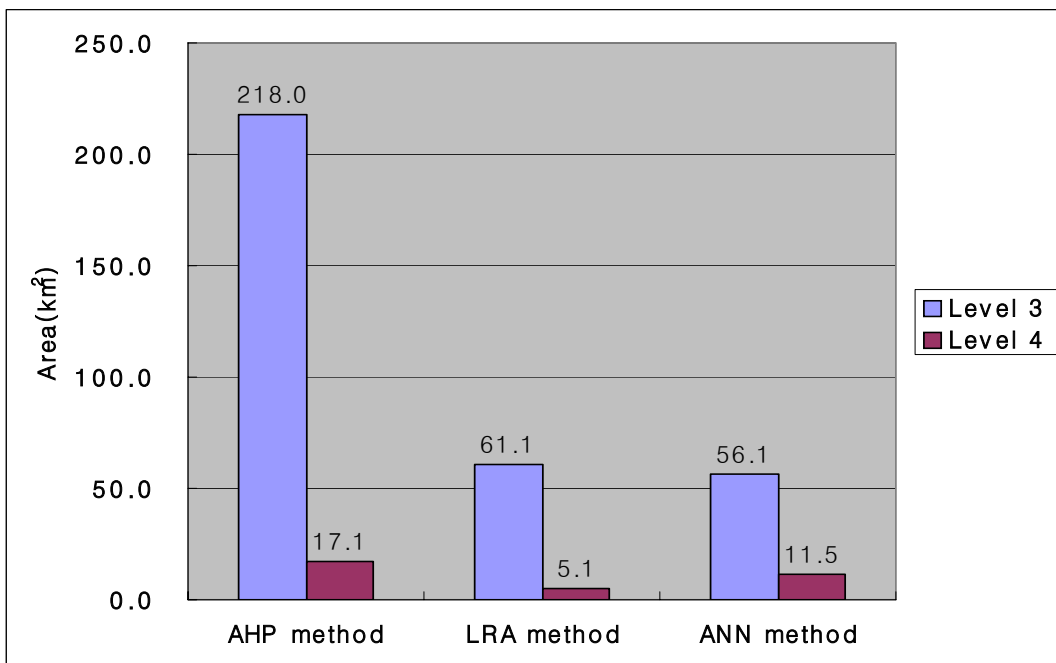


Fig. 6.5 The comparison of areas generated by three methods in level 3 and 4.

## 6.2 The accuracy analysis of the susceptibility areas by field data

To analyze an accuracy of the susceptibility maps generated by three different methods, we used six areas among 12 areas where landslide had occurred and the rest of the areas were considered to be more dangerous after the field survey. The information about the field data is shown in Table 6.1 and Table 6.2. The distribution of the field area is shown in Fig. 6.6.

After the comparison between three susceptibility maps and field data, 7 areas of the field data were recognized as susceptibility areas in the AHP method, 9 areas of the field data were recognized as susceptibility areas by the ANN method and 5 areas of the field data were recognized as susceptibility areas by the LRA method. More detail information is shown in Table 6.3. From Table 6.3, we finally knew that the susceptibility areas generated by the ANN method among three methods were more accurate.

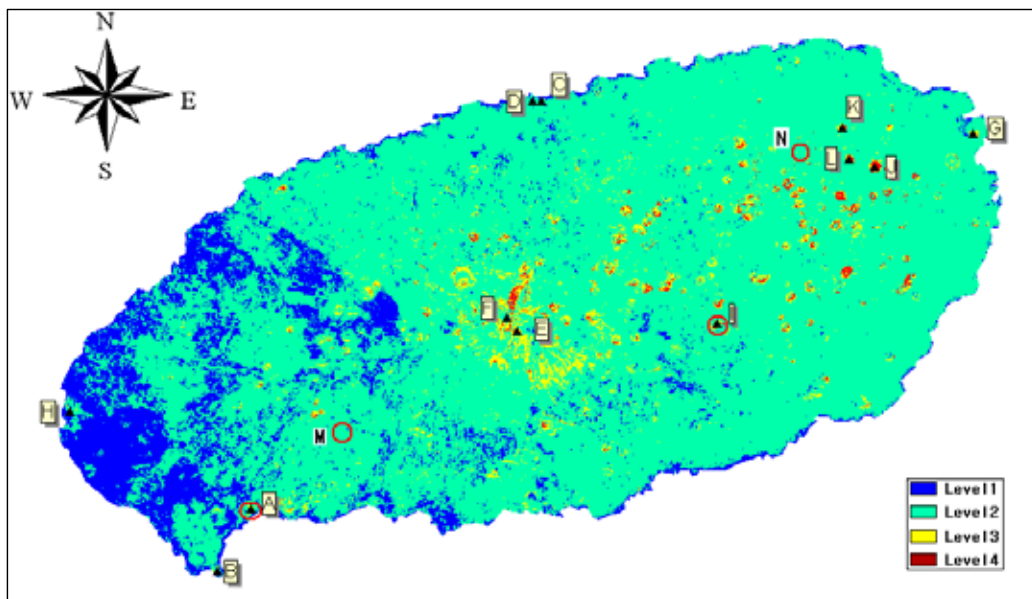







Fig. 6.6 The distribution of the field data.

Table 6.1 Field data.

<b>A(Sanbangsan)</b>		
	SL: 72m HL: 61.2m Elevation: 37.9m Slope: 32° Width: 17.4m Aspect: west	Geology: basalt Soil: B Forest: 6~16 Land cover: forest Rainfall intensity: 18.643mm/hr
<b>B(Songaksan)</b>		
	SL: 41.5m HL: 35.6m Elevation: 21.4m Slope: 31° Width: 11.6m Aspect: east	Geology: trachyte Soil: A Forest: - Land cover: grassland Rainfall intensity: 11.481mm/hr
<b>C(Byeoldobong)</b>		
	SL: 36.8m HL: 32.9m Elevation: 16.5m Slope: 26.6° Width: 23.2m Aspect: north	Geology: trachyte Soil: C Forest: - Land cover: grassland Rainfall intensity: 21.174mm/hr
<b>D(Sarabong)</b>		
	SL: 47.2m HL: 39.9m Elevation: 25.1m Slope: 32.2° Width: 61.9m Aspect: west	Geology: trachyte Soil: C Forest: - Land cover: grassland Rainfall intensity: 21.174mm/hr



**E(Baekrokdam)**

	SL:48.3m HL: 40m Elevation: 27m Slope: 34° Width: 8m Aspect: southeast	Geology: basalt Soil: B Forest: 6~16cm(diameter) Land cover: forest Rainfall intensity:21.174mm/hr
---	---	--

**F(North area in Hallasan)**

	SL: 60m HL: 51m Elevation: 32m Slope: 32° Width: 12m Aspect: north	Geology: basalt Soil: B Forest: 6~16cm(diameter) Land cover: forest Rainfall intensity:21.174mm/hr
---	---	--

Table 6.2 The information of the field data.

Area	Slope	Aspect	Geology type	Soil type	Forest (diameter)	Land cover	Rainfall intensity(mm/hr)
G	28.8°	S	trachyte	(A)	6-16cm	forest	21.116
H	47.2°	S	Sedimentary	(B)	6-16cm	forest	11.481
I	26.8°	N	trachyte	(B)	8-18cm	forest	18.643
J	29.6°	NW	trachyte	(A)	8-18cm	forest	21.116
K	32.4°	N	trachyte	(A)	6-16cm	forest	21.116
L	27.7°	SW	trachyte	(A)	6-16cm	forest	21.116

Table 6.3 The field data recognized as the susceptibility areas in each method.

Method type	Field data	Total number
AHP method	A, E, F, H, I, J, K	7
ANN method	A, C, D, E, F, G, I, J, K	9
LRA method	E, F, I, J, K	5

### 6.3 The landslide probability analysis

To inspect an accuracy of the susceptibility areas we also performed a landslide probability analysis in some susceptibility areas and safety areas in the susceptibility map generated by the ANN method.

To perform the probability analysis, we used the ANN method and 7 input layers as elevation, slope, porosity, dry density, lithology, USCS and permeability. These input layers were somewhat different from the input layers used in the susceptibility analysis. The input layers are shown in Fig. 6.7 and initial values of the hidden layer, output layer, learning rate and momentum are shown in Table 6.4 and 6.5. After the comparison of the RMSE values calculated by each different initial value, we found that the RMSE values were minimized when the hidden number was 14 and the learning rate and momentum value were 0.3 respectively as shown in Fig. 6.8. Thus, we calculated an importance value of each input layer by using this value. The importance value is shown in Fig. 6.9.

The probability analysis was performed in four areas such as A, I, M, N indicated in Fig. 6.6. Here, the areas of A and I belonged to susceptibility areas and the areas of M and N belonged to safety areas. After the calculation, we knew that the probability value of A, I, M, and N was 0.874, 0.942, 0.121, and 0.261 respectively as shown in Fig. 6.10.

Finally, we knew that the probability value belonging to the susceptibility areas was very high and the probability value belonging to the safety areas was very low and it also indicated that the susceptibility map was accurate.

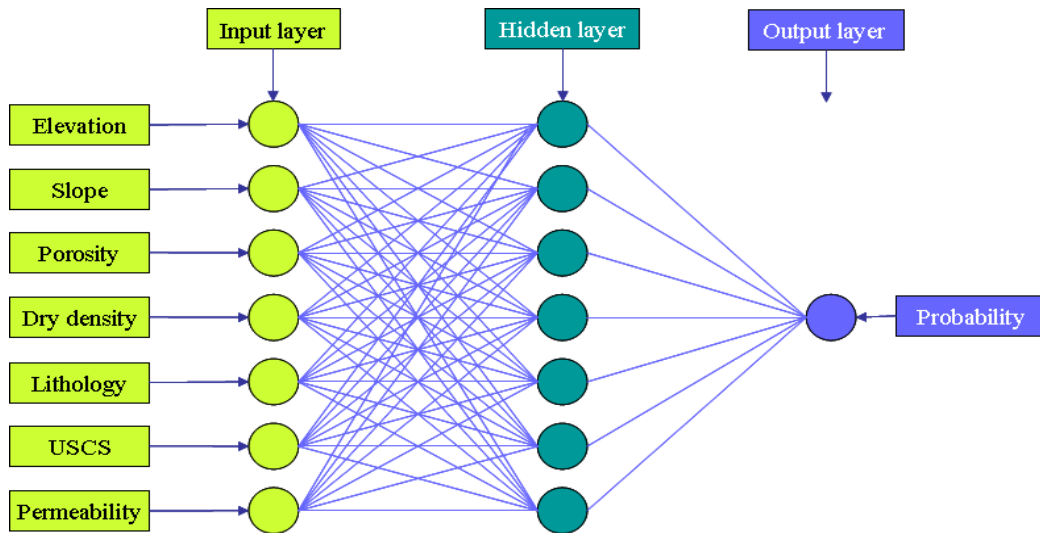


Fig. 6.7 The ANN model for the landslide probability analysis.

Table 6.4 Layer numbers.

Case \ Layer	Case1	Case2	Case3	Case4
Input layer	7	7	7	7
Hidden layer	7	14	21	28
Output layer	1	1	1	1

Table 6.5 The learning rates and momentum.

No \ Factor	1	2	3	4	5	6	7	8
Learning rate	0.01	0.01	0.01	0.01	0.1	0.1	0.1	0.1
Momentum	0.1	0.3	0.5	0.7	0.1	0.3	0.5	0.7
No \ Factor	9	10	11	12	13	14	15	16
Learning rate	0.3	0.3	0.3	0.3	0.5	0.5	0.5	0.5
Momentum	0.1	0.3	0.5	0.7	0.1	0.3	0.5	0.7

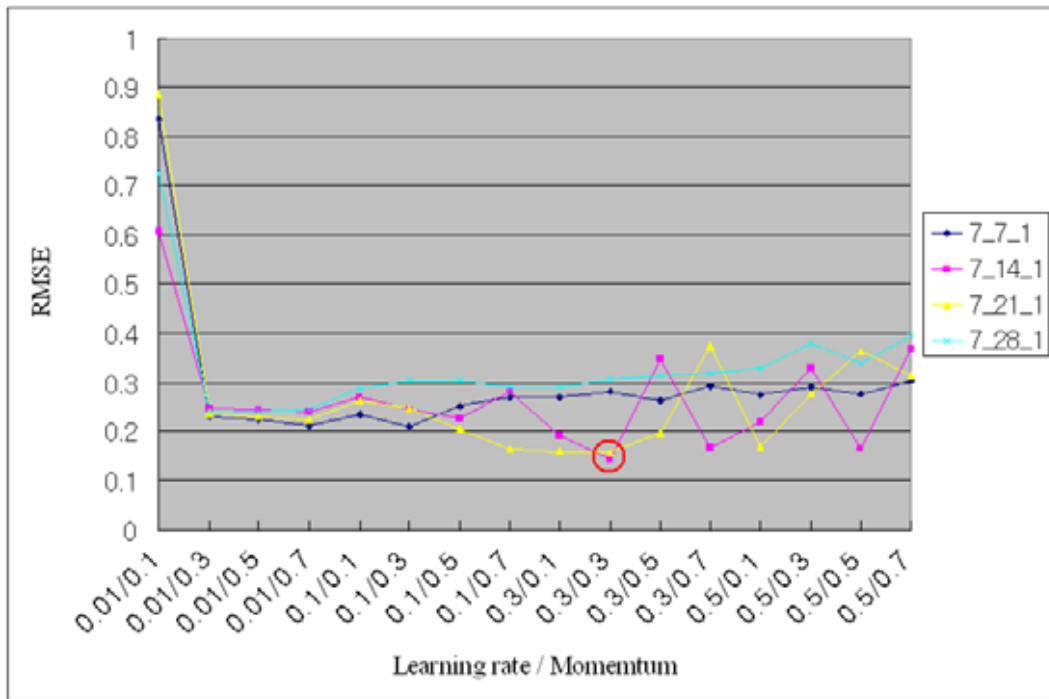


Fig. 6.8 The comparison of each RMSE value.

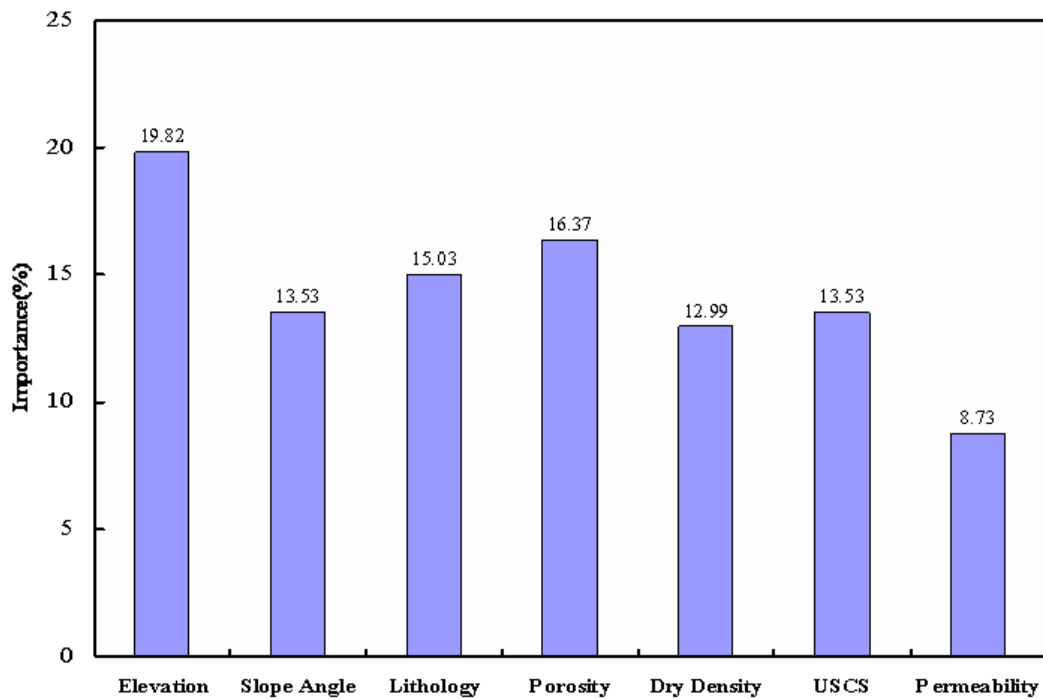


Fig. 6.9 The importance values of each input factor.

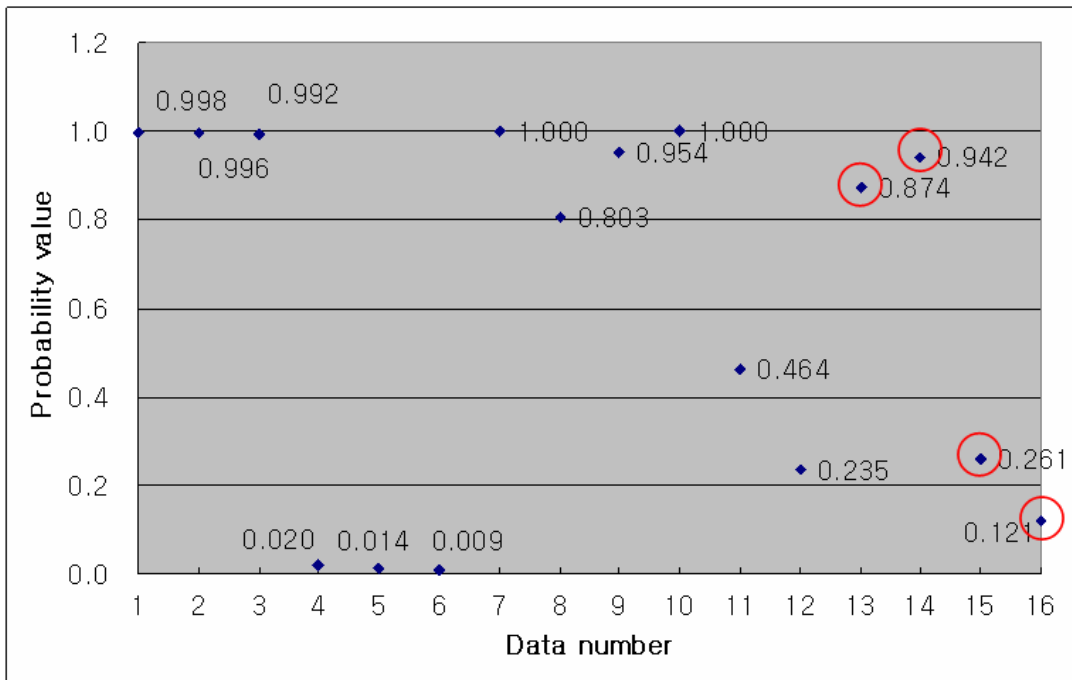


Fig. 6.10 The result of the landslide probability analysis.

## CHAPTER 7. CONCLUSIONS

In this study, we analyzed landslide susceptibility in Jeju Island by portraying the susceptibility maps using three methods such as the AHP, logistic regression analysis and artificial neural network and we had the following conclusions:

First, according to the weight values calculated by the AHP method, the weight values of slope, rainfall intensity, soil and forest were 35%, 24%, 16% and 10%, respectively, and these accounted for 85% of entire value. In the ANN method, the weight value of slope was 24.06% and there were no remarkable differences in weight values of rainfall intensity(16.96%), soil(16.77%) and forest(16.34%). However, these values also accounted for 74.13% of entire value. Then, we assumed that the slope, rainfall intensity, soil and forest were the most important factors to analyze landslide susceptibilities.

Second, to analyze the accuracy of the susceptibility maps generated by three different methods, we selected 12 areas for analysis after the field survey. After the comparison between three susceptibility maps and field data, 7 areas of the field data were recognized as susceptibility areas in the AHP method, 9 areas of the field data were recognized as susceptibility areas by the ANN method and 5 areas of the field data were recognized as susceptibility areas by the LRA method. From the results, we found that the map generated by the ANN method was more accurate, the map generated by the AHP method was secondly accurate and the map generated by the LRA method was the least accurate.

Third, according to the susceptibility maps, the most susceptibility areas belonging to level 4 generated by the AHP method, the LRA method and

the ANN method accounted for 0.93%(17.1 $km^2$ ), 0.28%(5.1 $km^2$ ) and 0.62%(11.5  $km^2$ ) of entire area, respectively, and almost all the susceptibility areas were distributed to the top and middle district of the Halla mountain and the outskirts of the island.

Fourth, from NDVI change images between 2001 and 2002 and between 2002 and 2007, we found that the NDVI values in some areas were significantly decreased. According to the conception of the NDVI, we found that the susceptibility areas where the NDVI values were significantly decreased were more dangerous than other susceptibility areas. To determine this dangerous area, we compared the NDVI change images with the susceptibility areas generated by the most accurate ANN method. From the results, we found that some susceptibility areas were distributed in the most decreased NDVI areas.

Finally, to inspect an accuracy of the susceptibility areas, we also performed a landslide probability analysis in some susceptibility areas and safety areas in the susceptibility map generated by the ANN method. The result of the probability analysis showed that the probability values in the susceptibility areas were very high and the probability values in the safety areas were very low and it also indicated that the susceptibility areas were accurately extracted.

## REFERENCES

- Aleotti, P., Chowdhury, R., 1999, Landslide hazard assessment: summary review and new perspectives. *Bulletin of Engineering Geology and the Environment* 58, pp.21-44.
- Arzandeh, S. and J. Wang, 2003, Monitoring the Change of Phragmites Distribution Using Satellite Data, *Canadian Journal of Remote Sensing*, 29(1): pp.24-35.
- Atkinson, P.M. and A. R. L. Tatnall, 1997, Neural Networks in Remote Sensing, *International Journal of Remote Sensing*, 18(4): pp.699-709.
- Baldelli P., Aleotti P. and Polloni G., 1996, Landslide susceptibility numerical at the messina Straits crossing site, Italy, *Proceedings of the seventh international symposium on landslides*, pp.153-158.
- Benediktsson, J.A. and J.R. Sveinsson, 1997, Feature Extraction for Multisource Data Classification with Artificial Neural Networks, *International Journal of remote sensing*, 18: pp.727-740.
- Benediktsson, J.A., Swain, P.H. and O. K. Ersoy, 1990, Neural Network Approaches Versus Statistical Methods in Classification of Multisource Remote Sensing Data, *IEEE Transactions on Geoscience and Remote Sensing*, 28: pp.540-552.
- Bischof, H., schneider, W. and A. Pi, 1992, Multispectral Classification of Landsat Images Using Neural Networks, *IEEE Transactions on Geoscience and Remote Sensing*, 30: pp.482-490.
- Bromhead, E. N., 1992, *The stability of slopes*, Blackie Academic & Professional.
- Brand, E. W., 1988, Landslide risk assessment in Hong Kong , *Proceedings of the fifth international symposium on landslide*, Vol.2, pp.1059-1074.
- Carrara, A., E. Catalano, M. Sorrosp-Valvo, C. Realli, and II. Ossi. 1978, Digital Terrain Analysis for Land Evaluation, *Geologia Applicata Idorgeologica*, Vol. 13, pp.69-127.
- Carrera A., M. Cardinali, R. Detti, F. Guzzetti, V. Pasqui, and P. Peichenbach,



- 1991, GIS Techniques and Statistical Models in Evaluating landslide Hazard. Earth Surface Processes and Landforms, Vol. 16, pp.427-445.
- Choi, G. S., 1999, Preliminary estimation of waste landfill sites using geo-spatial information system and analytic hierarchy process, Graduate School Gangwon University, Thesis for the Degree of Master.
- Chung C.F., A.G. Fabbri and C.J. van Westen, 1995, Multivariate Regression Analysis for Landslide Hazard Zonation, Geographical Information Systems in Assessing Natural Hazards, pp.135-175.
- Chun, K. S., 2005, A method of determining landslide susceptibility area using GIS, Gangwon university graduate school, PhD thesis.
- Civco, D.L., 1993, Artificial Neural Network for Land Cover Classification and Mapping, International Journal of Geographical Information System, 7: pp.179-186.
- Dai F.C, Lee C.F, 2002, Landslide characteristics and slope instability modeling using GIS, Lantau island, Hong kong, Geomorphology, v.42, pp.213-228.
- E. Yesilnacar, T. Topal, 2005, Landslide susceptibility mapping: A comparison of logistic regression and neural networks methods in a medium scale study, Hendek region(Turkey), Engineering Geology 79, pp.251-266.
- Fang, h., 1991, Foundation Engineering Handbook, Van Nostrand Einhold Company, pp.88-143, pp.410-446.
- F. Zahedi, 1986, The Analytic Hierarchy process-A Survey of the Method and Its Applications, Interfaces, 16(4), pp.96-108.
- Gonzalez, R. C. and R. E. woods, 2002, Digital Image Processing, New York: Addison-Wesley, pp.793.
- Gong, P., Pu, R. and J. Chen, 1996, Mapping Ecological Land Systems and Classification uncertainties from Digital Elevation and Forest-cover Data Using Neural Networks, Photogrammetric Engineering & Remote Sensing, 62: pp.1249-1260.
- Guzzetti, F., Carrara, A., Cardinalli, M., Reichenbach, P., 1999, Landslide hazard evaluation: areview of current techniques and their application in a

- multi-case study, central Italy. *Geomorphology* 31, pp.181-216.
- Hagan, M. T., Demuth, H.B., and Beale, M., 1996, *Neural Network Design*, Boston: PWS Publishing.
- Hansen, A., 1984, Landslide hazard analysis. In: Brunsden, D., Prior, D.B.(Eds.), *Slope Instability*. John Wiley and Sons, NewYork, pp.523-602.
- Haykin, S., 1994, *Neural networks: A Comprehensive Foundation*, New York: Macmillan College Publishing, pp.696.
- Hengl, T., 2002, *Neural Network Fundamentals : A Neural computing Primer*, *Personal Computing Artificial Intelligence*, 16(3), pp.32-43.
- Hwang, S. H., 2002, *Analysing and mapping landslide hazard based on GIS*, Gangwon university graduate school, Thesis for the Degree of Master.
- Jahne, B., 1997, *Digital Image processing: Concepts, Algorithms, and Scientific Applications*, New York: Springer-Verlag, pp.555.
- Jensen, J. R., 2000, *Remote Sensing of the Environment: An Earth Resource Perspective*, Upper Saddle River, NJ: Prentice-Hall, pp.544.
- Jensen, J. R., Qiu, F. and M. ji, 1999, Predictive Modeling of Coniferous Forest Age Using Statistical and Artificial Neural Network Approaches Applied to Remote Sensing Data, *International Journal of Remote Sensing*, 20(14): pp.2805-2822.
- Jensen, J. R., Qiu, F. and K. Patterson, 2001, A Neural Network Image interpretation System to Extract Rural and Urban Land use and Land Cover Information from Remote Sensor Data, *Geocarto International*, 16(1): pp.19-28.
- Ji, C. Y., 2000, Land-Use Classification of Remotely Sensed Data Using Kohonen Self-Organizing Feature Map Neural Networks, *Photogrammetric Engineering & Remote Sensing*, 66(12): pp.1451-1460.
- Journal of the Korean Society of Agriculture Engineers* Vol 37 No.6, pp.12-33.
- John R. jensen, 2005, *Introductory Digital Image Processing: a remote sensing perspective*, Pearson Education, Inc., pp.62-65.
- Kanellopoulas, I., Wilkinson, G.G., 1997, Strategies and best practice for neural network image classification. *International Journal of Remote Sensing* 18, pp.711-725.

- Kavzoglu, T., 2001, An investigation of the design and use of feedforward artificial neural networks in the classification of remotely sensed images, PhD thesis, University of Nottingham. School of Geography, pp.306.
- Keller, E. A., 1979, Environmental geology, Bell & Howell company, pp.111-154.
- Kim, G. H., 2000, GIS introduction, Daiyeongsa, pp.206-225.
- Korea disaster prevention association, 2001, Disaster prevention techniques for landslide, Disaster prevention information, Vol. 7, pp.44-45.
- Lee, B. G., 2003, Utilizing Principal Component Analysis in Unsupervised Classification Based on Remote Sensing Data, The graduate school Pusan National University, PhD thesis.
- Lee, M. J., 2003, Landslide susceptibility analysis using remote sensing, GIS, and neural network in the Kangneung area, Graduate School Yonsei University, Thesis for the Degree of Master.
- Lee, S. H., Ryu, J. H., Won, J. S., Park, H. J., 2004, Determination and application of the weights for landslide susceptibility mapping using an artificial neural network, Engineering Geology 71, pp.289-302.
- Lee, S. L., 2000, Development and application of landslide susceptibility analysis techniques using geographic information system(GIS), Graduate School Yonsei University , PhD thesis.
- Lillesand, T.M. and Kiefer, R., 2000, Remote sensing and image interpretation(4th edition), John Wiley & Sons, pp. 724.
- Lloyd, R., 1996, Spatial Cognition, Geographic Environments, Dordrecht, Netherlands: Kluwer Academic Publishers, pp.287.
- Lunetta, R. L. and J. G. Lyons(Eds.), 2003, Geospatial Data Accuracy Assessment, Las Vegas: US Environmental protection Agency, Report No. EPA/600/R-03/064, pp.335.
- Lunetta, R. S. and C. Elvidge, 2000, Remote Sensing Change Detection: Environmental Monitoring Methods and Applications, new york: Taylor & Francis, pp.340.
- Newman, E.B., A.R. Paradis, and E.E. Brabb, 1978, Feasibility and Cost of

- Using a Computer to Prepare Landslide Susceptibility Maps of the San Francisco Bay Region, California, U.S. Geological Survey, Reston, Vlo. 29.
- Qiu, F. and J. R. Jensen, 2004, Opening the Black Box of Neural Networks for Remote Sensing Image Classification, *International Journal of Remote Sensing*, in press.
- Rao, V. B. and H. V. Rao, 1993, *C<sup>++</sup> Neural Network and Fuzzy Logic*, New York: Management Information, pp.408.
- Russell, S. J. and P. Norvig, 2003, *Artificial Intelligence: A Modern Approach*, 2nd ed., Upper Saddle River, NJ: Prentice-Hall, pp.1080.
- Skempton, A. W. and Hutchinson, J. N., 1969, Stability of natural slopes and embankment foundations, *State-of-the-art Volume, 7th International Conference on Soil Mechanics and Foundation Engineering*, pp.291-340.
- Terzaghi, K., 1950, *Mechanism of Landslides*, Geological Society of America, Berkeley Volume, pp.83-123.
- T.L. Saaty, 1980, *The Analytic Hierarchy Process*, McGraw-Hill, pp.11-76
- Turner, K. A. and Schuster, R. L., 1996, *Landslides investigation and mitigation*, Transportation research board, National research council, Special report 247, pp.131-137.
- Turrini, C. M. and Visintainer, P., 1998, Proposal of a method to define areas of landslide hazard and application to an area of the Dolomites, Italy *Engineering Geology* 50, pp255-265.
- Varnes, D.J., 1978, *Slope Movement Types and Processes*, Landslides Analysis and Control, Special Report 176, Transportation Research Board, Washington, D.C. pp.11-80.
- Verstappen, H.T., 1983, *Applied Geomorphology: Geomorphological Surveys for Environmental Development*. Elsevier, Amsterdam.
- Walker, B. F., 1987, Soil slope instability and stabilization. A. A. Balkema, pp.2-52.
- Yu, B. M., 1998, *Geographic Information System*, Pakyoungsa, pp.1-5.
- Yu, B. M., 2003, *Modern digital photogrammetry*, Pearson Education Korea, pp.348-351.

## 요 약

제주도는 주 분화구였던 한라산을 중심으로 경사가 급하고 섬 변두리 부분에는 많은 절벽단층들이 분포하고 있으며 태풍과 폭우의 영향을 많이 받고 있으므로 하여 시간이 흐를수록 산사태문제가 지속적으로 발생하고 그에 따른 피해도 증가할 것으로 예상 된다. 따라서 제주도 전반지역에 대하여 산사태 취약성분석을 진행하고 취약한 지역에 대하여 집중적으로 조사 할 것이 필요하다.

산사태 취약성 분석을 진행하기 위하여 본 연구에서는 우선 제주도 전 지역에 대한 1:25000수치지도를 이용하여 수치표고모델을 추출하고 수치표고모델로부터 경사방향도, 경사도를 작성하고 기타 산사태에 영향을 주는 요소들인 강우강도, 지질, 임상, 토양, 토지피복 등에 대하여 산사태에 미치는 영향을 분석하였다. 위의 요소들을 이용하여 산사태 취약성분석을 하기 위하여 AHP 기법, 로지스틱 회귀분석 기법, 인공신경망기법을 이용하여 취약성도를 작성하고 각각의 결과를 비교분석하였다.

AHP기법에서는 기존의 연구와 달리 총 8개의 대안을 우선 설정한 다음 강우강도를 추가하여 산사태 발생에 영향을 주는 경사도, 경사방향도, 지질도, 토양도, 임상도, 토지이용도 등 요소들과 함께 사용하여 경중률을 계산한다. 다음으로 대안별로 경중률 값을 비교하여 최적의 대안을 선택하고 지형정보체계를 구축한 다음 GIS프로그램인 Arcview를 이용하여 위에서 선택된 최적대안의 경중률 값을 사용하여 모델을 구축하고 Weighted Overlay 기법을 이용하여 제주도 산사태 발생가능지역에 대한 취약성도를 작성한다.

로지스틱기법에서는 산사태 발생을 종속변수로 하고 산사태가 발생할 때 값은 1을 취하고 발생하지 않을 때 값은 0을 취하며 독립변수에는 경사, 경사방향, 토양, 지질, 임상, 강우강도, 토지피복 등 7개의 변수로 설정하여 산사태에 영향을 주는 요소들에 대하여 아래와 같은 방정식을 획득하고 이 방정식과 GIS 기법을 이용하여 취약성도를 작성하였고 취약성 분석을 위하여 이 방정식에 의하여 계산된  $P_z$ (사건발생확율)값에 의하여 취약성도를 총 4개의 위험등급으로 나누었다.

$$\begin{aligned} \ln(P_z/(1 - P_z)) = & (-10.158) + 0.783 * X_1(\text{slope}) + 0.364 * X_2(\text{aspect}) \\ & + 0.523 * X_3(\text{geology}) + 0.668 * X_4(\text{soil}) \\ & + 0.726 * X_5(\text{rainfall intensity}) \\ & + 0.400 * X_6(\text{forest}) + 0.575 * X_7(\text{landcover}) \end{aligned}$$

인공신경망 기법으로는 경사도, 경사방향도, 지질도 등 총 7개의 산사태 발생 인자에 대하여 입력층 7개, 은닉층 14개, 출력층은 1개로 하고 입력층과 은닉층을 연결하는 가중치 값은 총 98개, 은닉층과 출력층을 연결하는 가중치 값은 14개로 설정하여 인자들의 중요도를 추출한 다음 이 값들에 근거하여 GIS기법으로 취약성도를 작성하였다.

작성된 취약성지도에서도 가장 위험한 지역을 검출하기 위하여 동일지역에 대한 다년도 Landsat 영상을 이용하여 NDVI 값을 구하고 영상변화탐지기법을 사용하였다. 영상변화탐지를 위하여서는 2001, 2002, 2007년도 Landsat 영상을 이용하였으며 년도별 영상차를 통하여 NDVI 값이 현저히 감소한 지역을 추출하고 이 지역과 취약성지도를 중첩시키는 방법으로 가장 위험한 지역을 추출하였다.

AHP기법, 로지스틱 기법, 인공신경망 기법을 이용하여 작성된 산사태 취약성지도의 정확도를 검증하기 위하여 제주도 전 지역에서 현장조사를 통하여 산사태가 발생했던 지역과 비교적 취약한 지역을 선정하여 비교하여 보았다. 그 결과 인공신경망은 총 9개의 지역이 검출되었고 AHP기법은 7개, 로지스틱기법은 5개 지역이 검출되었다. 따라서 인공신경망기법이 가장 정확하다는 것을 알 수 있었다.

취약성지역에 대한 정확성을 진일보 검증하기 위하여 취약성지도에서 취약한 지역과 안전한 지역을 선정하여 산사태 가능성 분석을 진행하였다. 산사태 가능성분석을 진행함에 있어서는 인공신경망 기법을 사용하였고 입력인자는 취약성분석과 달리 토질인자들을 추가하여 분석하였다. 사용된 입력인자들은 고도, 경사, 지질, 건조단위중량, 간극율, 토양분류, 투수계수 등이다. 선정된 지역에 대하여 산사태 가능성분석을 한 결과 취약성지역에서 가능성 값이 현저히 높게 나오고 안전지역에서는 매우 낮게 나왔다.

## 감사의 글

본 논문이 완성되기까지 대학원 석사와 박사과정을 거쳐 오면서 부족한 저에게 많은 가르침을 주시고 항상 격려해주신 이병걸 교수님께 제일 먼저 감사의 인사를 드립니다. 그리고 저의 논문을 심사해주고자 멀리 중국 연변대학에서 와 주신 이백수 교수님, 부산대학교에서 와 주신 강인준 교수님, 박상렬 교수님, 남정만 교수님께 진심으로 감사드립니다. 또한 항상 저를 관심하고 배려해주신 양성기 교수님, 김남형 교수님, 김상진 교수님, 이동욱 교수님께도 감사드립니다.

대학원 생활 중 힘들 때 늘 곁에서 많은 조언을 해주고 도움을 주신 고영호 선배님, 김창훈 선배님, 승현이형, 승남이형에게 고마운 마음을 전합니다. 그리고 기쁠 때나 어려울 때나 항상 옆에 있어주고 함께 해온 친구들 조성환, 윤원수, 최슬기, 김준호, 김도형, 고행식, 양철영, 양태혁, 강규후, 박상훈에게도 감사드립니다. 그리고 연구실에서 매일 함께 공부하고 부족한 선배를 도와주느라 고생 많았던 연구실후배들 고정우, 부경훈, 외후 우르차이흐, 고경만, 홍성오, 장연수, 김원석, 부선진, 변지선에게도 정말 너무 고맙습니다.

6년간의 유학생 생활 동안 함께 동고동락해온 수길이형, 지강이형, 미선누나, 미경누나, 서권선생님, 박인호선생님, 림학, 박금룡, 김윤걸, 김해영, 최연희, 오금희, 홍진남, 전가, 정해매 그리고 지금은 떨어져 있지만 석사과정을 함께 해온 현이형, 향란누나, 김광일, 허미란에게도 고마운 마음 전합니다. 그리고 대학원 생활을 해오면서 많은 도움을 준 홍성협, 김경남, 문경태, 이창선, 김태건, 김영민, 김학재, 카오탄 녹탄, 문지원, 강향혜, 외국인 행사 때마다 항상 불러주고 좋은 추억을 만들어 준 부형주에게도 고맙다는 말을 하고 싶습니다.

마지막으로 지금까지 항상 저에게 힘이 되어주시고 사랑으로 뒷받침해 주신 부모님과 형님, 형수님, 귀여운 조카 성우, 그리고 사랑스러운 동생들에게 고마운 마음을 전하며 앞으로도 더욱 발전되고 열심히 사는 모습을 보여드리겠습니다.

-2009년 새해를 맞이하며